



PONTIFICIA UNIVERSIDAD CATOLICA DE CHILE  
ESCUELA DE INGENIERIA

# **RECYCLING OF FINES FROM CONSTRUCTION AND DEMOLITION CONCRETE WASTES**

**RICARDO SERPELL C.**

Thesis submitted to the Office of Research and Graduate Studies in  
partial fulfillment of the requirements for the Degree of Doctor in  
Engineering Sciences

Advisor:

**MAURICIO LÓPEZ**

Santiago de Chile, April, 2014

© 2014, Ricardo Serpell



PONTIFICIA UNIVERSIDAD CATOLICA DE CHILE  
ESCUELA DE INGENIERIA

# RECYCLING OF FINES FROM CONSTRUCTION AND DEMOLITION CONCRETE WASTES

**RICARDO SERPELL C.**

Members of the Committee:

**MAURICIO LÓPEZ**

**CARLOS VIDELA**

**BÁRBARA HERRERA**

**PATRICIA MARTÍNEZ**

**JEFFERY ROESLER**

**CRISTIÁN VIAL**

Thesis submitted to the Office of Research and Graduate Studies in  
partial fulfillment of the requirements for the Degree of Doctor in  
Engineering Sciences

Santiago de Chile, October, 2013

To my beloved wife Carola and my  
dearest children Martín and Gabriel:  
Your love and joy are my inspiration.

## **AKNOWLEDGEMENTS**

I would like to express my deep gratitude to my advisor, professor Mauricio López C., for sharing with me his passion for research and academic life. Along these years, he has constantly been a generous mentor, an inspiring model and a true friend for me. I would also like to thank professor Jeffery Roesler, my advisor during my stay as a visiting scholar at the Civil and Environmental Engineering Department of the University of Illinois at Urbana-Champaign, for giving me the exceptional opportunity of performing research at one of the leading centers in this field. I would like to extend my gratitude to the family and friends of professor Roesler, whose affection made me and my family feel truly at home during our one year stay in Urbana-Champaign.

I am grateful to the members of the Doctoral Thesis Committee, professors Carlos Videla, Barbara Herrera, Patricia Martínez and Cristián Vial, for the significant feedback they have provided to the development of this thesis, collectively and individually in several instances along these years.

I acknowledge the contributions of Professor José Miguel Aguilera, from the Department of Chemical and Bioprocess Engineering, and Professor Pablo Pasten, from the Department of Hydraulic and Environmental Engineering, who generously granted me access to critical research equipment in their respective laboratories. Likewise, I am grateful to Mr. Jose Miguel Pascual, Director of the Laboratorio de Resistencia de Materiales (RESMAT) from the Dirección de Investigación, Ciencia y Tecnología de la Universidad Católica (DICTUC) for granting me access to laboratory facilities, resources and equipment. I also thank the staff at RESMAT, and the staff at the Laboratorio de Materiales of the Department of Construction Engineering and Management, Mr. Mauricio Guerra and Mr. Fernando Palma, for their invaluable help.

My gratitude goes also to my colleagues at the Architecture School, professors Claudio Vasquez, Alejandro Prieto and Hernán Larraín, with whom I have taught the Introduction to Construction class, and professor Cristián Sandoval, with whom I have taught the Fundamentals of Structural Analysis and Design class.

I am grateful to my friends, professor José Quintanilla, and professor Loreto Muñoz, for sharing their personal insight on academic life in so many rewarding conversations. Likewise, I am grateful to my research mates at the Engineering and Technology of Concrete (ETC) group at the Department of Construction Engineering and Management, not only for their generous help and feedback, but also for the inspiring enthusiasm with which they dedicate themselves to cement and concrete research.

I acknowledge the scholarship for Doctorate studies awarded to me by the Comisión Nacional de Ciencia y Tecnología, CONICYT, de Chile, between March 2008 and August 2012.

Finally, I would like to express my profound gratitude to my wife, Carolina, my parents, Ricardo and Eloisa, and my siblings, Daniel, Eduardo, Ximena and Cristián, for their unconditional support throughout these years.

## TABLE OF CONTENTS

	Page
<b>DEDICATION.....</b>	<b>i</b>
<b>AKNOWLEDGEMENTS.....</b>	<b>ii</b>
<b>ABSTRACT .....</b>	<b>viii</b>
<b>RESUMEN.....</b>	<b>x</b>
<b>OUTLINE OF THE THESIS.....</b>	<b>xii</b>
<b>LIST OF PAPERS.....</b>	<b>xiv</b>
<b>LIST OF ABBREVIATIONS.....</b>	<b>xv</b>
<b>LIST OF TABLES .....</b>	<b>xvi</b>
<b>LIST OF FIGURES .....</b>	<b>xviii</b>
<b>1. INTRODUCTION .....</b>	<b>1</b>
1.1 Environmental impact of concrete and the role of recycling .....	2
1.2 Recycling of concrete aggregates and production of concrete fines .....	4
1.3 Characteristics of residual hydrated cement paste relevant to the recycling of concrete fines .....	7
1.3.1 Oxide composition .....	8
1.3.2 Unreacted cement and self-cementing behavior .....	9
1.3.3 Pozzolanic and alkaline activation capacity.....	11
1.3.4 Cementitious behavior after thermal treatment.....	14
1.4 Thesis objectives .....	17
1.4.1 General objectives.....	17
1.4.2 Specific objectives .....	18
1.5 Hypotheses .....	19

1.5.1	Hypotheses for the contribution of recycled aggregates to the performance of controlled low-strength materials .....	19
1.5.2	Hypotheses for the effects of material and process factors on the cementitious capacity of reactivated materials .....	20
1.5.3	Hypotheses for reactivation temperature and replacement level effects on the properties of reactivated material mortars .....	21
1.6	Outline of methodology .....	22
1.7	Synopsis of experimental results .....	24
1.7.1	Performance of controlled low-strength materials based on fine recycled concrete aggregates and fly ash .....	24
1.7.2	Materials and process factors significantly affecting the cementitious capacity of reactivated materials .....	28
1.7.3	Properties of mortars based on reactivated cementitious materials and supplementary cementitious materials.....	32
1.8	General conclusions .....	33
1.9	Additional research prospects .....	35
<b>2.</b>	<b>RELATIVE PROPORTIONING METHOD FOR CONTROLLED LOW-STRENGTH MATERIALS .....</b>	<b>37</b>
	Abstract.....	37
2.1	Introduction .....	38
2.2	Research significance .....	41
2.3	Experimental procedure .....	41
2.3.1	Experimental design.....	41
2.3.2	Materials .....	43
2.3.3	CLSM mixture and batching.....	46
2.4	Experimental results, modeling, and discussion .....	47
2.4.1	Slump-flow models .....	48
2.4.2	Subsidence models .....	54

2.4.3	28-day compressive strength models .....	55
2.5	Relative proportion CLSM mixture design principles .....	60
2.6	Conclusions .....	62
2.7	Acknowledgments .....	63
2.8	References .....	64
<b>3.</b>	<b>REACTIVATED CEMENTITIOUS MATERIALS FROM HYDRATED CEMENT PASTE WASTES .....</b>	<b>68</b>
	Abstract .....	68
3.1	Introduction .....	69
3.2	Experimental design, materials and methods .....	74
3.2.1	Experimental design and experimental factors .....	74
3.2.2	Materials and methods .....	77
3.3	Results and discussion.....	79
3.3.1	Estimated effects of factors and factor interactions .....	82
3.3.2	Identification of significant factor and factor-interaction effects ..	85
3.3.3	Analysis of estimated effects on compressive strength of RCM-based pastes.....	88
3.3.4	Response models.....	93
3.3.5	Optimum levels of factors.....	96
3.4	Conclusions .....	97
3.5	Acknowledgments .....	100
3.6	References .....	100
<b>4.</b>	<b>USE OF REACTIVATED CEMENTITIOUS MATERIALS FOR THE PRODUCTION OF MORTARS .....</b>	<b>105</b>
	Abstract .....	105
4.1	Introduction .....	106
4.2	Experimental Design .....	108

4.2.1 Mixture Design .....	110
4.3 Materials and methods .....	112
4.4 Results and discussion.....	115
4.4.1 Flow of RCM mortars .....	119
4.4.2 Strength of RCM mortars.....	122
4.4.3 Expansion of RCM mortars .....	129
4.5 Conclusions .....	132
4.5.1 Substitution level: .....	132
4.5.2 Reactivation temperature: .....	133
4.6 Acknowledgments.....	134
4.7 References .....	134
<b>GENERAL REFERENCES .....</b>	<b>138</b>
<b>APPENDICES .....</b>	<b>150</b>
Appendix A: Supplementary data from the FRCA-based CLSM study.....	151
Appendix B: Supplementary data from the multifactorial study of RCM.....	154
Appendix C: Supplementary data from the study of RCM-based mortars....	159

PONTIFICIA UNIVERSIDAD CATÓLICA DE CHILE  
ESCUELA DE INGENIERÍA

**RECYCLING OF FINES FROM CONCRETE  
CONSTRUCTION AND DEMOLITION WASTES**

Thesis submitted to the Office of Research and Graduate Studies in partial fulfillment  
of the requirements for the Degree of Doctor in Engineering Sciences by

**RICARDO JAVIER SERPELL CARRIQUIRY**

**ABSTRACT**

Produced at a rate of over 30,000 million metric tons per year, concrete is the most manufactured material in use in the world today, and as such, its environmental impact has been a matter of significant concern in recent years. Recycling of concrete wastes is generally regarded in the literature as an effective way to reduce its environmental footprint. However, over 50% of the output from the crushing of demolition concrete to produce coarse recycled aggregates is a finer sized material that finds limited use in conventional concrete mixtures due to its negative impact on performance, and thus is generally discarded or employed in lower value applications. Developing new construction materials based on these fines could significantly increase the fraction of concrete wastes being recycled. In this thesis, two recycling alternatives based on different degrees of processing of the wastes were explored, studying how the hydrated cement paste residues present in the fines contribute to the engineering properties of the recycled materials obtained in each case, simultaneously characterizing the effects that material and process factors associated with each alternative have on the performance of the materials, in order to provide relevant knowledge for their future development, optimization and application.

The first alternative explored, at the lower level of processing, was the development of controlled low-strength materials based on crushed concrete fines as produced. An alternative method for mixture design was proposed in order to enable the use of designed experiments to model the effects that mixture proportions have on the relevant properties

of the resulting materials. Comparing response models obtained when single constituents are replaced allowed unbiased identification of their relative contribution to material performance. Fine recycled concrete aggregate based materials exhibit improved flowability, segregation and subsidence characteristics, while achieving compressive strengths within prescribed limits, due to the physical and chemical characteristics of the aggregate particles and the hydrated cement paste residues present in them, respectively.

The second alternative explored was the production of reactivated cementitious materials based on the hydraulic behavior observed for the dehydrated and powdered product from hydrated cement paste wastes. A two-stage experimental program was developed to first identify material and process factors significantly affecting the strength of reactivated material pastes; and then characterize the effects of selected factors on a larger set of material properties and over a wider range of factor levels. Results from the first stage show strength developed by reactivated material pastes can be significantly increased adjusting the temperature of dehydration and the presence of silica fume in the new mixtures. Results from the second stage show the effects of dehydration temperature correlate to the concentration of a stabilized form of  $\alpha'$ -C<sub>2</sub>S detected in the reactivated materials, which forms during the reactivation process. It was concluded that strength gain of reactivated materials is due mostly to the formation of C-S-H by hydration of this polymorph of C<sub>2</sub>S. In addition, results from the second stage show, for the first time, that reactivated cementitious materials can be used for the production of mortars, developing compressive strengths exceeding 20 MPa at 28 days of hydration.

Members of the Doctoral Thesis Committee:

Mauricio López  
Carlos Videla  
Bárbara Herrera  
Patricia Martínez  
Jeffery Roesler  
Cristián Vial

Santiago, April, 2014

PONTIFICIA UNIVERSIDAD CATÓLICA DE CHILE  
ESCUELA DE INGENIERÍA

**RECICLAJE DE FINOS DE RESIDUOS  
DE CONSTRUCCIÓN Y DEMOLICIÓN DE HORMIGÓN**

Tesis enviada a la Dirección de Investigación y Postgrado en cumplimiento parcial  
de los requisitos para el grado de Doctor en Ciencias de la Ingeniería, por

**RICARDO JAVIER SERPELL CARRIQUIRY**

**RESUMEN**

El hormigón es el material manufacturado en mayor cantidad en el mundo en la actualidad, con una producción que excede las 30,000 millones de toneladas al año. Como tal, su impacto sobre el medio ambiente es materia de constante preocupación. El reciclaje de los residuos de hormigón es considerado en la literatura como una vía efectiva para reducir su huella ambiental. Sin embargo, más del 50% del material obtenido del chancado de hormigones de demolición para la producción de agregados gruesos reciclados es un material de graduación fina de limitado uso en hormigones convencionales, que es generalmente descartado o utilizado en aplicaciones de bajo valor. El desarrollo de nuevos materiales de construcción basados en estos finos podría aumentar significativamente la fracción de residuos de hormigón que pueden ser reciclados. En esta tesis se exploraron dos alternativas de reciclaje basadas en dos niveles distintos de procesamiento de los residuos, estudiando cómo los restos de pasta de cemento hidratada presentes en los finos contribuyen a las propiedades de ingeniería de los materiales reciclados obtenidos en cada caso, y caracterizando el efecto que los factores materiales y de proceso asociados a cada alternativa tienen sobre estas propiedades, con el fin de proveer conocimiento relevante para su desarrollo, optimización y aplicación futura.

La primera alternativa explorada fue la fabricación de materiales de baja resistencia controlada basados en agregados finos de hormigón reciclado sin procesamiento adicional. Se desarrolló un método mejorado de diseño de mezclas que facilita el uso de diseños experimentales sencillos para modelar los efectos que las proporciones de la mezcla tienen

sobre las propiedades de los materiales resultantes. La comparación de modelos obtenidos para materiales basados en distintos constituyentes permitió evaluar la contribución relativa de cada constituyente a las prestaciones del material. En comparación con los materiales basados en agregados finos vírgenes, los basados en agregados finos reciclados exhiben mejores características de fluidez, segregación y asentamiento, logrando resistencias a compresión dentro de los límites esperados.

La segunda alternativa explorada fue la producción de materiales cementicios reactivados basados en el comportamiento hidráulico que exhiben los productos obtenidos de la deshidratación de pastas de cemento hidratadas. Se desarrolló un programa experimental en dos etapas para primero: identificar factores materiales y de proceso que afecten significativamente a la resistencia a compresión de pastas de material reactivado, y segundo: caracterizar los efectos de factores seleccionados sobre un conjunto más amplio de propiedades. Los resultados de la primera fase muestran que es posible aumentar significativamente la resistencia desarrollada por las pastas ajustando la temperatura de deshidratación y el nivel de reemplazo de material reactivado por material cementicio suplementario en las nuevas mezclas. Los resultados de la segunda etapa muestran que los efectos de la temperatura de deshidratación se correlacionan con la concentración de una forma estabilizada de  $\alpha'$ -C<sub>2</sub>S presente en el material reactivado, formada durante el proceso de deshidratación. Esto permitió concluir que la ganancia de resistencia del material reactivado se debe principalmente a la formación de C-S-H por hidratación de este polimorfo de C<sub>2</sub>S. Adicionalmente, los resultados de la segunda fase muestran, por primera vez, que los materiales cementicios reactivados pueden ser usados para la producción de morteros con resistencias a compresión que superan los 20 MPa a 28 días de hidratación.

Miembros de la Comisión de Tesis Doctoral:

Mauricio López

Carlos Videla

Bárbara Herrera

Patricia Martínez

Jeffery Roesler

Cristián Vial

Santiago, Abril de 2014

## OUTLINE OF THE THESIS

The thesis is comprised of three journal articles in which I have communicated and discussed the main findings of the experimental work of my Doctorate research. Each article constitutes a separate chapter in the thesis. Full text, tables, figures and references included in the original publication or manuscript have been transcribed in each chapter. In addition, references have been collected in a unified master list at the end of the thesis.

The thesis is organized in four chapters:

Chapter 1, *Introduction*, presents the rationale behind recycling of concrete, summarizing main aspects of the impact of concrete on the environment over its whole life cycle. It presents a review of the current state of the art in recycling of concrete aggregates showing how additional research is required in order to find valuable applications for the large amount of finer materials generated as a by-product of the aggregate recovery process. It describes potential paths to recycling of these fines, based on a review of the characteristics and chemical composition of the hydrated cement paste residues present in them, and presents the two alternatives selected to be explored according to the objectives of the thesis, stating the specific hypotheses associated with each, and detailing the research methodology proposed to prove them. It briefly discusses the results obtained, – which are thoroughly presented in the following chapters–, and outlines general conclusions and additional research prospects on the subject.

Chapter 2, *Relative proportioning method for controlled low-strength materials*, presents the findings of original research work carried out to explore the use of finer material derived from the production of recycled concrete aggregates as a constituent of controlled low-strength materials. In order to evaluate the contribution of this recycled fine aggregate and of other non-standard constituents to the performance of the resulting materials, relative proportioning is proposed to establish mixture designs, thus enabling the use of designed experiments to model and compare the effects that changes to mixture

proportions have on the relevant properties of the end product when different constituents are used.

Chapter 3, *Reactivated cementitious materials from hydrated cement paste wastes*, presents the findings of the first stage of the experimental program proposed to explore the production of reactivated cementitious materials as a route to recycling of crushed concrete fines which have a high proportion of hydrated cement paste residues. It presents the results of a fractional factorial experiment designed to identify material and process factors significantly affecting the strength of reactivated cementitious material pastes, and discusses the selection of relevant factors for the development and optimization of the recycling process.

Chapter 4, *Use of reactivated cementitious materials for the production of mortars*, presents the findings of the second phase of the aforementioned experimental program. The two factors previously found to have the largest positive effect on the strength of reactivated cementitious material pastes (i.e. the reactivation temperature and the replacement level of reactivated material by supplementary cementitious material in new mixtures) were explored over a wider experimental region, and on a larger set of material properties, studying the flowability, compressive strength and expansion of mortars based on reactivated materials. It develops and discusses factor-response relationship models obtained by second order regression of the results from a central composite experiment designed to study both factors simultaneously, and compares them to results obtained from additional experiments where a different supplementary cementitious material was used. Finally, based on results from XRD analysis of the reactivated materials, it proposes a new hypothesis to explain their cementitious characteristics.

## LIST OF PAPERS

- Chapter 2.** Serpell, R., Henschen, J., Roesler, J. and Lange, D. Relative proportioning method for controlled low-strength materials. Submitted to *ACI Materials Journal* in May 2013.
- Chapter 3.** Serpell, R. and López, M. (2013). Reactivated cementitious materials from hydrated cement paste wastes. *Cement and Concrete Composites* 39 (1) pp. 104-114.
- Chapter 4.** Serpell, R. and López, M. Use of reactivated cementitious materials for the production of mortars. Submitted to *Cement and Concrete Composites*, in August 2013.

## LIST OF ABBREVIATIONS

### **Common abbreviations used throughout the thesis:**

C-S-H	Calcium Silicate Hydrates
FRCA	Fine Recycled Concrete Aggregate(s)
FVA	Fine Virgin Aggregate
HCP	Hydrated Cement Paste
OPC	Ordinary Portland Cement (ASTM C150 type I)
RCA	Recycled Concrete Aggregate(s)
RCM	Reactivated Cementitious Material(s)
SCM	Supplementary Cementitious Material(s)
SEM	Scanning Electron Microscope
VA	Virgin Aggregate
W/C	Water to Cement ratio (by mass)
W/CM	Water to Cementitious Material ratio (by mass)
XRD	X-Ray Diffraction

### **Cement chemistry notation:**

A	$\text{Al}_2\text{O}_3$	M	$\text{MgO}$
C	$\text{CaO}$	N	$\text{Na}_2\text{O}$
$\hat{\text{C}}$	$\text{CO}_2$	S	$\text{SiO}_2$
F	$\text{Fe}_2\text{O}_3$	$\hat{\text{S}}$	$\text{SO}_3$
H	$\text{H}_2\text{O}$	T	$\text{TiO}_2$
K	$\text{K}_2\text{O}$		

## LIST OF TABLES

### CHAPTER 2

<b>Table 2.1</b>	Experimental and coded levels of factors.....	42
<b>Table 2.2</b>	Experimental levels of additional cases .....	43
<b>Table 2.3</b>	Physical properties of constituent materials .....	44
<b>Table 2.4</b>	Chemical analysis of fly ash.....	45
<b>Table 2.5</b>	Results for individual cases in the central composite experiment.....	48
<b>Table 2.6</b>	Estimated effects (regression coefficients) of mixture proportions on slump-flow diameter (mm).....	49
<b>Table 2.7</b>	Estimated effects (regression coefficients) of mixture proportions on subsidence (as % of specimen height).....	54
<b>Table 2.8</b>	Estimated effects (regression coefficients) of mixture proportions on 28- day compressive strength (kPa).....	56
<b>Table 2.9</b>	Regression coefficients for Strength - W/CM ratio relationship for different sets of constituents at different levels of OPC/CM .....	60

### CHAPTER 3

<b>Table 3.1</b>	Assignment of experimental factors and their selected levels.....	73
<b>Table 3.2</b>	Composition of source pastes to supply HCP wastes (~2 L). ....	77
<b>Table 3.3</b>	Variance ( $S^2_R$ ) and standard deviation ( $S_R$ ) of responses and effects ( $S_E$ ) ....	83
<b>Table 3.4</b>	Effect of factors and interactions on response Y1: 7-day compressive strength of RCM pastes (MPa). 95% confidence interval: $\pm 0.94$ MPa .....	83
<b>Table 3.5</b>	Effect of factors and interactions on response Y2: 28-day compressive strength of RCM pastes (MPa). 95% confidence interval: $\pm 1.41$ MPa .....	84
<b>Table 3.6</b>	Effect of factors and interactions on response Y3: 90-day compressive strength of RCM pastes (MPa). 95% confidence interval: $\pm 1.74$ MPa .....	84

<b>Table 3.7</b>	Combinations of factor levels for optimum long term strength .....	97
------------------	--	----

## CHAPTER 4

<b>Table 4.1</b>	Design factor levels .....	110
<b>Table 4.2</b>	Mixture recipes: cases from the central composite experiment .....	111
<b>Table 4.3</b>	Mixture recipes: additional cases .....	112
<b>Table 4.4</b>	XRF analysis of fly ash .....	113
<b>Table 4.5</b>	NCh-158 normalized sand gradation.....	113
<b>Table 4.6</b>	Results: cases from the central composite experiment.....	118
<b>Table 4.7</b>	Results: cases from additional experiments .....	119
<b>Table 4.8</b>	ANOVA: flow test results .....	120
<b>Table 4.9</b>	ANOVA: 7-day strength results .....	123
<b>Table 4.10</b>	ANOVA: 28-day strength results .....	124
<b>Table 4.11</b>	ANOVA: Expansion results .....	130

## APPENDICES

<b>Table A.1</b>	Mixture compositions for the three replications of the CLSM central composite experiment.....	151
<b>Table B.1</b>	Weight loss on dehydration of source materials .....	154
<b>Table B.2</b>	RCM pastes: Individual case results for block 1, in execution order.....	155
<b>Table B.3</b>	RCM pastes: Individual case results for block 2, in execution order.....	156
<b>Table B.4</b>	RCM pastes: Individual case results for block 3, in execution order.....	157
<b>Table B.5</b>	RCM pastes: Individual case results for block 4, in execution order.....	158

## LIST OF FIGURES

### CHAPTER 1

<b>Figure 1.1</b>	Comparison of virgin and recycled aggregates (SEM backscatter image).....	5
<b>Figure 1.2</b>	Recycled aggregate cross-section showing cracking of residual hydrated cement paste matrix (SEM backscatter image). ....	5
<b>Figure 1.3</b>	Recycling alternatives for construction and demolition concrete wastes.....	8
<b>Figure 1.4</b>	Unreacted cement grains in HCP present in FRCA particle (SEM backscatter image). ....	10
<b>Figure 1.5</b>	Ettringite needles bridging fly ash particles in FRCA-based CLSM (fracture surface, SEM secondary electron image). ....	26
<b>Figure 1.6</b>	Effects of material and process factors and factor interactions on 7-day compressive strength of RCM pastes. ....	29
<b>Figure 1.7</b>	Effects of material and process factors and factor interactions on 28-day compressive strength of RCM pastes. ....	29

### CHAPTER 2

<b>Figure 2.1</b>	Relative proportions selected to establish mixture compositions.....	40
<b>Figure 2.2</b>	Graphical representation of the central composite experimental design, showing the experimental levels chosen for the factorial points (cube vertices). ....	42
<b>Figure 2.3</b>	Gradation of fine virgin aggregate (FVA) and fine recycled concrete aggregate (FRCA) compared to ASTM C33 limits.....	44
<b>Figure 2.4</b>	Predicted slump-flow diameter as a function of volumetric paste percent at 0.15 OPC/CM and 0.85 W/CM ratios. ....	49
<b>Figure 2.5</b>	Predicted slump-flow diameter as a function of the W/CM ratio at 42.5% paste fraction and 0.15 OPC/CM ratios.....	50

<b>Figure 2.6</b> Predicted slump-flow diameter for mixtures based on FVA and FA1 fly ash at different volumetric paste percentages and a fixed 0.15 OPC/CM ratio.....	51
<b>Figure 2.7</b> Predicted slump-flow diameter as a function of OPC/CM ratio of the mixture, at 42.5% paste and 0.85 W/CM ratios. ....	52
<b>Figure 2.8</b> Observed slump-flow diameter versus OPC/CM ratio at 40% VPP and W/CM=0.80 with detrimental effect on slump-flow at lower OPC/CM ratios and FRCA-based mixtures. ....	53
<b>Figure 2.9</b> SEM image of fracture surface of 28-day CLSM containing FRCA and FA2 fly ash with ettringite needles bridging fly ash particles.....	53
<b>Figure 2.10</b> Predicted mixture subsidence as a function of volumetric paste percent at 0.15 OPC/CM ratio and 0.85 W/CM ratio (except where indicated). ....	55
<b>Figure 2.11</b> Compressive strength results for mixtures containing FVA and fly ash (FA1) at W/CM and OPC/CM combinations yielding a fixed W/OPC ratio of 2.0.....	57
<b>Figure 2.12</b> 28-day strength results versus OPC/CM ratio for mixtures at fixed 0.80 W/CM ratio and 40% volumetric paste percent. ....	57
<b>Figure 2.13</b> 28-day compressive strength results versus W/CM ratio for mixtures with FVA and FA1 source fly ash at multiple OPC/CM ratios.....	58
<b>Figure 2.14</b> 28-day compressive strength results versus W/CM ratio for mixtures with FRCA and FA1 source fly ash at multiple OPC/CM ratios. ....	59
<b>Figure 2.15</b> 28-day compressive strength results versus W/CM ratio for mixtures with FRCA and FA2 source fly ash at multiple OPC/CM ratios. ....	59

### CHAPTER 3

<b>Figure 3.1</b> Schematic diagram of experimental steps, showing factors associated with each step. ....	73
<b>Figure 3.2</b> Time order scatter plot of observed strength for all cases. Frequency shows bi-modal distribution of response spreading over hydration time.....	80

<b>Figure 3.3</b>	Scatter plots of compressive strength observations. a) 28-day strength versus 7-day strength, b) 90-day strength versus 28-day strength. ....	80
<b>Figure 3.4</b>	Scatter plot of compressive strength observations versus SSD density observations for recycled paste specimens tested at 28 days. ....	81
<b>Figure 3.5</b>	Compressive strength observations at different testing ages. Average results of central cases deviate from average results of factorial cases.....	82
<b>Figure 3.6</b>	Half-normal probability plot of estimated effects on 7-day compressive strength (h.o.: higher order effect, not considered). ....	85
<b>Figure 3.7</b>	Half-normal probability plot of estimated effects on 28-day compressive strength (h.o.: higher order effect, not considered). ....	86
<b>Figure 3.8</b>	Half-normal probability plot of estimated effects on 90-day compressive strength (h.o.: higher order effect, not considered). ....	87
<b>Figure 3.9</b>	Average compressive strength of RCM-based pastes at different levels of substitution of RCM by silica fume in the mixtures (factor X6), showing factor and interaction effects. ....	89
<b>Figure 3.10</b>	Average compressive strength of RCM-based pastes at different levels of incorporation of NaOH solution to the mixtures (factor X3), showing factor and interaction effects. ....	90
<b>Figure 3.11</b>	Average compressive strength of RCM-based pastes at different levels of presence of silica fume in original composition of HCP wastes (factor X7), showing factor and interaction effects. ....	91
<b>Figure 3.12</b>	Average compressive strength of RCM-based pastes at different levels of dehydration temperature (factor X5), showing factor and interaction effects. ....	92
<b>Figure 3.13</b>	Average compressive strength of RCM-based pastes at different levels of degree of hydration of HCP wastes (factor X2) and at different levels of presence of inert siliceous fines along the HCP wastes (factor X8).....	93
<b>Figure 3.14</b>	Scatter plots of predicted (model) versus observed compressive strength at 7, 28, and 90 days, including residual versus observed values, and histogram of residuals. ....	95

## CHAPTER 4

<b>Figure 4.1</b> Experimental region covered by the central composite experimental design.....	109
<b>Figure 4.2</b> Percent of raw and reactivated material retained in #200 mesh (75 µm).....	116
<b>Figure 4.3</b> Evaporated water during initial mixing versus RCM reactivation temperature and RCM substitution level.....	117
<b>Figure 4.4</b> Predicted response for flow of RCM mortars at different RCM substitution levels.....	121
<b>Figure 4.5</b> Flow of RCM mortars versus RCM substitution level.....	122
<b>Figure 4.6</b> 28-day compressive strength of RCM mortars at different RCM substitution levels .....	124
<b>Figure 4.7</b> Predicted response for 7 and 28-day compressive strength of RCM mortars at different RCM substitution levels .....	125
<b>Figure 4.8</b> XRD scans of RCM produced at different reactivation temperatures.....	127
<b>Figure 4.9</b> Relative intensity of interest phases identified in the XRD scans of the RCM produced at different reactivation temperatures .....	128
<b>Figure 4.10</b> Predicted response for expansion of RCM mortars at different RCM substitution levels.....	131

## APPENDICES

<b>Figure A.1</b> Predicted response surface for 28-day compressive strength as a function of the W/CM and OPC/CM ratios for FVA-based CLSM incorporating class C fly ash.....	152
<b>Figure A.2</b> Predicted response surface for 28-day compressive strength as a function of the W/CM and OPC/CM ratios for FRCA-based CLSM incorporating class C fly ash.....	152
<b>Figure A.3</b> Predicted response surface for 28-day compressive strength as a function of the W/CM and OPC/CM ratios for FRCA-based CLSM incorporating a highly reactive class C fly ash.....	153

<b>Figure A.4</b> Comparison of slump-flow results for FRCA-based CLSM at high (left) and low (right) volumetric paste percent.....	153
<b>Figure B.1</b> 3-gang 20mm side mold for RCM-based pastes .....	154
<b>Figure C.1</b> Comparison of XRD patterns of OPC, hydrated paste and RCM produced at 800 °C, between 29 and 38 20 degrees.....	159

## **1. INTRODUCTION**

In scientific literature as well as in general interest publications it frequently reads that concrete is the most manufactured material in use in the world today. The statement by S. Brunauer and L.E. Copeland in a paper published in *Scientific American* in April 1964 (as cited by Mehta & Monteiro, 2006) reading that “man consumes no material except water in such tremendous quantities”, has remained true until today without exceptions. In 2011 the annual world production of Portland cement reached approximately 3,600 million metric tons (U.S. Geological Survey, 2013). A conservative estimate for world production of concrete exceeding 30,000 million metric tons annually can be obtained from that number. In the nearly 200 years period since Joseph Aspdin applied for a patent for “an improvement in the modes of producing an artificial stone”, which he called Portland cement because of its resemblance to the stone bearing the same name (Aspdin, 1824), cement based concrete has been constantly used and developed, successfully adapting it to an ever increasing variety of applications. It is an engineered material that can be designed and produced according to the requirements of each application, and based on the vast amount of knowledge accumulated through the years a high degree of control over the properties of the final product can be expected.

Nevertheless, concrete is far from being a simple material, and many times the product of a mixture turns out to be unsatisfactory. For Powers (1968), this non-conformity to the prescribed requirements is evident in the amount of research continuously carried out in developed countries. However, the growing effort put into cement and concrete research is also driven by the need to address ever changing material requirements. New requirements arise as industry and society concerns evolve over time, effectively altering the hierarchy of research subjects. As an example, whereas structural performance of concrete was for a long time the main area of research, since 1960 growing concern for durability of structures placed concrete durability performance on a center stage (Richardson, 2002).

Currently, concrete faces requirements beyond the scope of traditional performance indexes, echoing social demands for sustainable development. Although concrete is not a

particularly contaminating material, the magnitude of its impact on the environment is a matter of concern because of the large volume produced every year in the world. The urge to control the environmental impact of concrete over the whole life cycle of the material and the structures built with it has prompted cement and concrete institutions to place sustainability at the center of their agendas, as can be seen in several of their recent communications (ACI, 2008; PCA, 2008; RILEM, 2009).

## **1.1        Environmental impact of concrete and the role of recycling**

In terms of the life cycle assessment of concrete structures, the main sources of environmental impact can be grouped in four components: natural resources consumption, energy consumption, carbon dioxide emissions and solid wastes generation. The production of Portland cement and the manufacturing of concrete consume large amounts of raw materials, mainly: sources of calcium oxides, aluminum oxides, silicon and ferrous oxides for the production of cement, and water and aggregates for the production of concrete. Portland cement production is an energy intensive process requiring 3 – 6 GJ per metric ton of cement produced depending on the specifics of the process used (Gartner, 2004; Madlool, Saidur, Hossain, & Rahim, 2011). In comparison, sourcing of other concrete constituents and concrete mixing and placing consume very little energy. In addition, Portland cement production process contributes about 5% of global anthropogenic carbon dioxide emissions (Gartner, 2004; Hendricks, Jager, Blok, & Riemer, 1998; Huntzinger & Eatmon, 2009; Meyer, 2009), approximately half of which are related to the production of the energy required by the processes, the other half being derived from the decomposition of carbonated compounds in the raw materials (0.425 t CO<sub>2</sub>/t cement, according to Gartner, 2004; 0.507 t CO<sub>2</sub>/t clinker from stoichiometry for a 65% lime clinker). Finally, construction and demolition of concrete structures generates large amounts of wastes, which constitute the largest single component in solid wastes in developed countries (Meyer, 2009).

Environmental impact due to construction and demolition waste generation can be minimized by recovering and reusing. Generally, recovered wastes can be *reused*, with a minimum level of processing in lower value applications different than those originally intended (down-cycling), or *recycled*, using them as raw materials in the production of new materials of comparable value. Although in a strict sense recycling could produce a *closed loop material cycle*, where recovered materials are used in the production of a fresh supply of the same material, in practice this is often expensive or impractical, and therefore wastes are usually recycled into different materials instead. Nevertheless, in addition to reducing the environmental impact due to waste generation, reusing and recycling have the potential to reduce the consumption of natural resources associated with the production of new materials. Energy consumption can also be reduced by recycling, particularly for materials requiring higher energy input per unit mass produced. For construction materials it has been shown that the total amount of energy required in the life-cycle of the material is a good indicator of recycle-ability, with highest benefits to society accruing from material recycling rather than adaptive reusing (Brown & Buranakarn, 2003). According to a recent *energy*<sup>1</sup> analysis by Yuan, Shen, & Li (2011), in the case of concrete, recycled products have greater market value than non-recycled products, put less pressure on the environment, and whereas landfill is a classic consumer process, recycling options arrive at a balance between ecological circulation and economic development, particularly in the case of closed-loop recycling. Consequently, if recycled products can compete in terms of cost and quality, recycling can be a sustainable as well as economically viable trajectory for concrete wastes (Lauritzen, 2004). Concrete components –i.e. aggregates and hydrated paste– must be separated in order to source recycled materials for the production of new concretes.

---

<sup>1</sup> The concept of *energy* is a specific use of the term Embodied Energy, accounting for all the available energy of one kind that is used up in transformations directly or indirectly to make a product or service. It was developed by Howard T. Odum and David M. Scinceman in the 1990s. Extended explanation on energy analysis can be found in Odum, 1996.

## **1.2 Recycling of concrete aggregates and production of concrete fines**

Production of recycled concrete aggregates (RCA) started in the 1970s. Since approximately 80% of the weight in conventional concrete is aggregate (~75% by volume), its recovery would translate into a drastic reduction of concrete wastes. However, the use of recycled aggregates could be detrimental for the fresh and hardened properties of concrete. Engineering properties of the recycled aggregates, such as absorption, density, resistance to abrasion and intrinsic strength, are affected by hydrated cement paste (HCP) residues adhered to them (Sanchez de Juan & Alaejos Gutiérrez, 2009). In the recycled aggregates, the bonding between the hydrated paste residues and the original natural aggregates is affected by the characteristics of the interfacial transition zone formed between them in the original concrete. The characteristics of this old interfacial transition zone are highly dependent on the quality of the original cement paste (i.e. water to cementitious material ratio, addition of supplementary cementitious materials, presence of specific chemical admixtures), and are also affected by the mechanical strain imparted to the material in the crushing of the concrete wastes (**Figure 1.1**). Closer examination of polished cross-sections of recycled aggregates usually reveals a severely fractured surface, corresponding to the original hydrate cement matrix, with cracks surrounding the original aggregates (**Figure 1.2**). Depending on the degree of hydration of the original cement paste, un-hydrated cement grains are also seen embedded in the hydrated matrix. When recycled aggregates are incorporated in a new mixture, the characteristics of the adhered HCP and of its interfacial transition zone affect the mechanical and durability performance of the new concrete. Therefore, the impact of recycled aggregates on the properties of the new concrete depends primarily on the quantity and quality of the HCP residues found in them (Padmini, Ramamurthy, & Mathews, 2009; Poon, Shui, & Lam, 2004).

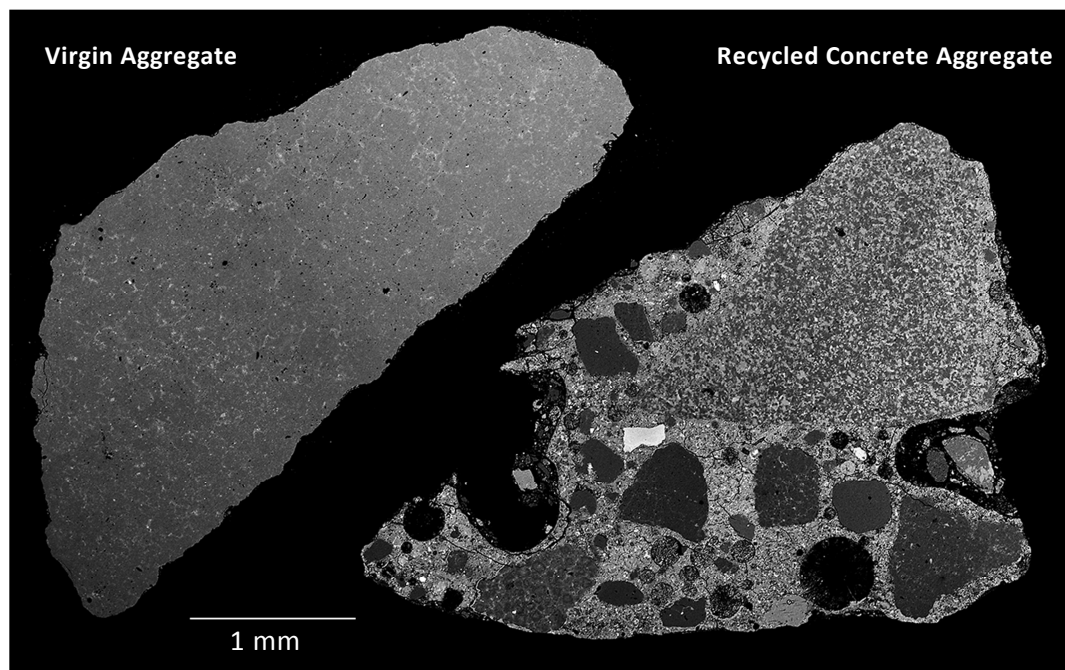


**Figure 1.1** Comparison of virgin and recycled aggregates (SEM backscatter image).

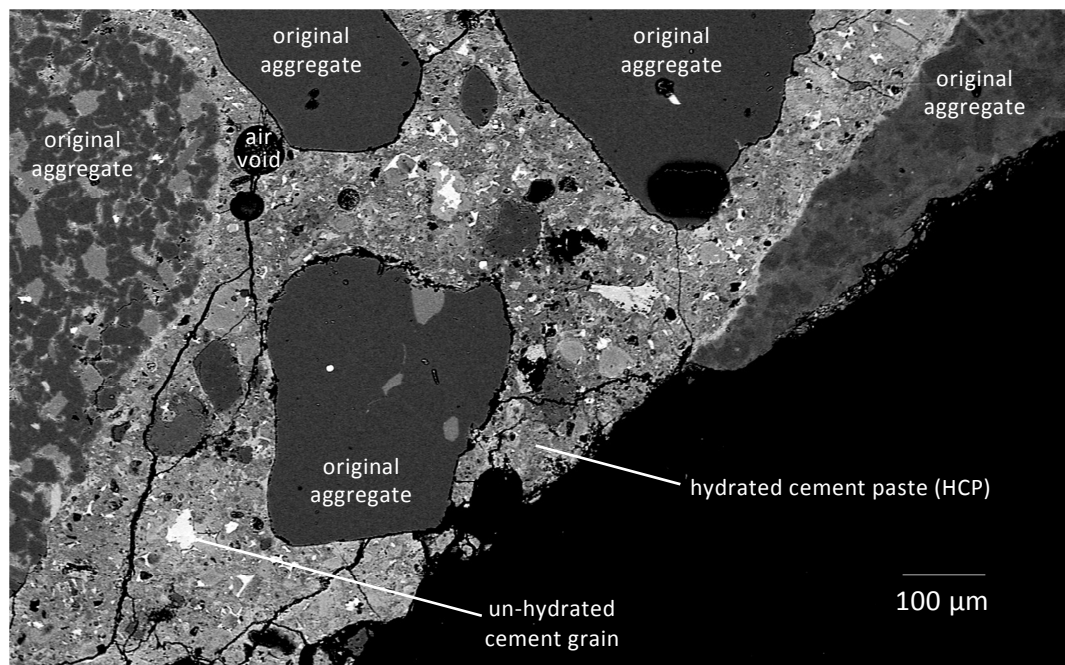


**Figure 1.2** Recycled aggregate cross-section showing cracking of residual hydrated cement paste matrix (SEM backscatter image).

Generally, as the replacement level of natural aggregates by RCA increases, compressive strength, splitting tensile strength, modulus of elasticity and abrasion resistance decrease, while drying shrinkage increases (Etxeberria, Vázquez, Marí, & Barra, 2007; Hansen & Boegh, 1985; Roesler, Lange, Salas, Brand, & Arboleda, 2013). In addition, due to the higher absorption, higher angularity and rougher texture of the recycled aggregates, workability decreases as the replacement level increases. Due to such negative effects, it is normally recommended to limit the amount of RCA used in structural concrete mixtures, particularly the smaller sized materials which have a higher concentration of HCP residues (Kenai, Debieb, & Azzouz, 2002; Shayan & Xu, 2003). Nevertheless, improved recycled aggregate production processes, appropriate characterization of the recycled materials and special mixture design methods have enabled the production of structural concretes performing within specifications with 100% coarse RCA (Abbas et al., 2009; Lin, Tyan, Chang, & Chang, 2004).

Because of the higher concentration of hydrated paste residues, the experience using fine recycled concrete aggregates (FRCA), with particles sizes ranging from 0 – 5 mm, has been less successful. A study by Evangelista & de Brito (2007) using laboratory produced FRCA showed that whereas compressive strength was not significantly affected by replacement ratios up to 30%, tensile splitting and modulus of elasticity were reduced with the increase of replacement ratio; although still within acceptable limits for replacement ratios under 30%. Likewise, in a study on self-compacting concrete made with FRCA, Kou & Poon (2009) showed no significant differences in 90-day compressive strength between mixtures using virgin fine aggregates and mixtures using FRCA in replacement levels up to 50%. Khatib (2005) showed that FRCA reduces 90-day compressive strength between 15 – 30%, for replacement levels between 25 – 100%, respectively.

Consequently, the industry has focused primarily on producing quality coarse RCA, by improving the separation of the original aggregates from the mortar –i.e. HCP and fine aggregate– adhered to them. Successive crushing stages and additional thermal or chemical processes can be combined to enhance the separation. However, as separation improves, the weight percent of crushed concrete reclaimed as coarse aggregate decreases. According

to Nagataki, Gokce, Saeki, & Hisada, (2004), the output of jaw crushing of concrete blocks followed by a single impact crushing stage is composed of 60% coarse aggregate with ~50% of adhered mortar, whereas adding two additional grinding stages reduces the output to 35% coarse aggregate with ~30% adhered mortar. Consequently, between 400 – 650 Kg of crushed concrete fines are produced per ton of demolition concrete in the production of coarse recycled aggregates. These fines are composed of crushed coarse aggregate, fine aggregate and HCP (as a fine powder and adhered to the aggregates). A fraction of the fines can be of enough quality to be used as FRCA in new concretes, particularly when original aggregate is of siliceous type and a thermal step was used to improve the separation, making use of the differences in the coefficient of thermal expansion between the paste and the aggregates (Kasai, 2004). However, since FRCA use in new concretes must be limited to low replacement levels, alternative applications must be developed in order to recycle the large amount of crushed concrete fines and powder produced. Nowadays most of these fines are discarded or used as backfilling material.

### **1.3 Characteristics of residual hydrated cement paste relevant to the recycling of concrete fines**

Just as the content of adhered mortar in the recycled coarse aggregates decreases as the separation improves, the concentration of HCP in the fines produced in the process increases. In developing potential recycling paths for these fines, it must be taken into account that these paste residues are comprised of the hydrated products of Portland cement, i.e. the higher costing component of the original concrete (both in an economical and environmental sense). Higher environmental benefit would be obtained developing recycled construction materials in which the HCP residues found in the fines can contribute to the engineering performance of the end product. In practice, it is possible to foresee several potentially viable alternatives to achieve this by developing construction materials for specific applications based on mixture designs that incorporate the fines as a recycled constituent material (**Figure 1.3**). Different recycled constituent materials can be developed based on different degrees of processing of the fines, with higher degrees

requiring higher energy input. Although the contribution to the engineering properties of the new mixtures is expected to depend on the degree of processing of the fines, the dependence relationship is expected to be property specific, and not necessarily linear, opening up opportunities for single and multi-response optimization of the end products.

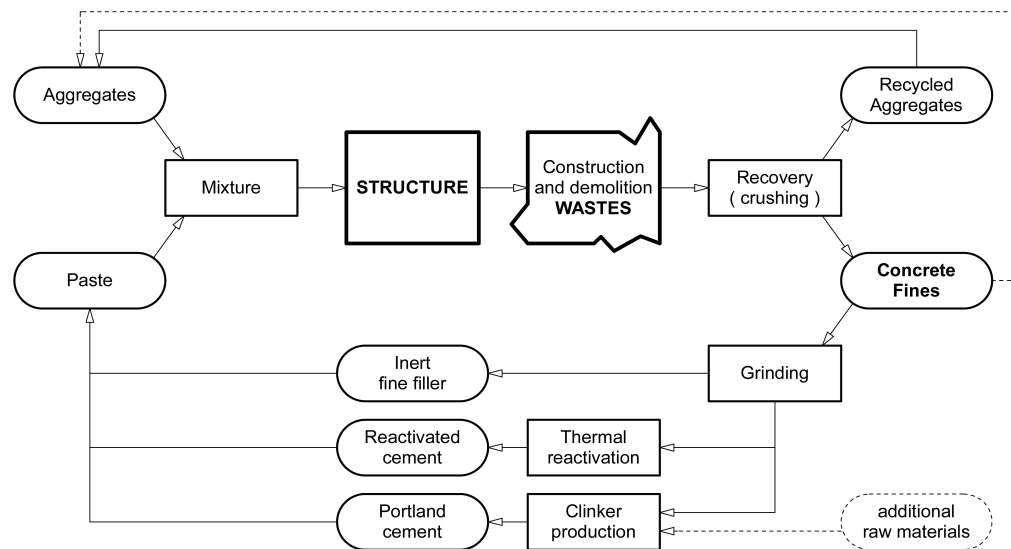


**Figure 1.3** Recycling alternatives for construction and demolition concrete wastes

### 1.3.1 Oxide composition

HCP residues are comprised of the hydration products of anhydrous phases found in Portland cement. Hydration of its major components, Alite (50 – 70 % by weight of cement), –tri-calcium silicate ( $\text{Ca}_3\text{SiO}_5$  or  $\text{C}_3\text{S}$  in cement chemistry notation)–, and Belite (15 – 30 %), –the *beta* polymorph of di-calcium silicate ( $\text{Ca}_2\text{SiO}_4$  or  $\beta\text{-C}_2\text{S}$ )–, produces calcium hydroxide (CH) and nearly amorphous calcium silicate hydrate (C-S-H). Aluminate (5 – 10 %), –tri-calcium aluminate ( $\text{Ca}_3\text{Al}_2\text{O}_6$  or  $\text{C}_3\text{A}$ )–, and Ferrite (5 – 15 %), –tetra-calcium aluminoferrite ( $\text{Ca}_4\text{AlFeO}_5$  or  $\text{C}_4\text{AF}$ )–, hydrate producing AFm phases (Alumino-Ferrite-mono), such as calcium aluminate hydrates or calcium aluminate mono-sulfate hydrates, AFt phases (Alumino-Ferrite-tri), such as calcium

aluminate tri-sulfate hydrates (e.g. ettringite), and other minor hydration products such as hydrogarnet, brucite, hydrotalcite and other related phases (Taylor, 1997). In addition, carbonated compounds are usually found intermixed with the hydrated products. A small amount of CO<sub>2</sub> can be incorporated in the hydrated products as a substitution during hydration reactions; however, much larger amounts are incorporated after hydrated products are formed, as they partially decompose to form calcium carbonates by reaction with atmospheric CO<sub>2</sub> in a degenerative process known as carbonation.

Besides the volatiles incorporated in the hydration and carbonation reactions, the elemental (or oxide) composition of the hydrated products found on the cement paste residues can be expected to be closely similar to that of the anhydrous Portland cement. In principle, crushed concrete fines containing a high proportion of hydrated cement residues can be recycled as a raw material for the production of Portland clinker (Fridrichová, 2007). Although the process is as energy intensive as the production of conventional clinker, it has lower CO<sub>2</sub> emissions from chemical origin as the hydrated products are a mostly carbon-free source of calcium, as opposed to the raw materials in the conventional process (calcite, CaCO<sub>3</sub>). Additional sources of calcium might need to be added together with the concrete fines to the raw feed in order to obtain the prescribed lime saturation factor, depending on the chemistry of the aggregates present in the fines. In addition, as a soluble compound, calcium hydroxide might have been leached in significant amounts from the concrete fines if they have not been stored properly.

### **1.3.2 Unreacted cement and self-cementing behavior**

HCP usually contain a fraction of un-hydrated cement, present as scattered unreacted cores of the original cement grains. The amount of un-hydrated cement relates to the degree of hydration and depends on the physical and chemical characteristics (e.g. particle size distribution and phase composition), the available volume for the precipitation of hydration products (i.e. the volumetric ratio of water to cement in the

original mixture), the availability of water for the hydration reactions (which relates to the initial amount of water and the subsequent curing conditions), and the time-temperature elapsed since the start of the hydration reaction (the age of hydration). The hydration model of Powers & Brownyard (1947), predicts a minimum initial water to cement ratio by weight (w/c) of 0.44 is required for the mixture to contain enough water for the complete hydration of the cement. Even though enough space for hydration products exists at lower ratios, hydration would not be complete unless additional water is added externally (curing water). In practice, unreacted cement grains can be observed in cement pastes manufactured at much higher initial water to cement ratios due to evaporation of water at exposed surfaces, unaccounted absorption of water by the aggregates, or water bleeding from the mixture before setting, all of which ultimately results in a lower degree of hydration (**Figure 1.4**).

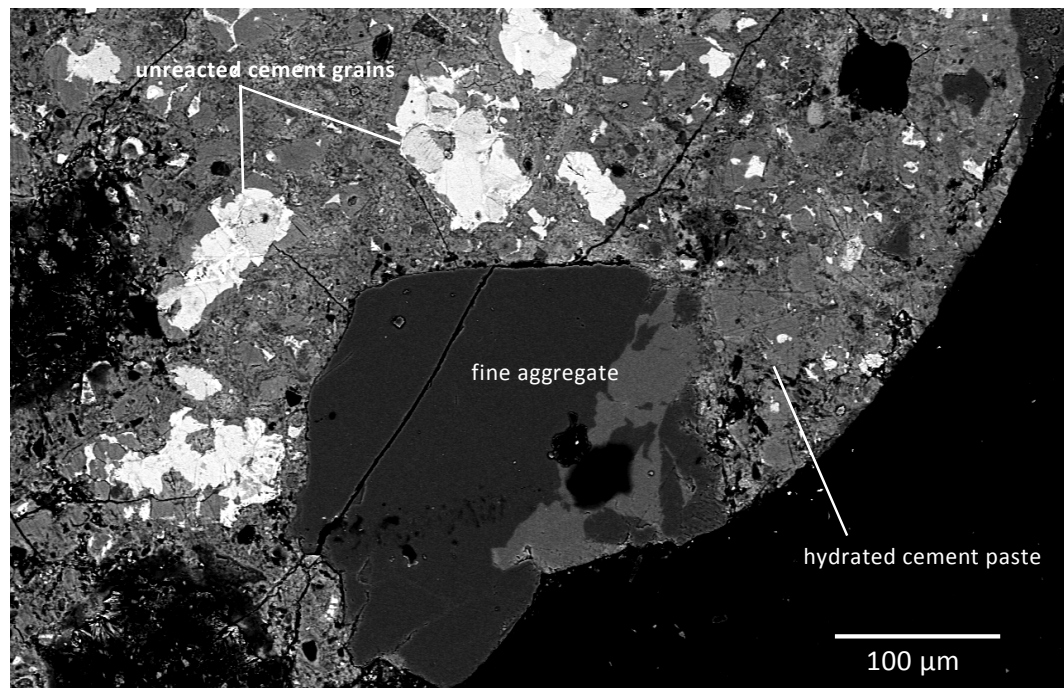


**Figure 1.4** Unreacted cement grains in HCP present in FRCA particle (SEM backscatter image).

When the surfaces of the unreacted grains are exposed again, e.g. by crushing and grinding, hydration reactions can proceed in the presence of water. This explains the self-cementing behavior observed in unbound sub-base materials obtained from the crushing of concrete wastes. In a study of FRCA-based granular materials wet-compacted to 200MPa and fog cured at 25 °C, Poon, Qiao, & Chan, (2006) show that specimens based on FRCA derived from relatively young structural grade concretes (16 month old, 45 MPa), and thus expected to contain a high proportion of unreacted cement, achieved a compressive strength of 2 MPa after 7 days of wet curing. From pH, strength and permeability tests, they conclude that unreacted cement present in the fines is principal cause of the self-cementing behavior and that the finer sized material (under 0.6 mm) is the largest contributor to the phenomenon. However, the cementitious capacity of the unreacted cement in the fines is too low for the requirements of most conventional applications. They could, nevertheless, be used as a combined aggregate-filler constituent in low-strengths materials, contributing to the rheology and strength gain of the mixtures. For these materials, special care would be needed during mixture design in order to account for the variability in the actual content of unreacted cement if maximum strengths are not to be exceeded or minimum strengths must be achieved.

### **1.3.3 Pozzolanic and alkaline activation capacity**

For HCP of high degree of hydration the content of calcium hydroxide (CH) is expected to be between 15 – 25 % compared to the ignited mass of the paste (Taylor, 1997). The actual value varies due to differences in the composition of cements. In addition, depending on the permeability of concrete, exposure to environmental agents such as CO<sub>2</sub> and water can significantly decrease the calcium hydroxide content of the paste due to carbonation ( Ca(OH)<sub>2</sub> + CO<sub>2</sub> = CaCO<sub>3</sub> + H<sub>2</sub>O ) and leaching, respectively.

As a soluble product, calcium hydroxide present in the hydrated paste residues present in FRCA is a source of Ca<sup>2+</sup> and OH<sup>-</sup> ions in aqueous solution. In agreement

with results reported by Poon, Qiao, & Chan (2006), it can be seen in Chapter 3 that a pH of 11.5 was measured immediately after dispersing 20g of FRCA in 100mL of distilled water. As water permeates the paste residues in the recycled aggregates, more calcium hydroxide dissolves and more alkalis enter solution raising pH over time. At 28 days a pH of 12.6 was measured in the same solution. It is believed that additional alkalis enter solution from the HCP.

The ionic products of calcium hydroxide and additional alkalis in solution can participate in hydration reactions of supplementary cementitious materials (SCM). These are inorganic materials that do not react significantly with water on their own, but can behave as hydraulic cements in the presence of other substances. They can be either pozzolanic materials or latent hydraulic cements. In a *pozzolanic* reaction, amorphous SiO<sub>2</sub> (and also Al<sub>2</sub>O<sub>3</sub>) present in high quantity in the pozzolanic material reacts with water to produce C-S-H in the presence of an external source of CaO. Latent hydraulic cements require the presence of minimal amounts of other substances, such as calcium hydroxide and alkalis, which act either as catalysts or activators, to hydrate (Taylor, 1997).

The pozzolanic and alkaline activation capacity of the HCP residues present in the FRCA can be beneficial in the production of controlled low-strength materials (CLSM), where it can be expected to reduce the amount of Portland cement required to achieve prescribed performance. CLSM are highly flowable, self-compacting, cementitious materials used in backfill applications primarily as an alternative to compacted fill. They are prescribed with a maximum strength, not exceeding 8.3 MPa as defined by ACI Committee 229 (1999), with most applications requiring less than 2.1 MPa (to allow for future excavation). Although its constituents are similar to those in concrete, CLSM can be manufactured with non-standard materials as they do not need to meet the same requirements, and as a result they can be a valuable application for industrial by-products which are normally rejected for concrete because of their negative impact on fresh and hardened properties.

Making use of the available alkalis and calcium hydroxide, Achtemichuk, Hubbard, Sluce, & Shehata (2009) investigated CLSM mixtures based on FRCA and SCM derived from industrial waste materials without addition of Portland cement. The fines used in their study exhibited self-cementing behavior and cubes containing only FRCA and water developed 0.17 MPa of compressive strength at 7-days. They found CLSM mixtures incorporating either class C fly ash or ground blast furnace slag gained significant additional strength. At comparable flowabilities (variable water to binder ratios), mixtures with fly ash contents ranging from 5 – 30 % by weight of FRCA achieved 7-day compressive strengths ranging from 0.20 – 1.77 MPa, respectively, whereas mixtures with slag contents ranging from 5 – 30 % by weight of FRCA achieved 7-day compressive strengths ranging from 0.55 – 6.54 MPa, respectively. Alkalies contributed by the FRCA studied were found to be 0.08 % by weight equivalent Na<sub>2</sub>O.

In a recent study on CLSM produced using recycled aggregates from mixed construction and demolition wastes, Portland cement and air entraining admixtures, Etxeberria, Ainchil, Pérez, & González (2013), found that strength gain between 7 and 28 days of hydration was higher for CLSM made with higher volume of recycled aggregate, probably due to pozzolanic reactions. However, they found recycled aggregate contents above 40 % negatively affected total 28-day compressive strength, requiring higher Portland cement contents and lower water to cement ratios to meet specifications. Flowability and setting time were also negatively affected above 50 % recycled aggregate contents. Nevertheless, they conclude that CLSM made with recycled aggregates achieves required fresh and hardened properties, being self-compacted and suitable for future excavation.

Although use of recycled aggregates is suggested in several CLSM guides, few articles report research on this topic in scientific and engineering journals. A possible cause for this is the lack of standard mixture design methods for CLSM. Most guides present reference designs based on conventional concrete materials in terms of absolute contents of constituents per unit volume of mixture, and suggest

adjustments to these contents in order to attain required performance (e.g. to increase the content of cement to increase compressive strength). Application of non-standard materials, such as FRCA, to the production of CLSM is complicated by this trial and error approach. In order to evaluate the contribution of the FRCA and of the HCP residues within it to the performance of CLSM, and enable the development and optimization of FRCA-based materials, an improved method of mixture design would be required.

#### **1.3.4 Cementitious behavior after thermal treatment**

Concrete structures that have been exposed to high temperatures due to a fire have been observed to recover some of the lost strength when they are re-wetted. The strength recovery could not be explained only by the presence of unreacted cement grains within the hydrated paste. As concrete increases temperature during a fire, its mechanical properties deteriorate due to physical and chemical transformations taking place in the HCP and in the paste-aggregate interface (Annerel & Taerwe, 2009). Ultrasonic pulse velocity measurements show the rate of deterioration increases above 300 °C (Handoo, Agarwal, & Agarwal, 2002). Gradual dehydration of C-S-H and abrupt decomposition of CH result in a drastic loss of strength when concrete reaches a temperature of 500 °C.

All hydrated phases in the hardened cement paste undergo modifications at high temperatures. Between 70 – 100 °C ettringite dehydrates (Castellote, Alonso, Andrade, Turrillas, & Campo, 2004), and above 200 °C it is not possible to detect it using X-ray diffraction (XRD). However, upon rehydration of specimens the same analysis shows ettringite is reconstituted in its original quantity (Shui, Xuan, Wan, & Cao, 2008). Likewise, CH de-hydroxilizes between 400 – 500 °C, remaining as free lime in the hardened paste, which can either rehydrate again upon contact with water (forming new CH), or carbonate on contact with ambient CO<sub>2</sub> (forming calcium carbonate). Although recrystallization of CH does not contribute cementitious behavior to the thermally treated material, it can participate in hydration reactions of

SCM. As temperature continues to increase C-S-H gradually dehydrates and decomposes. Consequently, the amount of free lime is expected to continue increasing with temperature, thus increasing the pozzolanic activation capacity of the thermally treated material.

Above 200 °C the packing density of the C-S-H decreases as it gradually dehydrates, as measured by nano-indentation techniques (DeJong & Ulm, 2007). As a consequence of the shrinkage of dehydrating C-S-H, mechanical properties of the material gradually deteriorate. In nuclear magnetic resonance ( $^{29}\text{Si}$  MAS NMR) of hydrated Portland cement pastes, Alonso & Fernandez (2004) showed changes in the structure of C-S-H occur gradually as temperature increases and C-S-H silicate chains separate: at 450 °C silicates appear forming dimmers, i.e. the maximum number of oxygen bridges between silicates is 1 ( $\text{Q}^1$ ), whereas at 750 °C separation is complete and all silicates appear in monomers ( $\text{Q}^0$ ). According to Alonso & Fernandez, this transformation results in the formation of a new neso-silicate morphologically different from the original un-hydrated calcium silicates, with a less ordered crystalline structure, although similar to  $\beta\text{-C}_2\text{S}$ . On contact with water, this newly formed product hydrates to form new C-S-H, developing cementitious behavior.

Powdered materials developing cementitious behavior can be obtained by grinding and heating of HCP to high temperatures. Cube specimens of pastes of powdered hydrated materials previously heated to 500 °C at 0.4 w/c ratio were observed to develop compressive strengths of 8.2 and 8.3 MPa, at 7 and 28 days of hydration, respectively (Shui et al., 2008). These results show cementitious behavior can be obtained from the HCPs, reactivating them by dehydration at high temperatures. In the same study, crystalline phases found in the XRD analysis of original HCP are seen to disappear in the analysis of the dehydrated materials, being replaced by high temperature products, and then reappear in the analysis of the same materials after rehydration.

According to results later reported by Shui, Xuan, Chen, Yu, & Zhang (2009), the cementitious capacity of the dehydrated materials is affected by the maximum temperature reached during the heating process. In their study, dehydrated cements were obtained by grinding laboratory sourced HCPs (produced using ordinary Portland cement at 0.5 w/c, and cured for 30 days), and then heating the powdered materials to seven different temperatures ranging from 300 to 900 °C. Compressive strength of cubic specimens of dehydrated cement pastes mixed at 0.65 water to solids mass ratio (w/s) increased with dehydration temperature from 300 to 800 °C, and decreased from 800 to 900 °C. According to results reported in their paper, pastes produced with material heated to 800 °C achieved compressive strengths of ~14 and ~19 MPa at 7 and 28 days of hydration, respectively. It could be implied that the thermal de-polymerization of C-S-H observed by Alonso & Fernandez (2004) is a partially reversible process that imparts a cementitious behavior to the dehydrated materials and contributes to their strength gain. In a recent study, the use of dehydrated-cement as an activator for fly ash in a geopolymers-like cementitious material system was investigated (Shui, Yu, & Dong, 2011). A design method based on the theoretical ratio of calcium to silicon was proposed, and strengths exceeding 60 MPa were achieved for steam cured pastes at 24 hours.

The dehydration process required to produce Reactivated Cementitious Materials (RCM) involves temperatures much lower than those required to produce new Portland cement, making it an interesting alternative for on-site recycling of fines derived from coarse RCA production, or for recycling of cementitious materials from wash waters and rejected batches in concrete mixing plants. However, development of a recycling alternative based on the reactivation of the cementitious capacity of the HCP wastes would require consideration of the variable properties of the recovered materials, the multiple parameters of the reactivation process and the options for the composition of the recycled mixtures produced. Source material factors to be studied include the concentration of HCP in the wastes (i.e. the dilution effect of inert materials in the wastes), its composition (e.g. whether OPC or blended cement was used, or whether a SCM was added), its degree of hydration (i.e. amount of

unreacted cement), its carbonation level, and others. Likewise, process factors such as the grinding regime of the source materials, the reactivation temperature, and RCM mixture composition factors, such as the addition of different SCMs, the use of alkaline activators, intermixing of OPC, or the effect of admixtures need to be addressed. Finally, it would be necessary to determine if significant interactions affecting the cementitious capacity of the RCM exist between these factors.

An exploratory study of this wider set of factors and interactions would be required to estimate the practical limits of this alternative and to identify relevant routes to optimize it. Although it can be foreseen that practical application of HCP recycling in the near future would require extensive additional research, the answers to these initial questions would provide a comprehensive starting point for it.

## **1.4 Thesis objectives**

The main objective of this thesis is to gain fundamental understanding of the potential contribution of hydrated cement paste residues to the engineering properties of recycled construction materials based on fines from construction and demolition concrete wastes. It is hoped that this knowledge would contribute to the development of new viable recycling alternatives, and to the improvement of existing ones, ultimately leading to an increase in the fraction of concrete wastes that can be recycled.

### **1.4.1 General objectives**

Exploration of two alternatives for the recycling of fines from construction and demolition concrete, based on different degrees of processing of the wastes:

- I. Development of controlled low-strength materials based on fine recycled concrete aggregates obtained from the crushing of concrete wastes without additional processing (reported in chapter 2).

- II. Development of reactivated cementitious materials based on thermally treated hydrated cement paste wastes (reported in chapters 3 and 4).

#### **1.4.2 Specific objectives**

Specific objectives relate to each of the recycling alternatives explored. The main specific objectives related to the development of CLSM based on FRCA were:

- I.1 Explore the contribution of HCP residues to the performance of CLSM based on FRCA, providing evidence-based explanations for the observed behavior.
- I.2 Model the effect of mixture proportions on the relevant properties of the FRCA-based CLSM, in order to develop mixture designs that maximize the contribution of the recycled constituent to the performance of the end product.
- I.3 Develop a mixture design guide for FRCA-based CLSM for research and practical applications.

The main specific objectives related to the development of RCM from HCP wastes were:

- II.1 Identify material and process factors and factor interactions significantly affecting the cementitious capacity of the RCM produced from HCP wastes.
- II.2 Model the factor-response relationship of selected material and process factors and relevant properties of mixtures based on RCM, providing evidence-based explanations for the observed behavior.
- II.3 Determine if optimal combinations of factor levels exist that maximize the performance RCM and RCM-based mixtures.

## **1.5        Hypotheses**

According to the exploratory emphasis of the thesis objectives, specific hypotheses that can be effectively supported or rejected by experimental means were favored, as they can serve as a set of well-established starting points for future research on this topic. Particular hypotheses were proposed for each of the recycling alternatives explored, in order to explain, in the first case, the expected contribution of the HCP residues present in the fines to the performance of CLSM based on FRCA and fly ash, and in the second case, the effects that material and process factors involved in the production of RCM and RCM-based mixtures have on the properties of the end products (pastes and mortars). The general assumptions are: that new recycled materials can be developed that benefit from the residual HCP found in large amounts in the fines from construction and demolition concrete wastes, and that different levels of contribution, suitable for different applications, can be obtained from the fines at different degrees of processing.

### **1.5.1      Hypotheses for the contribution of recycled aggregates to the performance of controlled low-strength materials**

The following hypotheses were proposed to explain the expected contribution of the HCP residues present in the recycled aggregates to the performance of the CLSM mixtures based on FRCA and fly ash:

I.a *Soluble compounds in the HCP residues present in the FRCA provide alkali ions that participate in hydration reactions with compounds found in fly-ash*

I.b *Hydrated phases thus formed contribute to the setting and strength gain of mixtures based on fine recycled concrete aggregates and fly ash*

Consequently,

- Mixtures based on FRCA and fly-ash were expected to gain higher strengths compared to FVA-based mixtures, particularly at low OPC contents.

### **1.5.2 Hypotheses for the effects of material and process factors on the cementitious capacity of reactivated materials**

The following hypotheses were proposed to explain the effects that each of the nine material and process factors studied were expected to have on the strength of pastes based on the RCM obtained:

II.a *Main hydraulic compounds found in the RCM are formed at temperatures between 700 and 800 °C from the dehydration of the C-S-H present in the source material.*

Consequently,

- Cementitious capacity of the RCM was expected to increase as the concentration of C-S-H increases due to higher degree of hydration of the source material (factor X2 in chapter 3).
- Cementitious capacity of the RCM was expected to increase as the concentration of C-S-H in the source material increases due to pozzolanic reactions involving SCM added in its original composition (factor X7 in chapter 3).
- Cementitious capacity of the RCM was expected to decrease as the concentration of C-S-H in the source material decreases due to presence of inert fines derived from the crushed aggregates (factor X8 in chapter 3), or from crushed clay bricks (factor X9 in chapter 3).

II.b *Dehydration of HCP also results in significant latent hydraulic or non-hydraulic silicates (i.e. silicon oxide, calcium-silicates and alumino-silicates) in the RCM.*

Consequently,

- Addition of an alkaline activator solution to the RCM-based mixtures, as a partial replacement of mix water was expected to increase the

cementitious capacity of the RCM due to formation of geopolymers-like macromolecules (factor X3 in chapter 3).

- II.c *Grinding of HCP exposes unreacted phases present in it (i.e. OPC or SCM) making them available for reactions during rehydration of RCMs.*

Consequently,

- Cementitious capacity of the RCM was expected to increase with increasing grinding of the HCP wastes, particularly for HCP having lower degree of hydration and HCP incorporating SCM (factor X1, and interactions X1·X2 and X1·X7 in chapter 3).

- II.d *Significant amounts of CH, formed by hydration of the free lime found in the RCM as a consequence of the decomposition of hydration products, are available to participate in pozzolanic reactions with SCM added to the RCM-based mixtures.*

Consequently,

- The strength developed by the RCM-based mixtures was expected to increase with the addition of SCM to the mixtures as a partial replacement of RCM (factor X6 in chapter 3).

### **1.5.3 Hypotheses for reactivation temperature and replacement level effects on the properties of reactivated material mortars**

The following hypotheses are proposed to explain the effects that the factors selected in the first stage of the reactivated cementitious material study (i.e. the reactivation temperature and the level of replacement of RCM by SCM in the new mixture) were expected to have on the performance of mortars based on the RCM obtained:

II.e *The relative concentration of hydraulic compounds in the RCM evolve as the maximum reactivation temperature changes, increasing and decreasing at different rates in the range between 660 and 940 °C.*

Consequently,

- The effect of reactivation temperature on the properties of the RCM was expected to be non-linear. Therefore, mortars achieving optimal response values were expected when using RCM produced at a specific –i.e. optimal– temperature.
- The contribution of partial replacement of RCM by SCM to the properties of the mortars was expected to depend on the reactivation temperature used to produce the RCM (i.e. display a significant interaction effect).

II.f *Contribution of SCM to the properties of the RCM-based mortars is due to pozzolanic reactions involving amorphous compounds found in the SCM and calcium ions provided by soluble phases found in large amounts in the RCM.*

Consequently,

- The contribution of partial replacement of RCM by SCM to the properties of the mortars was expected to be non-linear, reaching optimal values at specific replacement levels.
- The general contribution and the specific replacement levels at which optimal values for the properties of the mortars are achieved were expected to depend on the type of SCM used.

## **1.6        Outline of methodology**

The study of new alternatives for the recycling of fines from construction and demolition concrete wastes demands an exploratory approach to be accounted for in the research

methodology. Although experimental programs were purposely designed to meet the specific objectives of the thesis for each of the alternatives studied, -i.e. to answer the initial set of questions-, they also sought to provide opportunities to observe new or unexpected phenomena that could be the subject of future research on this topic. Detailed descriptions of the experimental program developed for the study of FRCA-based CLSM can be found in chapter 2, whereas, experimental programs developed for the study of RCM produced from HCP wastes can be found in chapters 3 and 4.

In the case of the RCM study, research was divided in two stages: an initial single-response multifactor experimental program oriented at the identification of material and process factors significantly affecting the cementitious capacity of the RCM, which could be followed by additional multi-response multilevel experimental programs oriented at the in-depth study of factors selected in the first stage. The work reported in chapter 3 corresponds to the first stage of the research, whereas the work reported in chapter 4 corresponds to a second stage study of two factors identified in stage one as having a large potential for RCM optimization. Chapter 4 is thus presented as a model for the study of additional factors.

A Design of Experiments (DOE) approach was used throughout the thesis in order to optimize experimental resources available, minimizing the number of experimental runs required to estimate statistical models for the factor-response relationships under study. Development of response surface models describing the combined effect of three mixture proportions on the properties of CLSM was based on a central composite experimental design. Second order response models obtained for materials based on fine virgin aggregate and on FRCA were compared in order to characterize the contribution of FRCA to the performance of CLSM. The estimation linear effects and linear by linear interaction effects of nine material and process factors on the cementitious capacity of the RCM was based on a fractional factorial design in two levels. Center point experimental runs were added to the design in order to estimate the variance and check for non-linearity of the response. Finally, in the second stage of the RCM study a central composite design was used to obtain second-order response surface models describing the effect of two selected

factors on relevant properties of RCM-based mortars. Assessment of significance of estimated coefficients was based on analysis of variance with a 95 % confidence interval (except in cases explicitly stated otherwise). Accordingly, models considered in the discussion of results were based exclusively on factor and factor interaction effects exceeding the 5 % significance level.

Additional experiments were carried out in order to extend the experimental region explored in directions that complement or help explain the results of the main experiments. These generally consisted of series of experimental runs where a single factor is adjusted beyond the levels explored in the main experiment. In addition, source materials and end products were characterized using a variety of experimental techniques, including sieving, pH measurements, thermo-gravimetric analysis, powder X-ray diffraction analysis (XRD) and scanning electron microscopy (SEM) imaging.

## **1.7        Synopsis of experimental results**

Significant findings from the exploration of the two recycling alternatives selected are presented in brief in the following subsections. Detailed discussion of experimental results, and of the models derived from them, can be found in chapters 2, 3 and 4.

### **1.7.1      Performance of controlled low-strength materials based on fine recycled concrete aggregates and fly ash**

CLSM mixtures studied were established using three relative proportions that can be adjusted independently from each other: the volumetric paste percent (VPP) of the mixture, i.e. the percent ratio of paste volume to total volume of the mixture; the water to cementitious material mass ratio of the paste (W/CM), i.e. the ratio of water mass to the mass of solids in the paste; and the Portland cement to total cementitious materials mass ratio of the paste (OPC/CM), i.e. the ratio of Portland cement mass to total mass of solids in the paste. Response models were obtained for the effects of these proportions and their interactions on the flowability, subsidence and 28-day

compressive strength of CLSM mixtures based on different combinations of constituents. The contribution of specific constituents (e.g. FRCA) to CLSM performance was evaluated by comparing the models obtained for different constituent combinations.

Fresh properties of FRCA-based CLSM:

Average flowability results were lower for FRCA-based CLSM mixtures compared to fine virgin aggregate (FVA) based mixtures. According to the response models, in the experimental region explored, the VPP is the mixture proportion having the largest effect on flowability. However, flowability of FRCA-based CLSM is less affected by changes to the VPP of the mixture, and therefore minimum flowability requirements can be achieved at lower paste contents when using FRCA. Although increasing W/CM ratio increases flowability, its effect is much lower than that of the VPP, and higher segregation was observed at higher W/CM ratios. Nevertheless, these observations also showed that FRCA-based mixtures were less affected by segregation, even at the highest W/CM ratios explored. According to the models, increasing OPC/CM ratio increases flowability of the FRCA-based mixtures only. In additional experimental cases, mixtures of FRCA and fly ash without Portland cement achieved the lowest flowability, and in the case of very reactive fly ash exhibited false set behavior. Average subsidence was much lower for FRCA-based mixtures. According to the response models derived for all constituent combinations studied, in the experimental region explored subsidence increases if any of the mixture proportions is increased. However, the estimated effects are higher for FVA-based mixtures, showing FRCA-based CLSM has improved resistance to subsidence.

Lower flowability and higher resistance to segregation and subsidence observed for FRCA-mixtures are due to the higher fines content in the FRCA gradation and the lower density and higher angularity of its particles increasing cohesiveness of the paste fraction. In addition, the higher cohesiveness decreases the effect of VPP on flowability. However, this is partly compensated by the additional fines increasing the effective VPP of the FRCA-based mixtures.

The higher resistance to subsidence and the estimated effect of OPC/CM ratio on flowability support the hypothesis that soluble compounds in the HCP participate in hydration reactions, since both phenomena can be linked to the formation of ettringite from compounds in the fly ash and ions provided by the HCP residues present in the FRCA (**Figure 1.5**). At the pH levels measured in fresh FRCA mixtures (~11.5), ettringite crystals of maximum length to thickness ratio are known to form, which affects the flow characteristics of the mixture and can lead to false set behavior. When the OPC/CM ratio of the mixture is increased, the rate of ettringite formation decreases and due to increased pH crystals of lower length to thickness ratio form.

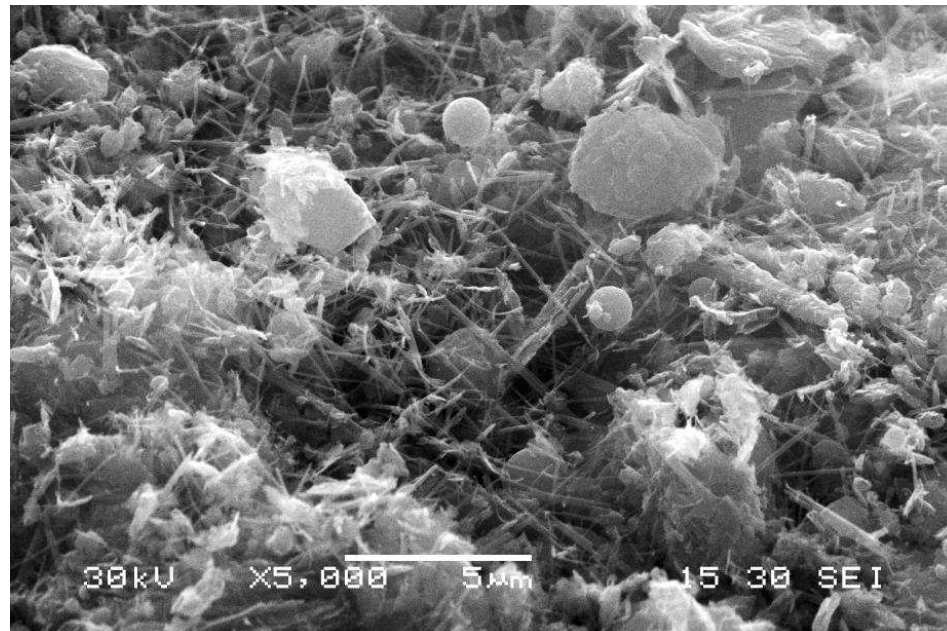


**Figure 1.5** Ettringite needles bridging fly ash particles in FRCA-based CLSM (fracture surface, SEM secondary electron image).

Compressive strength of FRCA-based CLSM:

According to the response models derived for all constituent combinations studied, in the experimental region explored, only the W/CM and OPC/CM ratios affect strength, with both factors displaying significant non-linearity and mutual dependence (interaction). For a given type of fly ash, FRCA-based mixtures achieved lower average compressive strengths compared to FVA-based mixtures. However, at the lower end of OPC/CM and W/CM ratios explored, FRCA-based mixtures achieved slightly higher compressive strengths compared to FVA-based mixtures. The additional strength in this region could be linked to the formation of hydration products (e.g. ettringite), partially supporting the hypothesis that reactions involving compounds in fly ash and ions released into solution from the HCP contribute to setting and strength gain of mixtures. At higher OPC/CM ratios no significant contribution to strength from pozzolanic reactions involving fly ash and CH from HCP residues could be detected in the 28 day hydration period observed. In agreement with results reported by Achtemichuk et al. (2009), in short hydration periods the strength gain of FRCA-based CLSM appears to be controlled by the reactivity of the SCM used. In additional experimental cases, the strength of FRCA-based mixtures at low OPC/CM ratios was observed to be highly dependent on the fly ash source used. However, at higher OPC/CM ratios the compressive strength appears to be limited by the characteristics of the recycled aggregate. The combined effect of W/CM and OPC/CM on the strength response surfaces is shown in figures in **Appendix A**, for all constituent combinations tested. In the experimental region explored with the central composite experiment, higher compressive strengths were observed for FRCA-based CLSM incorporating a highly reactive source of class C fly ash.

Guidelines for CLSM mixture design:

Comparison of response models showed mixture proportions have similar general effects on properties of CLSM across different combinations of constituents. General guidelines for mixture design of CLSM based on fine aggregate, cement and fly ash

were proposed based on this correspondence of effects. The VPP is recommended to control the flowability of the mixture with minimum impact on strength. Conversely, the W/CM ratio is not recommended for this purpose because of its detrimental effect on segregation, subsidence and strength. Consequently, the W/CM ratio must be kept at the lower value achieving flowability requirements. Finally, for a given W/CM ratio strength can be controlled adjusting the OPC/CM ratio. These recommendations allow achieving required performance at reduced OPC contents.

### **1.7.2 Materials and process factors significantly affecting the cementitious capacity of reactivated materials**

Reactivated materials have significant cementitious capacity as indicated by the strength gain of RCM pastes. Higher compressive strengths were 20.0 ( $\pm 1.4$ ), 32.8 ( $\pm 2.0$ ), and 39.0 ( $\pm 2.5$ ) MPa at 7, 28, and 90 days of hydration, respectively. These maximum values were observed at different combinations of factor levels, indicating effect of material and process factors evolve over time. Largest differences were observed between factor effects estimated from 7 and 28 day results.

Average strength of central cases, i.e. those performed with all factors set at their medium level, was significantly higher than the average strength of the rest of the cases in the experiment. This indicates significant non-linearity of the response in the experimental region explored, due to the non-linear effect of one or more factors. Identification of factor(s) causing the non-linearity is not possible due to the limitations of the experimental design, which is optimized for linear regression of results. Factors and interactions having largest effect on compressive strength of RCM pastes at 7 and 28 days are shown in **Figures 1.6 and 1.7**, respectively.

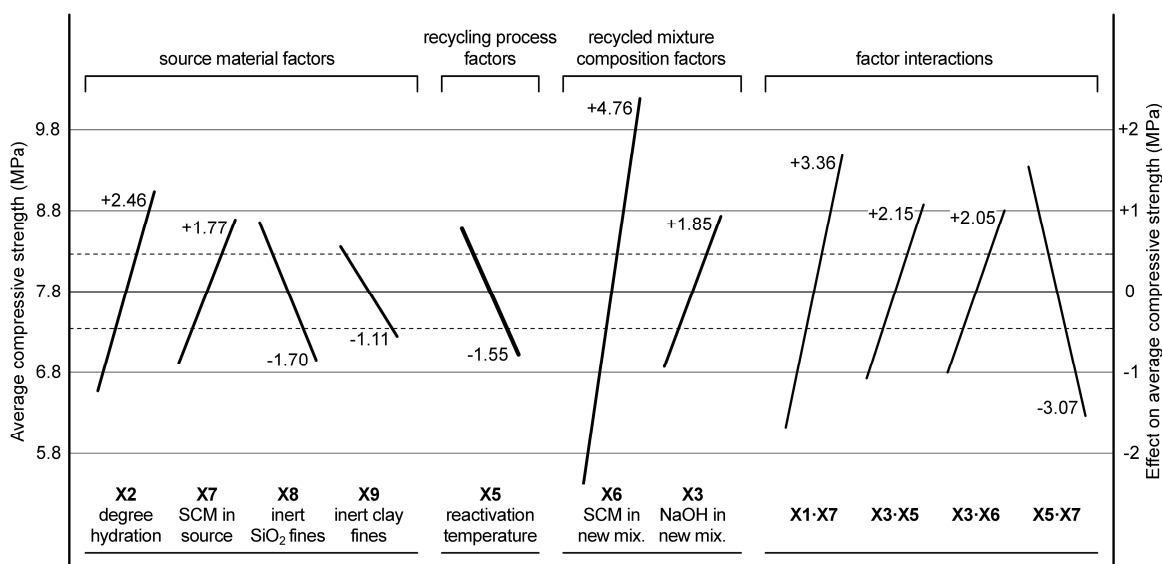


**Figure 1.6** Effects of material and process factors and factor interactions on 7-day compressive strength of RCM pastes (central horizontal line is the average response of all cases, and dashed lines indicate 95% confidence interval for effects).

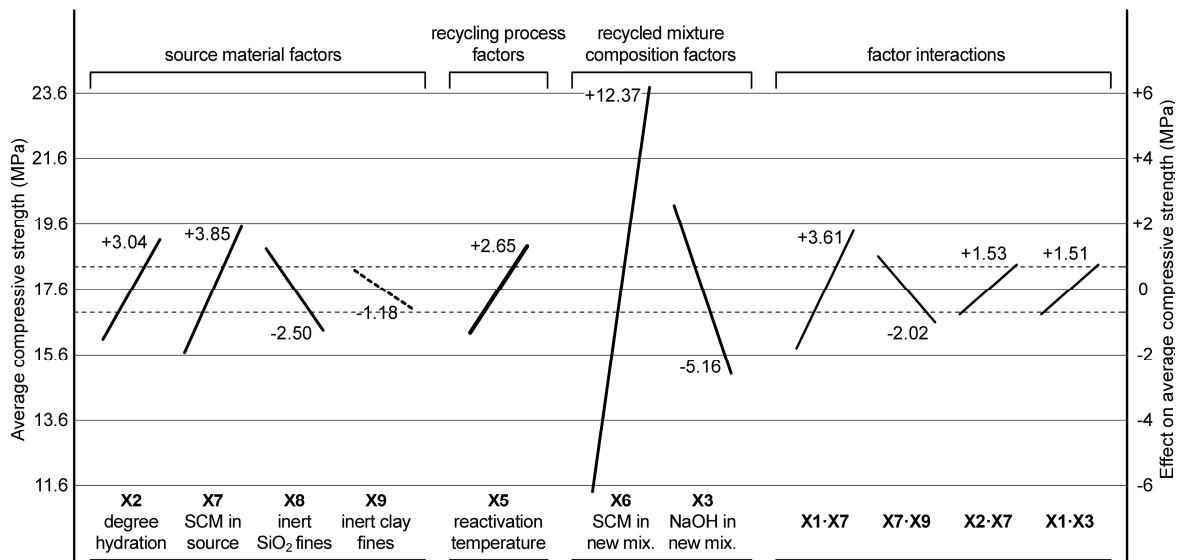


**Figure 1.7** Effects of material and process factors and factor interactions on 28-day compressive strength of RCM pastes (central horizontal line is the average response of all cases, and dashed lines indicate 95% confidence interval for effects).

Source material factors:

In the experimental region explored, increasing the W/CM ratio of the source material (i.e. increasing its degree of hydration) increases strength of RCM pastes at all ages tested. Likewise, increasing the level of silica fume added to the source material increases compressive strength of RCM pastes at all ages tested. Conversely, increasing the level of inert siliceous fines added to the source material decreases strength of RCM pastes at all ages tested. These results support the hypothesis that hydraulic phases in the RCM are formed by chemical transformation of C-S-H present in the source material occurring during the thermal reactivation. Higher degree of hydration and higher addition of silica fume to the source paste increase the concentration of C-S-H in the source material, whereas addition of inert fines reduces it.

Although a reduced concentration of C-S-H can also be expected from the addition of inert fines from clay bricks to the source material, additional aluminates and silicates present in the clay were expected to react with calcium compounds in the source material during reactivation, increasing strength of RCM pastes. According to the regression analysis, increasing the level of inert clay fines added decreases 7-day strength of RCM pastes but has no significant effect on 28 and 90-day strength. A possible contribution of clay fines to the formation of hydraulic compounds in the RCM during the reactivation process may not be discarded at this point.

Reactivation process factors:

According to regression analysis, the different processes used to grind the source material to different fineness have no significant effect on the strength of the RCM pastes. However, this factor was involved in several significant interactions with other factors. According to the largest of these, strength of RCM pastes significantly increases when both the fineness and the level of silica fume addition to the source material are at a high level. This interaction is probably caused by unreacted silica fume in the source material becoming available for reactions during RCM hydration

as it is exposed during the grinding process. Likewise, according to another interaction involving this factor, strength of RCM pastes increases when source pastes having lower degrees of hydration are grinded to higher fineness. The lack of significant main effect for the fineness might be due to RCM achieving large specific surface during dehydration regardless of the specific surface of source material.

Whereas increasing the reactivation temperature, from 700 to 800 °C, decreases 7-day compressive strength of RCM pastes, the effect reverts over time, significantly increasing 28 and 90-day compressive strength in agreement with results reported by Shui et al. (2009). In addition, the estimated effect decreases when silica fume is present in the source materials. At a higher temperature the rate of crystallization of amorphous silica is expected to increase. This probably results in a larger fraction of the original silica fume becoming an inert phase, thus, diluting reactive compounds in the RCM.

Recycled material factors (due to composition of RCM pastes):

Partial substitution of reactivated material by silica fume in the RCM pastes was the factor having the largest effect on their compressive strength. In the experimental region explored, increasing the level of substitution increases strength of RCM pastes at all ages tested, supporting the hypothesis that RCM have a significant capacity for participating in pozzolanic reactions due to the significant amount of CH formed from hydration of the CaO present in the reactivated material. On the other hand, the effect of NaOH addition to the RCM pastes evolved over time, increasing 7-day strength but decreasing 28 and 90-day strength. Similar behavior has been reported for the effects of high alkalinity on strength of Portland cement pastes (Juenger & Jennings, 2001), which suggests hydraulic compounds present in RCM might react and develop strength in a similar way as compounds in Portland cement. This contradicts the hypothesis that latent hydraulic products are present in the RCM which would hydrate in the presence of externally supplied alkalis.

### **1.7.3 Properties of mortars based on reactivated cementitious materials and supplementary cementitious materials**

According to the results of the first stage, the substitution level of SCM in the RCM-based mixtures, and the reactivation temperature used to produce the RCM, were selected for the second stage of the study because of the large positive effect on compressive strength of the former, and the potential interactions between both factors that could arise from the different compositions of the RCM obtained at different temperatures. Although results from this second stage indicate both factors significantly affect the flowability, compressive strength and expansion of RCM mortars, interaction effects were not detected at the 5 % significance level.

#### Effect of substitution level of SCM

Effects of SCM on the properties of the RCM mortars depend on the type of SCM used. The central composite experiment was performed using silica fume. Additional experiments were performed using either silica fume or a local source of class F fly ash. According to the response model, flowability of RCM mortars decreases when the silica fume substitution level increases. Conversely, in additional experiments flowability was observed to increase as the fly ash substitution level increased. Likewise, whereas the response model shows 28-day compressive strength of RCM mortars increases as the silica fume substitution level increases, additional experiments show increasing fly ash substitution level decreases strength. Higher strengths were observed for mortars based on RCM produced at 800 °C at a 40% silica fume replacement level (25.8 MPa). In the range of substitution levels explored in the composite experiment, increasing the silica fume substitution level increases expansion of RCM mortars. Finally, it was observed that increasing the substitution level decreased the heat evolved by the RCM-based mixtures in the first minutes regardless of SCM type used, due to the dilution effect.

### Reactivation temperature:

Effects of reactivation temperature on all mortar properties tested display significant non-linearity. According to the response models, for RCM produced at reactivation temperatures in the range from 660 – 800 °C, increasing reactivation temperature decreases flowability, increases 28-day compressive strength, and has no net effect on expansion. Conversely, in the range from 800 – 940 °C, increasing reactivation temperature increases flowability, decreases compressive strength and significantly increases expansion. These results support the hypothesis that relative concentration of hydraulic compounds in the RCM depends on the maximum reactivation temperature used. Estimated effects of reactivation temperature correlate with the relative abundances of reactive phases identified in XRD analysis of the RCM produced: free lime,  $\beta$ -C<sub>2</sub>S and a stabilized form of  $\alpha'$ -C<sub>2</sub>S. Free lime content in the RCM is seen to increase with increasing dehydration temperature, and at a higher rate in materials produced at temperatures above 800 °C. Accordingly, higher expansion behavior of RCM mortars can be explained by delayed hydration of free lime in the set mixtures. The relative abundance of free lime also agrees with initial heat evolved by RCM mixtures, which increases with increasing reactivation temperature. According to the XRD analysis, the relative concentration of  $\alpha'$ -C<sub>2</sub>S in the RCM increases as reactivation temperature is increased in the range from 660 – 800 °C. However, in the range from 800 – 940 °C,  $\alpha'$ -C<sub>2</sub>S decreases while  $\beta$ -C<sub>2</sub>S increases. Apparently, a larger fraction of the high temperature polymorph reverts to the less reactive  $\beta$ -C<sub>2</sub>S on cooling when the RCM is produced at temperatures above 800 °C. Consequently, strength developed by RCM-based mixtures can be explained by the concentration of  $\alpha'$ -C<sub>2</sub>S in the reactivated material.

## **1.8 General conclusions**

Valuable recycled construction materials based on fines from construction and demolition concrete wastes can be developed so that hydrated cement paste (HCP) residues present in the fines contribute to their engineering properties. The affected properties and extent of

contribution depends mostly on the degree of processing of the fines and the mixture design of the recycled construction material.

At the lowest degree of processing, the fines can be used as fine recycled concrete aggregate (FRCA) for the production of special purpose products such as controlled low-strength materials (CLSM). Overall, FRCA positively contribute to the fresh and hardened properties of CLSM based on fine aggregate, cement and fly ash. At low Portland cement contents, hydration products formed in reactions involving fly ash and soluble ions released from the HCP residues in the recycled aggregate contribute to the compressive strength of FRCA-based CLSM, outperforming materials based on fine virgin aggregates. Early hydration products formed (e.g. ettringite) also contribute higher resistance to subsidence to the material after placement. On the other hand, lower particle density and higher fines content in the gradation of the recycled fines contribute higher cohesiveness and enhanced resistance to segregation to the mixtures. The reduction in flowability associated with the higher cohesiveness is partly compensated by the increase in the effective volumetric percent of paste in the mixture. FRCA-based mixtures incorporating class C fly ash achieve minimum flowability requirements at lower W/CM ratios, thus reducing the content of Portland cement required to achieve prescribed strengths.

However, reactions involving fly ash and soluble ions from the HCP residues can also have a detrimental effect on flowability of CLSM. FRCA-based mixtures incorporating highly reactive fly ashes can exhibit false set behavior at low Portland cement contents. Consequently, fresh and hardened properties of FRCA-based CLSM are highly sensitive to the characteristics of the SCM used.

At a higher degree of processing, materials having cementitious behavior can be obtained from the HCP residues present in the fines by heating them to 800 °C. The reactivated cementitious materials (RCM) obtained by grinding and heating of HCPs have significant cementitious capacity as indicated by the strength gain of recycled pastes and mortars made with them. Hydraulic compounds found in the RCM are formed as C-S-H present in the HCP dehydrates during the reactivation process. Consequently, composition and

degree of hydration of the HCP affects the cementitious capacity of the RCM. The type and concentration of hydraulic compounds in the RCM depend on the maximum temperature reached during the reactivation process. Early strength developed by the RCM pastes is due to hydration of  $\alpha'$ -C<sub>2</sub>S, a high temperature polymorph of C<sub>2</sub>S. The concentration of this polymorph in the RCM at room temperature increases as the reactivation temperature used to produce it is increased, reaching a maximum value for materials produced at 800 °C. Concentration of  $\alpha'$ -C<sub>2</sub>S in the RCM drops as reactivation temperature is further increased.

Likewise, concentration of free lime in the RCM increases with reactivation temperature, particularly above 800 °C. Hydration of free lime temporarily reduces the flowability of mixtures and is a highly exothermic process that increases evaporation of mix water. Consequently, RCM-based mixtures require higher W/CM ratios to achieve a prescribed flowability. In addition, mortars based on RCM produced above 800 °C exhibit larger expansion due to delayed hydration of free lime. Nevertheless, calcium hydroxide formed from hydration of free lime can have a positive effect on strength of RCM-based mixtures due to pozzolanic reactions involving SCM. However, up to 28 days of hydration, the contribution of the pozzolanic reactions is largely dependent on the characteristics of the SCM used. Overall, SCM additions affects the fresh and hardened properties of RCM-based mixtures in a similar way as they affect Portland cement based mixtures, suggesting that besides the high content of free lime RCM performs as a conventional cement.

## **1.9 Additional research prospects**

Short term application of knowledge gathered in this thesis can be anticipated in the production of CLSM based on FRCA and fly ash. The proposed guideline for CLSM mixture design included in the manuscript submitted to publication is expected to contribute in this regard. Although FRCA sourced from different crushing plants would certainly deviate from the behavior observed in the reported work, proposed adjustments should be appropriate to compensate for much of the variability. Nevertheless, the

proposed method is oriented at effective adjustment of trial batches to required performance, but has no predictive power over the outcome of the initial mixtures. Knowledge of the basic set of characteristics of the FRCA that affect the properties of the mixtures would allow for specific aggregate tests results to be incorporated in a predictive mixture design method.

Practical application of RCM would require more additional research. Knowledge of the actual mechanism allowing  $\alpha'$ -C<sub>2</sub>S to remain stable on cool down to room temperature is required to allow control over its concentration and thus, optimization of strength gain of RCM-based mixtures. In the same line, as reactivation temperature and RCM substitution level can be ruled out, the cause of the large non-linearity of the strength response observed in the first stage of the study remains to be determined. Although the concentration of free lime and CH in the RCM implies a significant capacity to activate pozzolanic reactions, additional research is required in order to investigate the long term mechanical properties of the RCM-based mixtures incorporating less reactive SCM (e.g. class C and F fly ash). Careful examination of heat evolved during initial hydration of RCM is required to develop methods to control the temperature raise of the mixtures. Knowledge of the effect of chemical admixtures on the properties of RCM-based mixtures would be particularly important, e.g. to achieve flowability requirements despite the high water demand of the materials. Determination of energy requirements of the reactivation process would be particularly important to guide future research decisions. Finally, the knowledge acquired studying RCM produced from synthetically sourced pastes would have to be validated using actual fines from concrete wastes as the raw material.

## **2. RELATIVE PROPORTIONING METHOD FOR CONTROLLED LOW-STRENGTH MATERIALS**

Ricardo Serpell, Jacob Henschen, Jeffery Roesler, David Lange

Submitted, May 2013: *ACI Materials Journal*

### **Abstract**

Controlled low-strength material (CLSM) mixture design remains a trial and error process. A new approach using relative proportioning of the constituent materials instead of prescribed mass contents is proposed. Relative proportions allow for independent adjustments that enable unbiased estimation of their effects on CLSM properties. For the CLSM mixtures studied, a central composite experimental design was defined using three relative proportions: volumetric paste percentage (VPP), water to cementitious material ratio (W/CM) and Portland cement to total cementitious materials ratio (OPC/CM). Second order response models for slump-flow, subsidence, and 28-day compressive strength were obtained for different sets of constituents including virgin and recycled concrete fine aggregates and two fly ash sources. Slump-flow and subsidence were most affected by the VPP and W/CM ratio respectively, whereas strength was explained by the combined effect of the W/CM and OPC/CM ratios. The W/OPC ratio was not a reliable predictor of CLSM strength.

**Keywords:** Controlled low-strength material (CLSM); flowable fill; mixture design; fine recycled concrete aggregates; experimental design.

## **2.1      Introduction**

Controlled low-strength material (CLSM) is a highly flowable, self-compacting, cementitious material used in many applications including as an alternative to compacted fill. Although its constituents are similar to those in concrete, CLSM does not need to meet the same performance requirements as concrete. CLSM is prescribed with a maximum strength, not to exceed 8.3 MPa (1200 psi), as defined by ACI 229, with most applications requiring less than 2.1 MPa (300 psi) to allow for future excavation (ACI Committee 229, 2013). As a result, CLSM can be a valuable application for non-standard materials, such as industrial and by-product wastes, which are normally rejected for conventional concrete because of their negative impact on hardened properties. With the growing emphasis on sustainability, CLSM can also be a suitable solution for construction and demolition solid wastes. The underlying motivation for this work was the development of CLSM containing fine recycled concrete aggregates (FRCA). The crushing process of demolition concrete can produce as much as 50% (by weight) of aggregates sizes less than 4.75mm (3/16’’), which have a higher proportion of residual cement paste. The residual paste alters the engineering properties of FRCA (Sanchez de Juan & Alaejos Gutiérrez, 2009) and adversely affects the fresh and hardened properties of concretes made with them (Kenai et al., 2002; Khatib, 2005; Shayan & Xu, 2003).

ACI 229 places few restrictions on constituents for CLSM except to avoid materials that swell, most organic materials, and environmentally harmful materials. Nevertheless, non-standard materials should be characterized along with trial batching to assess the material's effect on CLSM performance indicators. Traditionally, a new CLSM mixture design is achieved empirically by adjusting previous mixture proportions until the desired CLSM performance requirements are met. However, these reference mixtures and recommendations to adjust their performance, such as those provided in ACI 229, come primarily from experiences based on already approved concrete constituents. Non-standard materials may affect mixture properties in less predictable ways which renders the recommended adjustments less effective and thus increases the number of trial batches required (Alizadeh, Helwany, Ghorbanpoor, & Sobolev, 2014; Bhat & Lovell, 1997).

Consequently, the classic trial and error mixture approach is inefficient for proportioning CLSM based on non-standard materials and may not result in an optimal mixture design.

Several studies have systematically evaluated the performance of CLSM incorporating different industrial wastes and by-product materials as major constituents of the mixture (Du & Folliard, 2002; Hanson, Stone, & Yesiller, 2012; Katz & Kovler, 2004; Lachemi, Sahmaran, Hossain, Lotfy, & Shehata, 2010; Naganathan, Razak, & Hamid, 2012; Tarun R Naik et al., 2006; Nataraja & Nalanda, 2008; Pierce, Tripathi, & Brown, 2003; Taha, Alnuaimi, Al-Jabri, & Al-Harthy, 2007; Tikalsky, Gaffney, & Regan, 2000). Generally, these studies have compared the impact of alternative constituents on the performance of CLSM, either adjusting the content of a non-standard constituent in the mixture or using it to partially or totally replace a conventional constituent. However, since the contents of constituents in a mixture are interrelated they cannot be adjusted independently without affecting the mixture proportions, e.g., adding water to achieve a minimum slump-flow requirement affects several mixture proportions. Even when the contents are fixed, constituent weight replacement affects mixture proportions due to differences in the constituents' specific gravities. As a consequence, much of the CLSM performance observed in these studies is a coupled result of specific constituent's characteristics and changing mixture proportions. Although this approach can be satisfactory for developing a single CLSM mixture design for a particular project, it compromises unbiased interpretation of results within each study, and impairs comparison of results between studies since it negates the independence of the variables.

In order to achieve CLSM performance requirements without an extensive trial and error approach, mixture designs need to be established using a set of independent parameters. The proposed approach establishes CLSM mixture compositions through a set of relative proportions between constituents which can be adjusted independently of each other. As independent factors, these relative proportions can be studied using experimental design to estimate their main and interaction effects on the relevant CLSM responses (e.g., slump-flow, subsidence, or strength).

In this study, the proposed methodology was used to evaluate CLSM mixtures with either FRCA or fine virgin aggregates (FVA) and two sources of Class C fly ash. The CLSM mixtures studied were composed of four constituents: fine aggregate, cement, supplementary cementitious material (SCM) and water. Mixture compositions were established using three independent relative proportions (**Figure 2.1**): the volumetric paste percent (VPP), which corresponds to the volume of the paste (water, cement and SCM) compared to the total volume of the mixture, the mass ratio of water to cementitious materials (W/CM), and the mass ratio of the Portland cement to cementitious materials (OPC/CM). In the proposed approach, these relative proportions are the only independent variables adjusted to achieve the desired CLSM performance. All other characteristics of the mixture and of the constituent materials are considered either as dependent variables (e.g. density, entrapped air), or fixed variables (e.g. aggregate type and gradation, type of cement and fly ash, etc.). A central composite experimental design was selected to estimate the main and interaction effects of the mixture proportions on the CLSM performance, since this type of experimental design allows for a second order regression model to approximate the response surface.

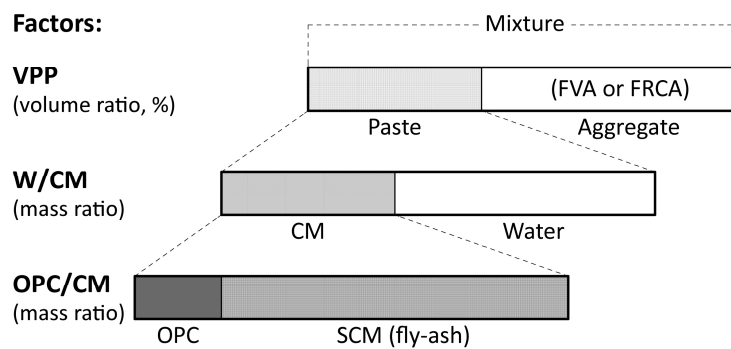


**Figure 2.1** Relative proportions selected to establish mixture compositions.

## **2.2 Research significance**

The purpose of this study was to efficiently attain the desired CLSM properties through an improved method for mixture design and optimization. When mixture compositions are established using independent parameters, such as the relative proportions between constituents, the relationship between mixture parameters and CLSM properties (e.g. slump-flow, subsidence, strength) can be experimentally determined. Response models derived for a specific set of constituents can be used to set initial mixture proportions and predict adjustments required to achieve specific CLSM performance objectives. In addition, models obtained from different sets of constituents can be used to evaluate the contribution of specific constituents to CLSM properties.

## **2.3 Experimental procedure**

### **2.3.1 Experimental design**

In order to model the factor-response relationship, a central composite experimental design for three factors of the Box-Wilson type (Box & Wilson, 1951) was selected. This second-order design, shown in **Figure 2.2**, is based on a full factorial design in two levels, augmented with six axial points, outside the range covered by the factorial points, and a central point at the average level of the factors. The factorial points of the design allow estimation of the linear effects of the independent factors, while the central and axial points allow derivation of second-order regression models for the factor-responses relationships. The central point is replicated to estimate the experimental variance of the responses in order to provide a statistic for identification of significance. Along each factor axis, the level of the factor at the axial points is chosen to be  $(n_f)^{1/4}$  times the level at the factorial points (with  $n_f$  = number of factorial points in the design). In this way, a rotatable design is obtained, i.e. one in which the variance of the estimated response depends only on the distance from the center of the design (Box & Hunter, 1957). This is a desirable characteristic

for a second order design when the trends of the responses are not known in advance. The experimental levels of factors (**Table 2.1**) were mapped to their coded levels in the design covering most of the experimental region encompassed in CLSM literature (Du & Folliard, 2002; Hanson et al., 2012; Katz & Kovler, 2004; Lachemi et al., 2010; Naganathan et al., 2012; Tarun R Naik et al., 2006; Nataraja & Nalanda, 2008; Pierce et al., 2003; Taha et al., 2007; Tikalsky et al., 2000).

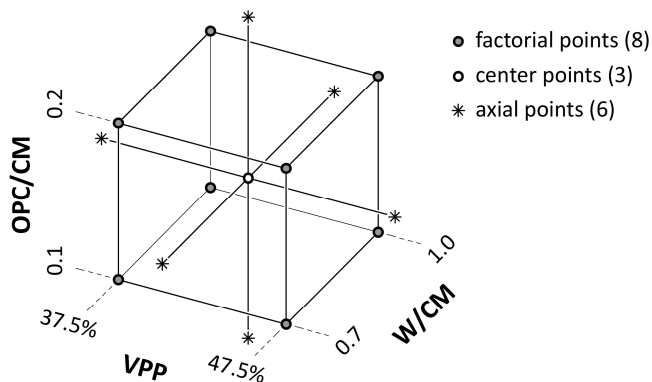


**Figure 2.2** Graphical representation of the central composite experimental design, showing the experimental levels chosen for the factorial points (cube vertices).

**Table 2.1** Experimental and coded levels of factors

Coded Factors (CLSM mixture proportions)			
	1: W/CM Water to Cementitious Materials ratio	2: VPP Volumetric Paste Percent	3: OPC/CM Portland to Cementitious Materials ratio
Coded levels	(w/w)	(v/v * 100)	(w/w)
-1.682	0.51	34.1%	0.07
-1	0.65	37.5%	0.10
0	0.85	42.5%	0.15
1	1.05	47.5%	0.20
1.682	1.19	50.9%	0.23

The measured responses representing the basic performance indicators of CLSM mixtures from fresh to hardened state were the ability to flow (slump-flow), subsidence, and unconfined compressive strength. Response models were developed independently for three alternative sets of constituents, replicating the experimental design at the same factor levels for each set. Additional experimental cases were performed to explore CLSM performance at mixture proportions outside the experimental region covered by the central composite design. Experimental levels of factors for these cases (**Table 2.2**) were seven mixtures at OPC/CM ratios ranging from 0.0 to 1.0 (i.e. 100% SCM to 100% OPC at fixed 40% VPP and 0.8 W/CM ratio) and five mixtures at combinations of W/CM and OPC/CM ratios resulting in a fixed water to Portland cement ratio (W/OPC) of 2.0 for a 40% fixed VPP. These additional cases were also replicated for two sets of constituents.

**Table 2.2** Experimental levels of additional cases

Case	AR1	AR2	AR3	AR4	AR5	AR6	AR7
VPP	40%	40%	40%	40%	40%	40%	40%
W/CM	0.8	0.8	0.8	0.8	0.8	0.8	0.8
OPC/CM	0.0	0.1	0.2	0.4	0.6	0.8	1.0

Case	AR10	AR11	AR12	AR13	AR14
VPP	40%	40%	40%	40%	40%
W/CM	0.4	0.6	0.8	1.0	1.2
OPC/CM	0.2	0.3	0.4	0.5	0.6
W/OPC	2.0	2.0	2.0	2.0	2.0

### 2.3.2 Materials

Physical properties of constituents are shown in **Table 2.3**. The FVA was natural river sand while the FRCA was obtained from fractionating crushed concrete at the Chicago O’Hare International Airport. A comparison of both fine aggregate gradations relative to ASTM C33 limits is shown in **Figure 2.3**. Ordinary Portland cement (OPC) conforming to ASTM C150 Type I was used for all mixtures. The following two fly ash sources, shown in **Table 2.4**, were utilized: a conventional

Class C (FA1) and a fly ash conforming to Class C but not recommended by the producer for use in concrete due to its rapid setting characteristics (FA2).

**Table 2.3** Physical properties of constituent materials

True Density ASTM C188 Dry g/cm <sup>3</sup>	Specific Gravity		Bulk Density		Absorpt. Capacity ASTM C128	Moisture Content Stock		
	ASTM C128		ASTM C29 M					
	OD	SSD	OD	Voids %				
OPC	3.119	--	--	--	--	--		
FA1	2.689	--	--	--	--	--		
FA2	2.645	--	--	--	--	--		
FVA	2.670	2.592	2.631	1,738	32.8%	1.48%		
FRCA	2.599	2.190	2.385	1,422	34.9%	8.90%		
						9.00%		

Notes: 1 g/cm<sup>3</sup> = 62.428 lb/ft<sup>3</sup>; 1 kg/m<sup>3</sup> = 1.685 lb/yd<sup>3</sup>;  
OD: Oven Dry condition; SSD: Saturated Surface Dry condition.

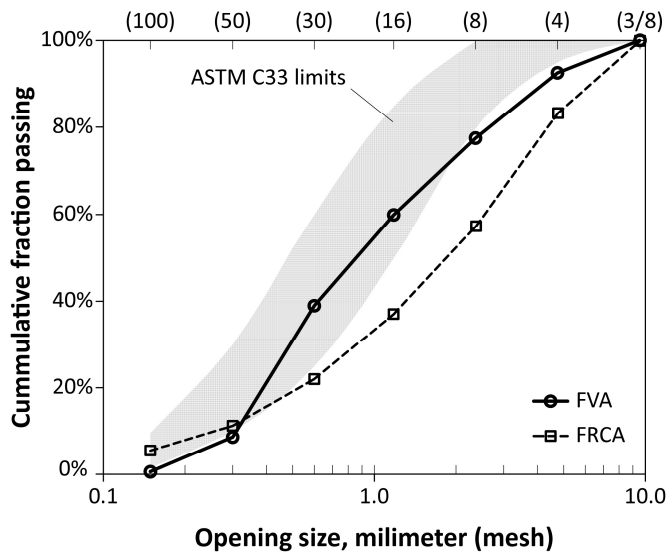


**Figure 2.3** Gradation of fine virgin aggregate (FVA) and fine recycled concrete aggregate (FRCA) compared to ASTM C33 limits.

**Table 2.4** Chemical analysis of fly ash

	FA1 (%)	FA2 (%)	ASTM C618 Class C Specification
SiO <sub>2</sub>	41.75	31.01	
Al <sub>2</sub> O <sub>3</sub>	21.85	17.19	
Fe <sub>2</sub> O <sub>3</sub>	5.19	5.51	
SiO <sub>2</sub> +Al <sub>2</sub> O <sub>3</sub> +Fe <sub>2</sub> O <sub>3</sub>	68.79	53.71	50 Min
CaO	18.59	26.67	
MgO	3.82	6.13	
SO <sub>3</sub>	1.71	2.27	5.0 Max
Na <sub>2</sub> O	1.54	3.47	
K <sub>2</sub> O	0.83	0.53	
Moisture Content	0.08	0.28	3.0 Max
Loss On Ignition	0.79	2.63	6.0 Max

Notes: Chemical analysis provided by Lafarge North America

Besides the role of FRCA as an aggregate phase in the CLSM mixture, alkalis released from the hydrated paste residues in the FRCA might promote additional pozzolanic reaction of the fly ash, which would contribute to CLSM strength gain. Achtemichuk et al. (Achtemichuk et al., 2009) demonstrated that CLSM mixtures based on recycled aggregates and either ground granulated blast furnace slag or Class C fly ash gained sufficient strength without Portland cement. The contribution of the FRCA to the pozzolanic reactions cannot be clearly established from their work because no control mixtures were cast with virgin aggregates. Recently, Etxeberria, Ainchil, Pérez, & González (2013), produced CLSM with increasing amounts of FRCA and found higher cement paste contents and lower water to cement ratios were required in order to achieve the CSLM performance of virgin aggregates. In this laboratory study, a direct comparison of response models obtained from both virgin and recycled fine aggregates provides the quantitative contribution of FRCA to CLSM performance.

### **2.3.3 CLSM mixture and batching**

The experiment was executed in two separate blocks: a factorial portion (cases R1-R9 in **Table 2.5**) and an axial portion (cases R10-R17 in **Table 2.5**). The execution order of each specific mixture was randomized within each block. Constituents' masses were determined from the required volumes according to the specific gravities of the materials. Water adjustments were made to compensate for the aggregate moisture content.

Since the fresh properties of CLSM mixtures can change rapidly in the first minutes after mixing, testing the fresh properties at the end of the mixing phase might not reflect workability in the field where longer times from mixing to placing can be expected. Therefore, the mixing process was split into three periods: 2.5 minute initial mixing period, 10 minute rest period, and 2.5 minute final mixing period. All CLSM mixtures were batched in 4.0 liter (1.0567 gallons) volumes and mixed in a mortar mixer.

Flowability was evaluated by the slump-flow diameter according to ASTM D6103-04 within 30 seconds of final mixing. The fresh CLSM mixture was cast in 75 by 150 mm (3 x 6 in) cylindrical, split molds for ease of specimen removal. The molded specimens were cured at 23°C and 100% relative humidity for 14 days and then removed and moist cured until 28 days. Due to the potential excessive bleeding and material consolidation, the subsidence of the CLSM molded-specimen was measured at 10 days at three independent points on the top surface of the specimen. The average compressive strength (ASTM D4832-10) was determined from three specimens. Unbonded metal caps fitted with sorbothane pads (Shore OO durometer hardness of 50) were used to avoid damage to the specimen surface (Du, Folliard, & Trejo, 2004).

## 2.4 Experimental results, modeling, and discussion

The individual case results for all the central composite experiment are presented in **Table 2.5**. Second-order response models describing the relationship between the mixture responses (slump-flow, subsidence, and strength) and mixture proportions were estimated using ordinary least squares regression shown in **Equation 2.1** below, where  $y$  is the predicted response,  $\beta_0$  is the average response for the all cases,  $x_i$  and  $x_j$  are the coded levels of factors, and  $\beta_i$ ,  $\beta_{ij}$ , and  $\beta_{ii}$  are the regression coefficients (i.e.,  $\beta_i$  is the linear effect of  $x_i$ ,  $\beta_{ij}$  is the linear interaction effect between  $x_i$  and  $x_j$ , and  $\beta_{ii}$  is the quadratic effect of  $x_i$ ). The regression coefficients represent the effect of each input factor expressed in the units of the response, i.e. millimeters of slump-flow diameter, percentage loss of height for subsidence, and kPa for compressive strength.

$$\hat{y} = \beta_0 + \sum_{i=1}^3 \beta_i x_i + \sum_{i < j}^3 \beta_{ij} x_i x_j + \sum_{i=1}^3 \beta_{ii} x_i^2 + e \quad (2.1)$$

The regression coefficients for slump-flow, subsidence, and compressive strength models are shown in **Tables 2.6**, **2.7** and **2.8**, respectively. In the three tables, the row named “Intercept” shows the average response ( $\beta_0$ ) for all cases. Rows numbered 1, 2 and 3, show the linear effects of factors W/CM, VPP and OPC/CM, respectively; rows numbered 12, 13, and 23 show effects due to the interactions of these factors ( $\beta_{ij}$ ); and rows numbered 11, 22, and 33 show their quadratic effects ( $\beta_{ii}$ ). A positive value for the estimated effect of a factor indicates the response (e.g., slump-flow) is increased when the factor level (e.g., VPP) is increased. Statistical significance of estimated effects was assessed at a 5% level for effects on slump-flow and strength and at 10% significance level for effects on subsidence (subsidence response exhibited higher experimental variance). The relative proportions that had a significant effect on the CLSM response parameter are indicated in bold.

**Table 2.5** Results for individual cases in the central composite experiment

Case	Factor levels						Experimental Results								
	Coded			Experimental			FVA + FA1			FRCA + FA1			FRCA + FA2		
	1:	2:	3:	W/ CM	VPP	OPC/ CM	S-flow (mm)	Subs. (%)	Strength (kPa)	S-flow (mm)	Subs. (%)	Strength (kPa)	S-flow (mm)	Subs. (%)	Strength (kPa)
R1	-1	-1	-1	0.65	37.5	0.10	140	1.2	254	195	0.0	261	75	0.0	538
R2	1	-1	-1	1.05	37.5	0.10	140	1.9	181	195	1.0	101	115	0.0	171
R3	-1	1	-1	0.65	47.5	0.10	440	1.4	217	425	0.7	279	2401	0.0	676
R4	1	1	-1	1.05	47.5	0.10	540	6.5	131	490	0.7	71	250	0.0	148
R5	-1	-1	1	0.65	37.5	0.20	110	1.6	3437	255	1.0	1304	170	0.0	3608
R6	1	-1	1	1.05	37.5	0.20	140	3.0	1343	250	0.8	370	230	0.7	752
R7	-1	1	1	0.65	47.5	0.20	420	2.2	3068	460	1.0	1310	350	1.2	3017
R8	1	1	1	1.05	47.5	0.20	545	7.9	1497	535	1.8	304	455	2.4	818
R9	0	0	0	0.85	42.5	0.15	375	3.3	630	355	0.7	293	260	0.9	646
R10	-1.68	0	0	0.51	42.5	0.15	280	1.4	1335	280	0.1	1068	180	0.4	3282
R11	1.68	0	0	1.19	42.5	0.15	445	3.8	530	335	0.7	123	310	0.6	303
R12	0	-1.68	0	0.85	34.1	0.15	75	1.3	761	195	0.0	251	145	0.0	746
R13	0	1.68	0	0.85	50.9	0.15	585	5.2	403	520	0.8	211	465	0.6	472
R14	0	0	-1.68	0.85	42.5	0.07	420	1.6	52	300	0.0	107	135	0.0	213
R15	0	0	1.68	0.85	42.5	0.23	405	3.4	2408	475	1.6	775	275	1.4	2236
R16	0	0	0	0.85	42.5	0.15	425	3.0	564	330	0.2	265	285	0.8	704
R17	0	0	0	0.85	42.5	0.15	405	2.8	536	360	0.5	255	280	0.5	627

Notes: 1 mm = 0.0394 inch; 1 kPa = 0.145 psi

#### 2.4.1 Slump-flow models

Average slump-flow results were higher for virgin aggregates and mixtures with conventional Class C fly ash. As seen in **Table 2.6**, the VPP had the largest effect on the CLSM flowability for all tested constituents. The estimated effect of the VPP is larger for FVA-based mixtures, but becomes comparable to FRCA-based mixtures above 45% VPP (**Figure 2.4**). As seen in the **Figures 2.4** to **2.7**, the CLSM regression model predicts slump-flow results above the recommended minimum slump-flow diameter (200 mm) for most of the experimental region.

**Table 2.6** Estimated effects (regression coefficients) of mixture proportions on slump-flow diameter (mm).

Factors	FVA + FA1		FRCA + FA1		FRCA + FA2	
	Effect mm	p value	Effect mm	p value	Effect mm	p value
Average	<b>393</b>	<b>&lt;0.0001</b>	<b>350</b>	<b>0.0007</b>	<b>272</b>	<b>0.0001</b>
1 W/CM	<b>40</b>	<b>0.0009</b>	17	0.1059	<b>32</b>	<b>0.0024</b>
2 VPP	<b>166</b>	<b>&lt;0.0001</b>	<b>114</b>	<b>&lt;0.0001</b>	<b>91</b>	<b>&lt;0.0001</b>
3 OPC/CM	-5	0.4805	<b>35</b>	<b>0.0074</b>	<b>56</b>	<b>0.0001</b>
12 interaction	<b>25</b>	<b>0.0275</b>	18	0.1681	2	0.8534
13 interaction	7	0.4343	1	0.9507	16	0.1085
23 interaction	2	0.7895	-4	0.7430	13	0.1634
11 W/CM	<b>-21</b>	<b>0.0278</b>	-15	0.1835	-12	0.1372
22 VPP	<b>-32</b>	<b>0.0044</b>	3	0.7707	9	0.2578
33 OPC/CM	-3	0.6774	13	0.2421	<b>-26</b>	<b>0.0117</b>

Notes: 1 mm = 0.0394 inch

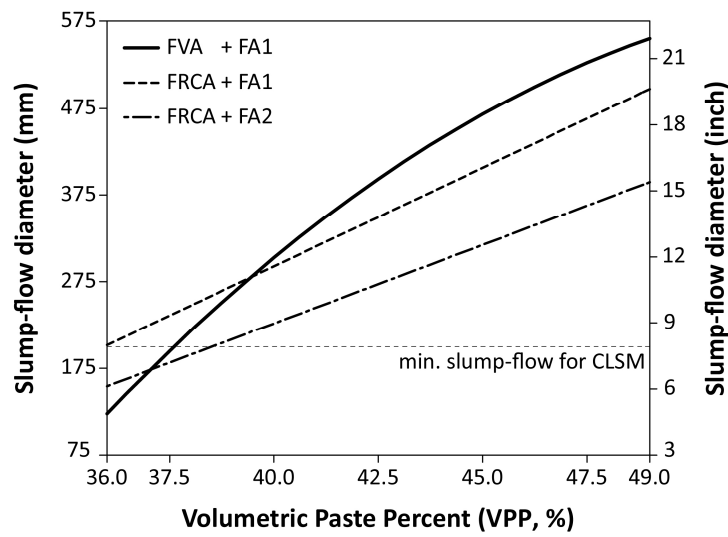


**Figure 2.4** Predicted slump-flow diameter as a function of volumetric paste percent at 0.15 OPC/CM and 0.85 W/CM ratios.

According to the fitted regression model, the effect of W/CM ratio on flowability is 3 to 6 times lower than the effect of VPP. For FVA-based mixtures, the estimated effect of W/CM ratio for a fixed VPP exhibits significant nonlinearity (**Figure 2.5**), decreasing progressively and becoming insignificant at higher W/CM ratios. Furthermore, the estimated effect of the W/CM ratio increases as the paste percent increases as seen in **figure 2.6**. The individual experimental cases of FVA demonstrated similar trends in regards to slump-flow with segregation more noticeable at higher W/CM ratios. For the FRCA-based mixtures, the models predict slump-flow to be insensitive to changes in W/CM for FA1 fly ash as seen in **Figure 2.5**, while for FA2 fly ash it increases linearly with increasing W/CM. Overall, the FRCA-based mixtures exhibited higher resistance to segregation relative to FVA due to the lower density and increased angularity of the recycled aggregates, and the higher fines content in its gradation.

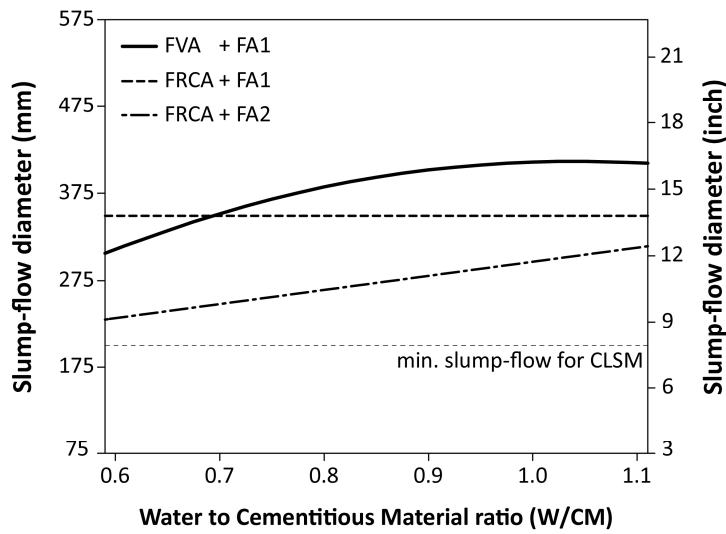


**Figure 2.5** Predicted slump-flow diameter as a function of the W/CM ratio at 42.5% paste fraction and 0.15 OPC/CM ratios.

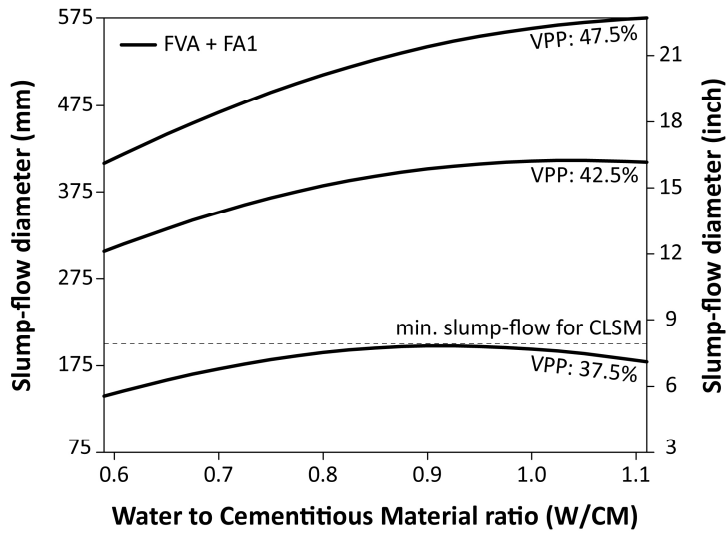


**Figure 2.6** Predicted slump-flow diameter for mixtures based on FVA and FA1 fly ash at different volumetric paste percentages and a fixed 0.15 OPC/CM ratio.

The estimated effect of the OPC/CM ratio on flowability depends on the set of constituents selected (**Figure 2.7**). In the range of OPC/CM ratios explored, the regression model predicts an insignificant effect on slump-flow for FVA-based mixtures. Conversely, for FRCA-based mixtures, the models predict slump-flow increases with increasing OPC/CM ratios. As shown in **Figure 2.8**, additional experimental case results outside the range covered by the central composite experiment show increasing OPC/CM ratio, i.e., decreasing the level of substitution of Portland cement by fly-ash, generally decreased slump-flow diameter. However, in the range from 0.0 to 0.2 OPC/CM ratios for FRCA-based mixtures, the slump-flow diameter increased with increasing OPC/CM ratio. The reduction of flowability for FRCA-based mixtures at very low OPC/CM ratios can be linked to the formation of ettringite crystals from sulfates present in both fly ashes (Taylor, 1997). Ettringite crystal stability and morphology is strongly dependent on the pH of the solution (Cody, Lee, Cody, & Spry, 2004). A pH of 11.5 was measured immediately after dispersing 20g of FRCA in 100mL of distilled water. If formed at this pH, ettringite

crystals reach a maximum length-to-thickness ratio (Lo Presti et al., 2007; Stark & Bollmann, 2000). These elongated crystals could bridge other mixture constituents, as is seen in SEM observations of the FRCA-based mixture in **figure 2.9**. Consequently, depending on the chemical composition and content of fly ash, mixtures can display reduced flowability, shorter time of setting or even false set behavior (Tarum R Naik & Singh, 1997; Tanikella & Olek, 2009). For this study, FRCA-based mixtures at very low OPC/CM ratios (i.e. higher fly ash contents), displayed generally lower slump-flow results. In addition, at 0.0 OPC/CM ratio, mixtures incorporating FA2 fly ash, which had higher sulfate content, exhibited false set behavior in the resting period between mixing. As OPC/CM ratio is increased, the pH of the solution continually increases favoring the formation of shorter ettringite crystals improving flowability and eliminating false setting.

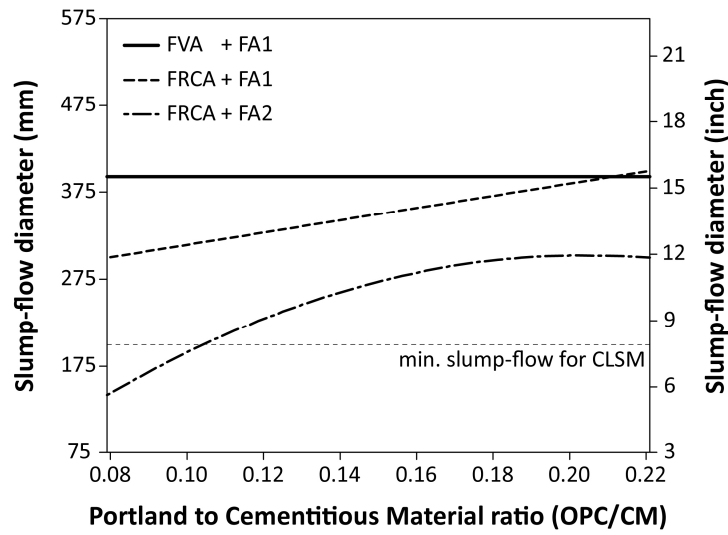


**Figure 2.7** Predicted slump-flow diameter as a function of OPC/CM ratio of the mixture, at 42.5% paste and 0.85 W/CM ratios.

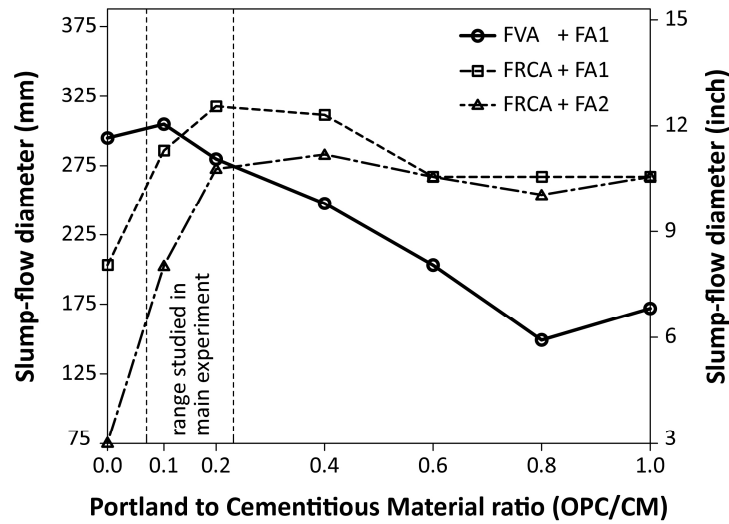


**Figure 2.8** Observed slump-flow diameter versus OPC/CM ratio at 40% VPP and W/CM=0.80 with detrimental effect on slump-flow at lower OPC/CM ratios and FRCA-based mixtures.

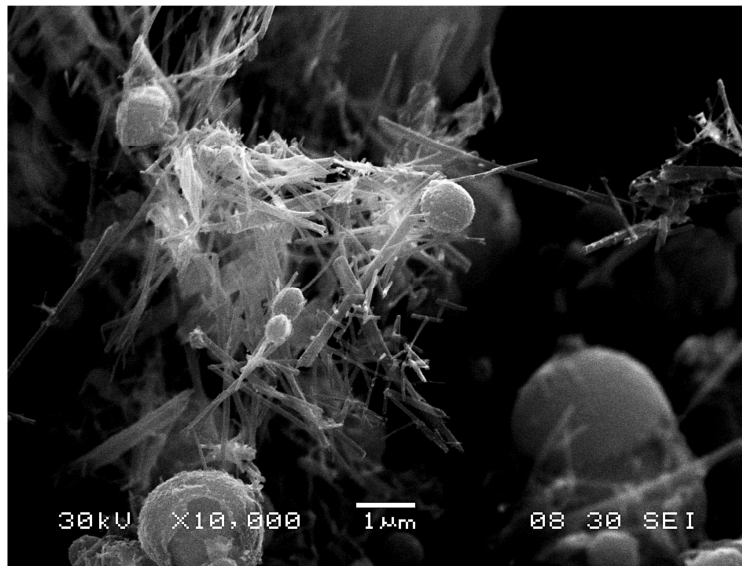


**Figure 2.9** SEM image of fracture surface of 28-day CLSM containing FRCA and FA2 fly ash with ettringite needles bridging fly ash particles.

## 2.4.2 Subsidence models

For all sets of constituents tested, the regression model coefficients listed in **Table 2.7** predict higher CLSM subsidence if VPP, W/CM, or OPC/CM are increased. The estimated effects of VPP and W/CM on subsidence are much stronger for FVA-based mixtures. Average subsidence was also significantly higher for FVA-based mixtures relative to FRCA. However, regardless of aggregate type, the lowest subsidence was observed in mixtures having lower paste percentages due to increased contact between aggregate particles. As seen in **Figure 2.10**, for FVA-based mixtures, the effect of VPP significantly increases at higher W/CM ratios.

**Table 2.7** Estimated effects (regression coefficients) of mixture proportions on subsidence (as % of specimen height).

Factors	FVA + FA1		FRCA + FA1		FRCA + FA2	
	Effect %	p value	Effect %	p value	Effect %	p value
Average	<b>3.10</b>	<b>0.0026</b>	<b>0.51</b>	<b>0.0395</b>	<b>0.76</b>	<b>0.0031</b>
1 W/CM	<b>1.23</b>	<b>0.0006</b>	<b>0.19</b>	<b>0.0745</b>	<b>0.17</b>	<b>0.0543</b>
2 VPP	<b>1.23</b>	<b>0.0006</b>	<b>0.21</b>	<b>0.0567</b>	<b>0.28</b>	<b>0.0067</b>
3 OPC/CM	<b>0.51</b>	<b>0.0341</b>	<b>0.36</b>	<b>0.0062</b>	<b>0.49</b>	<b>0.0004</b>
12 interaction	<b>1.07</b>	<b>0.0043</b>	0.00	0.9752	0.06	0.5161
13 interaction	0.16	0.5249	-0.04	0.7179	<b>0.24</b>	<b>0.0367</b>
23 interaction	0.09	0.7331	0.07	0.5600	<b>0.37</b>	<b>0.0069</b>
11 W/CM	-0.10	0.6558	0.02	0.8381	-0.09	0.3147
22 VPP	0.13	0.5554	0.03	0.7984	-0.16	0.0858
33 OPC/CM	-0.13	0.5451	0.16	0.1591	-0.02	0.8248

Notes: Effect corresponds to percentage of initial specimen height

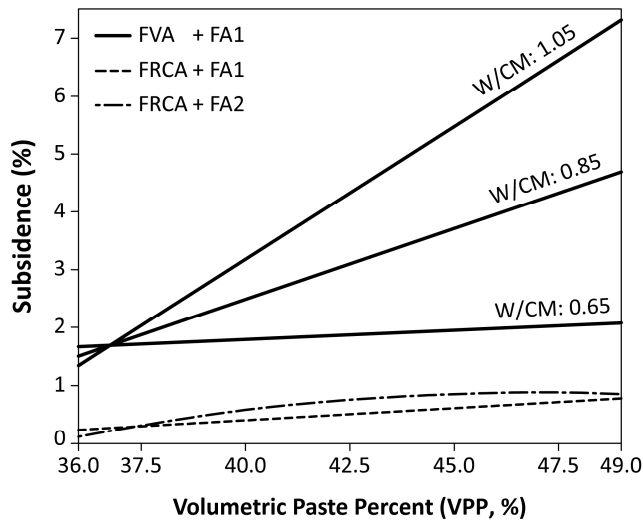


**Figure 2.10** Predicted mixture subsidence as a function of volumetric paste percent at 0.15 OPC/CM ratio and 0.85 W/CM ratio (except where indicated).

#### 2.4.3 28-day compressive strength models

Compressive strength results were highly dependent on the set of constituents tested with FRCA-based mixtures incorporating FA1 fly ash displaying the lowest average strength. The regression model coefficients in **Table 2.8** demonstrate that the effect of volumetric paste percent on strength is not significant regardless of the aggregate type and fly ash source. As expected, for each set of constituents the model predicts that the compressive strength increases with decreasing W/CM ratios. Likewise, the compressive strength is positively correlated to the OPC/CM ratio as well as dependent on the interaction between W/CM and OPC/CM, as noted in **Table 2.8**. The principal and interaction effects estimated for the W/CM and OPC/CM ratios explain the significant variation observed in strength for each set of constituents.

**Table 2.8** Estimated effects (regression coefficients) of mixture proportions on 28-day compressive strength (kPa).

Factors	FVA + FA1		FRCA + FA1		FRCA + FA2	
	Effect kPa	p value	Effect kPa	p value	Effect kPa	p value
Average	<b>621</b>	<b>0.0012</b>	<b>281</b>	<b>0.0001</b>	<b>655</b>	<b>0.0001</b>
1 W/CM	<b>-379</b>	<b>0.0069</b>	<b>-285</b>	<b>&lt;0.0001</b>	<b>-803</b>	<b>&lt;0.0001</b>
2 VPP	-66	0.5085	-10	0.6981	-64	0.3563
3 OPC/CM	<b>917</b>	<b>0.0001</b>	<b>271</b>	<b>&lt;0.0001</b>	<b>737</b>	<b>&lt;0.0001</b>
12 interaction	64	0.6230	-15	0.6629	62	0.4852
13 interaction	<b>-438</b>	<b>0.0119</b>	<b>-197</b>	<b>0.0010</b>	<b>-520</b>	<b>0.0008</b>
23 interaction	-16	0.9008	-6	0.8606	-80	0.3744
11 W/CM	<b>168</b>	<b>0.1611</b>	<b>123</b>	<b>0.0046</b>	<b>398</b>	<b>0.0014</b>
22 VPP	45	0.6874	-6	0.8474	-21	0.7807
33 OPC/CM	<b>274</b>	<b>0.0409</b>	<b>69</b>	<b>0.0500</b>	<b>197</b>	<b>0.0330</b>

The significant interaction between W/CM and OPC/CM ratios suggests that the water to Portland cement mass ratio (W/OPC) alone may be a good predictor of CLSM strength. However, CLSM mixtures produced with a fixed W/OPC ratio can be obtained at different combinations of W/CM and OPC/CM ratios resulting in significantly different compressive strengths as seen in the additional experimental cases shown in **Figure 2.11**.

The results of the testing and regression parameters in **Table 2.8** confirm that the compressive strength of FRCA is highly dependent on the fly ash source. In **Figure 2.12**, compressive strength results over the full range of OPC/CM ratios demonstrate the CLSM strength appears to be limited by the type of aggregate at higher OPC/CM ratios with FRCA mixtures achieving lower strengths. However at lower OPC/CM ratios, higher CLSM strengths were observed for FRCA-based mixtures and FA2 source fly ash. This additional strength can be linked with the increased ettringite formation in the hardened paste shown in **Figure 2.9**, which can explain the higher average strength results obtained with this set of constituents compared to the FRCA-based mixture incorporating FA1 source fly ash.

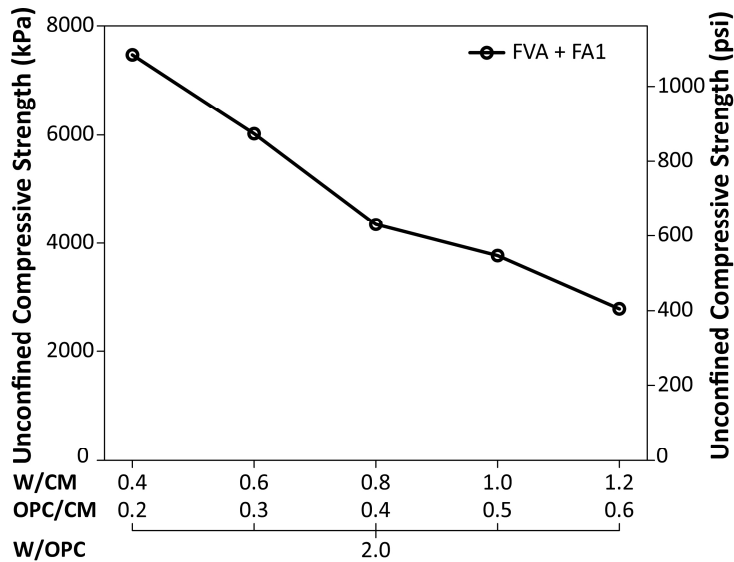


**Figure 2.11** Compressive strength results for mixtures containing FVA and fly ash (FA1) at W/CM and OPC/CM combinations yielding a fixed W/OPC ratio of 2.0.

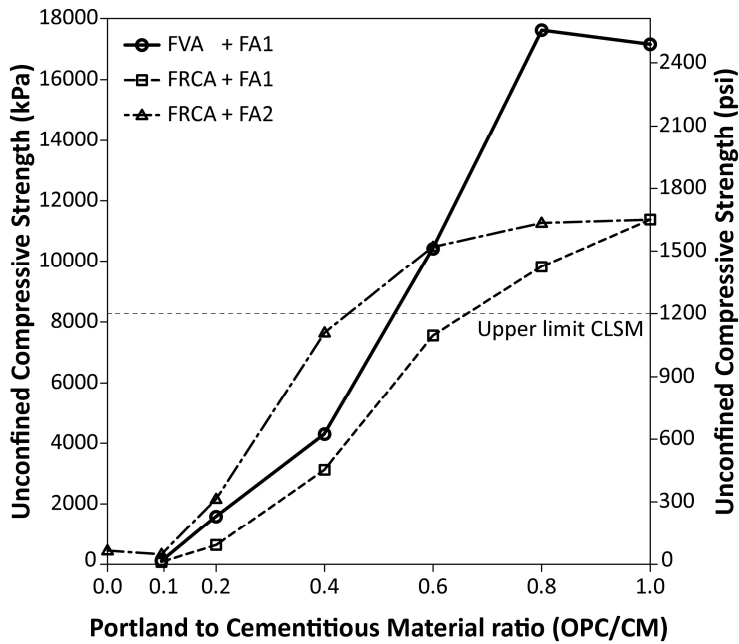


**Figure 2.12** 28-day strength results versus OPC/CM ratio for mixtures at fixed 0.80 W/CM ratio and 40% volumetric paste percent.

**Figures 2.13, 2.14, and 2.15** show compressive strength results versus W/CM ratio for all mixtures produced with a specific set of constituents and varying OPC/CM ratio. The strength trend for a particular level of OPC/CM ratio can be described by a power law with greater strength at lower W/CM and higher OPC/CM. Considering:  $S = a \cdot (W/CM)^b$ , where  $S$  is the 28-day compressive strength of the CLSM, the coefficients of the power law relationship,  $a$  and  $b$ , depend on the set of constituents selected (e.g., aggregate type and fly ash source) and the OPC/CM ratio (**Table 2.9**). With this predictive relationship, for a given set of constituents and OPC/CM ratio, W/CM ratio alone can be used to predict strength of CLSM mixture. Decreasing the W/CM ratio maximizes the strength achievable at any given OPC/CM ratio, with each set of constituents achieving a different magnitude of compressive strength for a fixed W/CM and OPC/CM ratio. The observed relationship suggests that W/CM should be minimized in order to reduce the required amount of Portland cement to achieve a targeted strength.

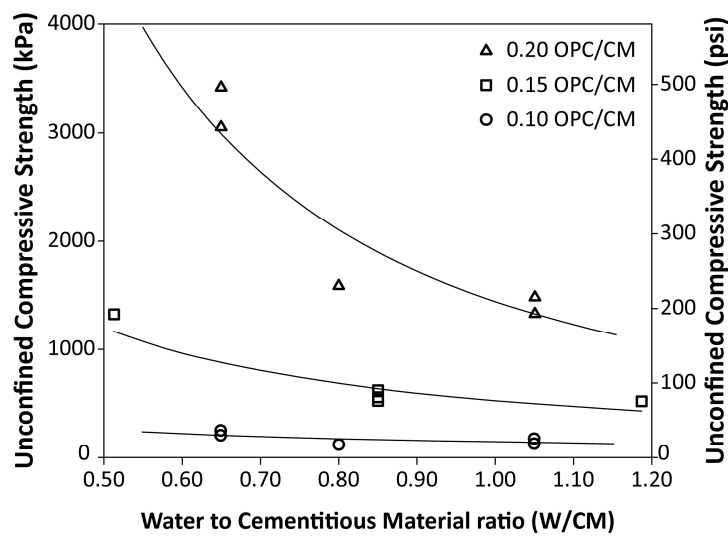


**Figure 2.13** 28-day compressive strength results versus W/CM ratio for mixtures with FVA and FA1 source fly ash at multiple OPC/CM ratios.

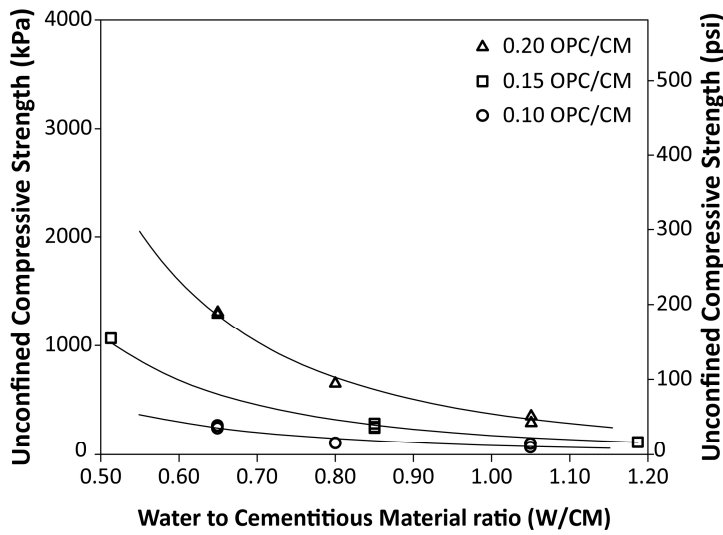


**Figure 2.14** 28-day compressive strength results versus W/CM ratio for mixtures with FRCA and FA1 source fly ash at multiple OPC/CM ratios.

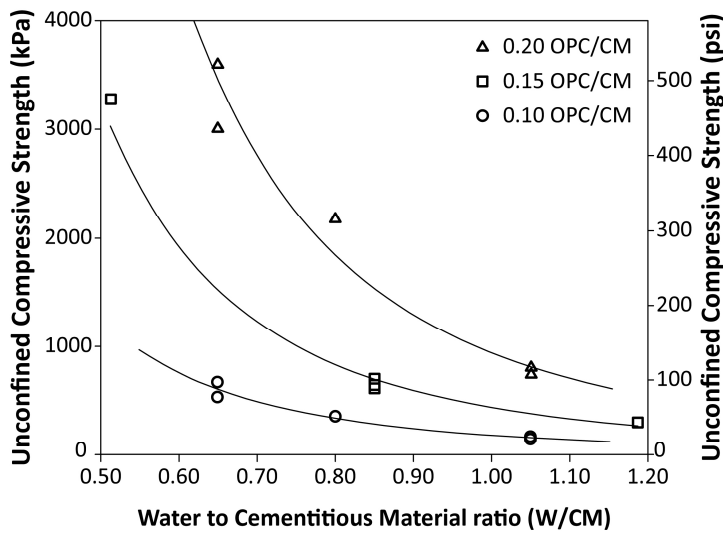


**Figure 2.15** 28-day compressive strength results versus W/CM ratio for mixtures with FRCA and FA2 source fly ash at multiple OPC/CM ratios.

**Table 2.9** Regression coefficients for Strength - W/CM ratio relationship for different sets of constituents at different levels of OPC/CM

OPC /CM	FVA+ FA1		FRCA + FA1		FRCA + FA2	
	a	b	a	b	a	b
0.10	163	-0.86	97	-2.38	183	-2.79
0.15	573	-1.14	183	-2.57	459	-2.85
0.20	1547	-1.72	387	-2.83	909	-3.00

## 2.5 Relative proportion CLSM mixture design principles

Whenever recycled or by-product materials are used to produce CLSM, significant changes in its fresh and hardened properties can be expected. The findings from the CLSM regression models can help establish more systematic mixture proportioning guidelines and adjustments for similar sets of constituents (i.e. cement, SCM or fine filler material, fine aggregate, and water). Although predictions from each regression model are limited to a specific set of constituents, comparison of models obtained in this study show several estimated effects of mixture proportions are similar across all the sets of constituents tested. The following mixture design principles are based on these observed effects.

Achieving flowability requirements: Slump-flow of CLSM mixtures is best controlled by adjusting its volumetric paste percent. When the VPP is set at values exceeding the void content of the aggregate, the VPP has a strong effect on slump-flow diameter. Since the VPP has the least effect on strength (see **Table 2.8**), it can be adjusted after selecting other mixture proportions for strength. Nevertheless, in order to maximize aggregate content, VPP should be set to the minimum value to achieve the required slump-flow. Depending on the gradation of the aggregate an initial starting point for the VPP can be between 1.1 and 1.2 times the voids content of the aggregate. The oven-dry aggregate content required per unit volume of mixture can be calculated from the target VPP.

$$\text{Aggregate Content (kg/m}^3\text{)} = 1000 \times \text{BSG}_{OD} \times \frac{100 - VPP}{100 - AVP} \quad (2.2)$$

where,  $\text{BSG}_{OD}$  is the bulk specific gravity (oven dry) of the aggregate, VPP is the target volumetric paste percent of the mixture, and AVP is the percent of voids of the oven dry aggregate. The resulting quantity needs to be corrected to account for the moisture content of the aggregate from the stockpile.

Contrary to common practice and references for CLSM mixture proportioning, the findings of this research clearly showed that W/CM ratio is less effective in controlling flowability (**Figure 2.5 and 2.6**), has a detrimental effect on segregation, bleeding, and subsidence of the mixture, and negatively affects strength. When slump-flow test results change due to changes in the type, particle size distribution, and chemical composition of the aggregates or SCM, CLSM mixture proportions must be adjusted, i.e., VPP must be increased or decreased to maintain desired slump-flow.

Controlling subsidence: Since highly flowable mixtures are prone to subsidence, VPP, W/CM and OPC/CM ratios of the mixture must be kept at their minimum practical levels as seen in **Table 2.7**. Lower values of VPP and W/CM produce a higher proportion of solid to fluid phases at all levels in the mixture, resulting in increased particle to particle interactions while lower values of OPC/CM produce a greater proportion of lower specific gravity particles in the paste.

Achieving strength requirements: The W/CM ratio should be selected to achieve the target strength and workability while minimizing the OPC content. The minimum W/CM ratio to achieve the required flowability for the selected VPP can be rapidly determined by performing a series of slump-flow tests. However, it is important to test for minimum W/CM ratio at an OPC/CM ratio close to the desired strength criteria (**Figures 2.13 to 2.15**) since the OPC/CM ratio also affects the flowability of the mixture (**Figure 2.7 and 2.8**). In order to change the W/CM ratio without affecting the VPP, the following formula can be used to determine the content of cementitious material required:

$$CMT(kg/m^3) = \frac{1000 \times VPP}{W/CM + 1/(\rho_{SCM} \times (1 - OPC/CM) + \rho_{OPC} \times OPC/CM)} \quad (2.3)$$

where, CMT is the total cementitious material (OPC + SCM), VPP is the volumetric paste percent of the mixture,  $\rho_{SCM}$  is the density of the SCM or fine filler,  $\rho_{OPC}$  is the density of the Portland cement, and W/CM and OPC/CM are the selected water to total cementitious material and Portland cement to total cementitious material mass ratios, respectively.

For the aggregate and fly ash combinations in this study, a W/CM ratio 0.7 was found to be appropriate for achieving a flowable mixture with a VPP approximately 1.2 times the percent of voids in the aggregate. This W/CM ratio is suggested as a starting point for either recycled or virgin fine aggregate CLSM mixtures. Once W/CM ratio is set, the 28-day strength is controlled adjusting the OPC/CM ratio. As shown in **Figures 2.13 to 2.15**, the sensitivity of CLSM strength to OPC/CM change is specific to the aggregate and SCM combination. Therefore, whenever alternative aggregates or SCMs are used, a series of mixtures at the selected paste percent and W/CM ratio need to be produced for different OPC/CM ratios to characterize the actual 28-day compressive strength of the new combined materials.

## 2.6 Conclusions

With the need to utilize recycled and by-product materials, a more systematic method to rapidly determine the optimal CLSM mixture proportions is required. In this study, a set of relative proportions comprising of the volumetric paste percent of the mixture (VPP), the water to cementitious material ratio (W/CM), and the Portland cement to cementitious material ratio (OPC/CM) was shown to provide adequate control over relevant CLSM properties including flowability, subsidence, and 28-day compressive strength. Central composite experimental design and regression analysis were used to estimate the main and interaction effects of the mixture proportions on the properties of CLSMs based on either virgin or recycled fine aggregate and two fly ash sources.

Overall, similar relative mixture proportion adjustments exhibited similar effects across the sets of constituent materials studied. The VPP was found to have the strongest effect on flowability, whereas W/CM ratio had a comparatively minor effect. Due to its detrimental effect on segregation, bleeding, and subsidence, increasing W/CM is not recommended to increase flowability of CLSM. In addition, decreasing the W/CM ratio increases the compressive strength obtained at any given OPC/CM ratio, thus minimizing cement requirements. When the VPP and W/CM ratio of the mixture are fixed, the OPC/CM ratio can be used to control compressive strength with minimal influence on flowability and subsidence.

Comparison of response models and experimental observations showed FRCA-based mixtures achieved minimum slump-flow diameter at lower paste percent and exhibited improved segregation, bleeding, and subsidence characteristics than similar FVA mixtures. Fresh properties of FRCA-based CLSM benefit from the higher powder content in FRCA gradation and the lower density of its particles. In addition, formation of early reaction products due to chemical interaction between fly ash and soluble species released from the recycled aggregate might provide additional subsidence resistance after placement. However, depending on the fly ash source, these early reaction products can also induce false setting of FRCA-based CLSM, particularly at lower OPC/CM ratios. Although FVA-based mixtures achieved generally higher strengths, FRCA-based mixtures at low OPC/CM and low W/CM ratios achieved higher strengths compared to similar FVA-based mixtures.

## **2.7 Acknowledgments**

We acknowledge the O'Hare Modernization Program and the City of Chicago for financing this research work through the Center of Excellence for Airport Technology at the Department of Civil and Environmental Engineering, University of Illinois at Urbana-Champaign. We appreciate the fly ash samples and technical information provided by Lafarge North America.

## 2.8 References

- Achtemichuk, S., Hubbard, J., Sluce, R., & Shehata, M. H. (2009). The utilization of recycled concrete aggregate to produce controlled low-strength materials without using Portland cement. *Cement and Concrete Composites*, 31(8), 564–569. doi:10.1016/j.cemconcomp.2008.12.011
- ACI Committee 229. (2013). *ACI 229R-13 Controlled Low-Strength Materials* (pp. 1–13). Farmington Hills.
- Alizadeh, V., Helwany, S., Ghorbanpoor, A., & Sobolev, K. (2014). Design and application of controlled low strength materials as a structural fill. *Construction and Building Materials*, 53, 425–431. doi:10.1016/j.conbuildmat.2013.12.006
- Bhat, S. T., & Lovell, C. W. (1997). Flowable Fill Using Waste Foundry Sand: A Substitute for Compacted or Stabilized Soil. In M. A. Wasemiller & K. B. Hoddinott (Eds.), *Testing Soil Mixed With Waste or Recycled Materials, ASTM STP 1275*. American Society for Testing and Materials.
- Box, G. E. P., & Hunter, J. S. (1957). Multifactor experimental designs for exploring response surfaces. *Annals of Mathematical Statistics*, 28(1), 195–241.
- Box, G. E. P., & Wilson, K. B. (1951). On the experimental attainment of optimum conditions. *Journal of the Royal Statistical Society Series B (Statistica Methodology)*, 13(1), 1–45.
- Cody, A. M., Lee, H., Cody, R. D., & Spry, P. G. (2004). The effects of chemical environment on the nucleation, growth, and stability of ettringite  $[Ca_3Al(OH)_6]_2(SO_4)_3 \cdot 26H_2O$ . *Cement and Concrete Research*, 34(5), 869–881.
- Du, L., & Folliard, K. (2002). Effects of constituent materials and quantities on water demand and compressive strength of controlled low-strength material. *Journal of*

- materials in civil engineering*, 14(6), 485–495. doi:10.1061/(ASCE)0899-1561(2002)14:6(485)
- Du, L., Folliard, K., & Trejo, D. (2004). A New Unbonded Capping Practice for Evaluating the Compressive Strength of Controlled Low-Strength Material Cylinders. *Cement, Concrete, and Aggregates*, 26(1), 1–8. doi:10.1520/CCA11895
- Etxeberria, M., Ainchil, J., Pérez, M. E., & González, A. (2013). Use of recycled fine aggregates for Control Low Strength Materials (CLSMs) production. *Construction and Building Materials*, 44, 142–148. doi:10.1016/j.conbuildmat.2013.02.059
- Hanson, J. L., Stone, G. M., & Yesiller, N. (2012). Use of Post-Consumer Corrugated Fiberboard as Fine Aggregate Replacement in Controlled Low-Strength Materials. *Journal of ASTM International*, 9(2), 562–579. doi:10.1520/JAI103843
- Katz, A., & Kovler, K. (2004). Utilization of industrial by-products for the production of controlled low strength materials (CLSM). *Waste management (New York, N.Y.)*, 24(5), 501–12. doi:10.1016/S0956-053X(03)00134-X
- Kenai, S., Debieb, F., & Azzouz, L. (2002). Mechanical Properties and Durability of Concrete made with Coarse and Fine Recycled Aggregates. In R. K. Dhir, T. D. Dyer, & J. E. Halliday (Eds.), *Sustainable Concrete Construction: Proceedings of the International Conference Held at the University of Dundee, Scotland, UK on 9-11 September, 2002* (pp. 383–392). London: Thomas Telford.
- Khatib, J. M. (2005). Properties of concrete incorporating fine recycled aggregate. *Cement and Concrete Research*, 35(4), 763–769. doi:10.1016/j.cemconres.2004.06.017
- Lachemi, M., Shahmaran, M., Hossain, K. M. a., Lotfy, a., & Shehata, M. (2010). Properties of controlled low-strength materials incorporating cement kiln dust and slag. *Cement and Concrete Composites*, 32(8), 623–629. doi:10.1016/j.cemconcomp.2010.07.011

- Lo Presti, A., Artioli, G., Bravo, A., Cella, F., Cerulli, T., & Magistri, M. (2007). Study of the Influence of Soluble Ions on Morphological and Microstructural Properties of Synthetic Ettringite. In *Proceedings of the 12th International Congress on the Chemistry of Cement*. Montreal, Canada.
- Naganathan, S., Razak, H. A., & Hamid, S. N. A. (2012). Properties of controlled low-strength material made using industrial waste incineration bottom ash and quarry dust. *Materials & Design*, 33, 56–63. doi:10.1016/j.matdes.2011.07.014
- Naik, T. R., & Singh, S. S. (1997). Influence of Fly Ash on Setting and Hardening Characteristics of Concrete Systems. *ACI Materials Journal*, 94(5), 355–360.
- Naik, T. R., Asce, F., Kraus, R. N., Ramme, B. W., Chun, Y., & Kumar, R. (2006). High-Carbon Fly Ash in Manufacturing Conductive CLSM and Concrete. *Journal of materials in civil engineering*, 18(6), 743–746. doi:10.1061/(ASCE)0899-1561(2006)18:6(743)
- Nataraja, M. C., & Nalanda, Y. (2008). Performance of industrial by-products in controlled low-strength materials (CLSM). *Waste Management*, 28(7), 1168–1181. Retrieved from <http://www.sciencedirect.com/science/article/pii/S0956053X07001456>
- Pierce, C. E., Tripathi, H., & Brown, T. W. (2003). Cement Kiln Dust in Controlled Low-Strength Materials. *ACI Materials Journal*, 100(6), 455–462. doi:10.14359/12951
- Sanchez de Juan, M., & Alaejos Gutiérrez, P. (2009). Study on the influence of attached mortar content on the properties of recycled concrete aggregate. *Construction and Building Materials*, 23(2), 872–877. doi:10.1016/j.conbuildmat.2008.04.012
- Shayan, A., & Xu, A. (2003). Performance and Properties of Structural Concrete Made with Recycled Concrete Aggregate. *ACI Materials Journal*, 100(5), 371–380.
- Stark, J., & Bollmann, K. (2000). Delayed Ettringite Formation in Concrete. *Nordic Concrete Research Publications*, 23, 4–28.

- Taha, R. A., Alnuaimi, A. S., Al-Jabri, K. S., & Al-Harthy, A. S. (2007). Evaluation of controlled low strength materials containing industrial by-products. *Building and Environment*, 42(9), 3366–3372.
- Tanikella, P., & Olek, J. (2009). Incorporating physical and chemical characteristics of fly ash in statistical modeling of binder properties. *Masters Abstracts International*, 48(2).
- Taylor, H. F. W. (1997). *Cement Chemistry* (2nd ed.). London: Thomas Telford.
- Tikalsky, P., Gaffney, M., & Regan, R. (2000). Properties of Controlled Low-Strength Material Containing Foundry Sand. *ACI Materials Journal*, 97(6), 698–702.  
doi:10.14359/9984

### **3. REACTIVATED CEMENTITIOUS MATERIALS FROM HYDRATED CEMENT PASTE WASTES**

Ricardo Serpell, Mauricio López

Published: *Cement and Concrete composites* 39 (1) 2013, pp. 104-114.

#### **Abstract**

Hydrated cement pastes subjected to high temperature dehydration have been shown to develop a cementitious behavior upon rehydration that could enable recycling of hydrated cement wastes as alternative binders of high environmental value. In order to evaluate the potential of this recycling option it is first necessary to identify material and process factors affecting the performance of the reactivated cementitious materials produced. This paper presents the findings of a fractional factorial experiment designed to screen factors based on their effect on the strength developed by pastes incorporating materials reactivated from laboratory sourced hydrated cement pastes. Results allowed identification of factor and factor-interaction effects involving 7 of the 9 factors under study, which would be relevant in optimizing the recycling process. Highest strengths observed in the experimental region explored were 20, 32.8 and 39 MPa at 7, 28, and 90 days, respectively, for reactivated material pastes mixed at 0.7 w/cm ratio.

**Keywords:** Thermal Treatment; Compressive Strength; Cement Paste; Cement Recycling; Recycled Concrete; Waste Management.

### **3.1        Introduction**

The cement and concrete industry faces an ever increasing demand to reduce its impact on the environment. Concrete is nowadays one of the most used manufactured materials, with worldwide production currently exceeding 20,000 million tons per year, as estimated from the 2.9 billion tons of Portland cement produced in 2009 (U.S. Geological Survey, 2009). Therefore, small changes in concrete technology have the potential to produce a significant change to the environmental footprint of the industry. Three main sources of impact can be identified: the consumption of natural resources and energy to produce both Portland cement and concrete, the greenhouse gas emissions due mostly to the production of Portland cement (Gartner, 2004; Huntzinger & Eatmon, 2009; Juenger, Winnefeld, Provis, & Ideker, 2011; Meyer, 2009), and the large contribution of concrete to the construction and demolition solid wastes (Meyer, 2009). Recycling cement and concrete wastes can reduce the impact derived from these sources, and, adding to the environmental benefit of a sound material cycle, this substitution can be economically viable due to the savings in energy and transportation that could be achieved (Lauritzen, 2004).

Major concrete components must be processed separately in order to source recycled materials for the production of new mixtures. In the case of aggregates, substitution of natural materials by recycled concrete aggregates (RCA) can reach 100% by adjusting mixing methods to RCA properties (Abbas et al., 2009; Lin et al., 2004). Quality RCA have to be freed from hydrated cement paste residues which would otherwise limit the performance of the new concrete (Poon et al., 2004). When an aggregate improvement process involving heating and grinding is used, 75% of the original wastes can be recovered as high quality fine and coarse RCA, leaving 25% of fine concrete powder waste comprised mostly of hydrated cement paste (HCP) (Kasai, 2004). These fines, however, are normally discarded or used in low value applications, despite being the by-product of the higher costing component of the original concrete both in economic and in environmental terms.

Recycling of HCP wastes as binders for the production of new concretes holds high environmental value for the cement and concrete industry. Impact from natural resources consumption and waste generation would be further reduced, and, depending on the technical characteristics of the recycling process developed, greenhouse gas emissions and energy consumption could also be reduced, as recycled materials partially substitute Portland cement.

Potential paths to recycling of HCP wastes identified in recent publications range from the production of controlled low-strength materials using fines from crushed concrete together with supplementary cementitious materials (SCM) (Achtemichuk et al., 2009; Poon et al., 2006), to the production of clinkers using concrete wastes as raw-feed (Ai, Wei, Bai, & Lu, 2011; Fridrichová, 2007). Somewhat in between the range above, a promising alternative is the reactivation of the cementitious properties of the HCP wastes by dehydration. Chemical transformations occur in the hydrated paste at high temperatures leading to unhydrated compounds with cementitious characteristics. This process explains the partial recovery of strength observed in concrete structures damaged by fire when subject to post-fire curing (Poon, Azhar, Anson, & Wong, 2001). Dehydration and decomposition reactions within the hydrated cement paste contribute to a rapid degradation of concrete properties, particularly beyond 300°C (Arioz, 2007; Handoo et al., 2002; Janotka & Mojumdar, 2005; Mendes, Sanjayan, & Collins, 2007; Phan, Lawson, & Davis, 2001), as all hydrated phases of cement paste dehydrate progressively to give anhydrous phases (Castellote et al., 2004), decreasing the packing density and increasing porosity of the pastes (DeJong & Ulm, 2007; Farage, Sercombe, & Gallé, 2003). Upon re-saturation, rehydration of the anhydrous phases is accompanied by partial recovery of the initial pore structure and partial recovery of the mechanical properties of the paste (Farage et al., 2003; Poon et al., 2001). However, despite the apparent reversibility, anhydrous phases obtained from dehydration are different from the anhydrous phases in the original cement. Poorly crystallized Calcium Silicate Hydrates (C-S-H) of Ca/Si ratio over 1.3 gradually decomposes over 300°C to produce  $\beta$ -C<sub>2</sub>S of high specific surface area (Okada, Sasaki, Zhong, Ishida, & Mitsuda, 1994). C-S-H from hydrated cement pastes decomposes at 750°C to form a neso-silicate similar in structure to  $\beta$ -C<sub>2</sub>S, which rehydrates upon contact

with ambient water producing new C-S-H (Alonso & Fernandez, 2004). This rehydration displays cementitious behavior similar to that of the calcium silicates present in Portland cement, developing strength and thus potentially enabling the production of construction materials (Shui et al., 2008).

Shui, Xuan, Chen, Yu, & Zhang (2009), explored the effect of dehydration temperature between 300°C and 900°C on several properties of dehydrated-cement pastes such as: water requirement for standard consistency, setting time, degree of rehydration, and compressive strength. Highest 28-day compressive strength reported, equivalent to 60% of the strength developed by ordinary Portland cement pastes at the same age, was observed for pastes incorporating materials dehydrated at 800°C. In a more recent study, the use of dehydrated-cement as an activator for fly ash in a geopolymers-like cementitious material system was investigated (Shui et al., 2011). A design method based on the theoretical ratio of calcium to silicon was proposed, and strengths exceeding 60 MPa were achieved for steam cured pastes at 24 hours.

The dehydration process required to produce Reactivated Cementitious Materials (RCM) involves temperatures much lower than those required to produce new Portland cement, making it an interesting alternative for on-site recycling of fines derived from RCA production, or for recycling of cementitious materials from wash waters and rejected batches in concrete mixing plants. However, considering the wide variety of HCP sources which would be available, and the multiple options for both the reactivation process and the proportioning of pastes incorporating RCM, a study of the effect of a wider set of factors and factor interactions is required to evaluate this recycling alternative and to identify relevant parameters to optimize it.

In order to address these requirements, a two phase experimental study was developed beginning with an exploratory phase to identify and screen relevant factors, followed by a second phase focused on the in-depth study and characterization of their effects. This paper presents the results of a factorial experiment designed for the first phase of the study, meant to identify factors and factor interactions having a significant effect on the

cementitious characteristics of the RCM as indicated by the strength development of paste specimens produced with them. A total of 9 factors were selected to represent the most relevant inputs of the recycling process (**Figure 3.1**). These factors were grouped according to their role in the process (**Table 3.1**). Factors from group I correspond to characteristics of the waste materials and account for foreseeable variations of real HCP wastes. The characteristics of the original HCP, such as its degree of hydration, composition and concentration relative to inert materials present in the wastes were expected to affect the cementitious characteristics of the RCM produced from them. In order to have control over these characteristics, cement pastes were produced under laboratory conditions to supply the HCP wastes for this study. Factors from group II correspond to parameters of the reactivation process expected to affect the cementitious characteristics of the RCM, such as the maximum temperature of the dehydration process and the fineness to which materials are grinded before dehydration. Factors from group III control the proportioning of mixtures based on RCM. In these mixtures, it was expected that free lime present in the RCM would hydrate and provide  $\text{Ca}(\text{OH})_2$  for pozzolanic reactions with SCM additions. It was also expected that inert fines present along the HCP wastes would undergo transformations during the thermal process producing materials which could benefit from the addition of an alkaline activator to the RCM-based mixtures. Finally, partial substitution of RCM by OPC in these mixtures would allow evaluation of possible interactions between both materials for potential applications of RCM as supplementary cements.

Screening of relevant factors by identifying significant factor and factor-interaction effects provides key information for future investigations on the subject, and helps guide the characterization of HCP wastes required to select appropriate recycling processes.

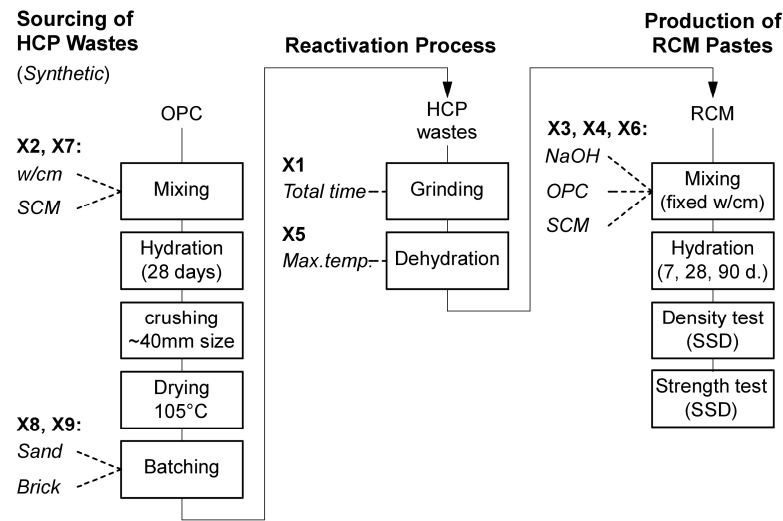


**Figure 3.1** Schematic diagram of experimental steps, showing factors associated with each step.

**Table 3.1** Assignment of experimental factors and their selected levels

Design factors	Experimental factors		Factor group	Levels					
	Name	Description		I	II	III	-1	0	+1
X1	<i>FGR</i>	additional grinding time (fine grinding)		o			0 min.	10 min	20 min.
X2	<i>DoH-s</i>	W/CM ratio of HCP waste (degree of hydration)		o			0.35	0.425	0.50
X3	<i>NaOH</i>	Alkaline activator content in RCM-paste			o		0 %	3 %	6 %
X4	<i>OPC</i>	Portland cement replacement in RCM-paste			o		0 %	2.5 %	5 %
X5	<i>T°DH</i>	Maximum temperature during dehydration			o		700 °C	750 °C	800 °C
X6	<i>SCM</i>	SCM replacement in RCM-paste			o		0 %	5 %	10 %
X7	<i>SCM-s</i>	SCM replacement in HCP waste			o		0 %	5 %	10 %
X8	<i>F.Si-s</i>	Inert siliceous fines in HCP waste (sand residues)			o		0 %	5 %	10 %
X9	<i>F.Al-s</i>	Inert clay brick fines in HCP waste (brick residues)			o		0 %	5 %	10 %
X10	B1	Blocking factor 1							
X11	B2	Blocking factor 2							

Notes: Factor groups indicate role of factors in the recycling process. Group I: source material factors. Group II: reactivation process factors. Group III: composition factors for RCM-based pastes.

### **3.2      Experimental design, materials and methods**

For identification and screening purposes the design of experiments approach enables an efficient use of experimental resources and time by reducing the number of observations required to assess relative factor relevance. It provides quantitative values for the effects of factors and factor interactions enabling fitting a linear model of the response within the experimental region explored. This model can be used to determine which factors merit further attention and can be expanded later with a minimal set of additional experimental runs to develop a detailed model of the response surface, which can be used to optimize the process parameters.

#### **3.2.1    Experimental design and experimental factors**

A fractional factorial experimental design was selected to keep the number of experimental cases within constraints. To accommodate the nine factors under study plus two blocking factors a  $2^{11-5}$  design was adapted from a published design (NIST/SEMATECH, 2003). This design requires only 64 experimental cases ( $2^6$ ), corresponding to a 1/32th fraction ( $2^{-5}$ ) of a full factorial design for 11 factors in two levels ( $2^{11}$ ). The fractioning was achieved using the defining relation  $I = 12347 = 13568 = 23569 = 345(10) = 126(11)$ . This means factor X7 is mapped to the interaction of factors X1\*X2\*X3\*X4, factor X8 is mapped to the interaction of factors X1\*X3\*X5\*X6, factor X9 is mapped to the interaction of factors X2\*X3\*X5\*X6, factor X10 is mapped to the interaction of factors X3\*X4\*X5, and factor X11 is mapped to the interaction of factors X1\*X2\*X6. Higher order interactions are not expected to have significant effect on the responses. However, as a consequence of fractioning some effects become aliased, *i.e.* some effects cannot be unambiguously estimated as they are confounded with effects of different factors or factor interactions. Nevertheless, in the selected design all main-factor effects and most of the 55 two-factor interaction effects are aliased to higher order interactions only (interactions of 3 or more factors). By careful assignment of experimental factors, most of the aliased two-factor interactions were made to involve blocking factors which are not expected to participate in interactions (Box & Hunter, 2005).

Only 6 two-factor interaction effects involving experimental factors remained aliased. Consequently, experimental factors least expected to display interaction effects were assigned to the design factors involved in the remaining aliased interactions.

Assignment of experimental factors to design factors is shown in **Table 3.1** including the experimental levels selected for each factor. Factors from group I were assigned design factors X2, X7, X8 and X9. Factor X2 (*DoH-s*) corresponds to the degree of hydration of the source pastes. The water to cementitious material mass ratio (W/CM) was used as an indirect way to obtain two different levels for the degree of hydration of the source pastes at a fixed hydration time. Preliminary tests showed that the selected 0.50 and 0.35 W/CM ratios produced a significant difference in non-evaporable water content –indicative of the degree of hydration– for OPC paste samples cured under water for a fixed period of time. Factor X7 (*SCM-s*) indicates the weight substitution level of OPC by silica fume in the source paste, and is meant to test for effects due to the use of SCM in the original composition of the wastes. Factors X8 (*F.Si-s*) and X9 (*F.Al-s*) were used to assess the effect of inert fine residues of siliceous (sand) and argillaceous (clay brick) composition, respectively, which are expected to be found along HCP wastes from actual concretes. Both inert materials were incorporated as substitution by weight of source paste.

Factors from group II were assigned design factors X1 and X5. Factor X1 (*FGR*) corresponds to the fineness to which the HCP wastes are grinded prior to dehydration. The different levels of fineness were achieved extending grinding time and changing the configuration of the mill. The grinding time used for the low level of fineness resulted in 85% of the material passing the No. 200 mesh (75 $\mu\text{m}$ ), while the time used for the high level resulted in 85% of the material passing the No. 325 mesh (45 $\mu\text{m}$ ). Factor X5 (*T°DH*) corresponds to the maximum temperature reached during dehydration. Although its general effect has been characterized (Shui et al., 2009), it was included it in order to assess its potential interactions with other factors.

Factors from group III were assigned design factors X3, X4 and X6. Factor X3 (*NaOH*), indicates the addition of sodium hydroxide as an alkaline activator to the RCM mixtures. The level to which the sodium hydroxide solution was incorporated is expressed as a percentage by weight of cementitious material, but substituting the equivalent volume of mixing water, following standard practice of studies on alkali activated materials (Dombrowski, Buchwald, & Weil, 2006). Factor X4 (*OPC*) indicates the weight substitution level of RCM by ordinary Portland cement in the mixtures. A low level of substitution was selected, as it was expected that Portland cement would outperform the corresponding amount of RCM being substituted. Finally, factor X6 (*SCM*) indicates the weight substitution level of RCM by silica fume in the mixtures.

To cope with the still large number of cases the design was divided in 4 blocks of 16 cases each according to the levels of the two blocking factors. Blocking factors were assigned design factors X10 and X11. Execution order of individual cases within each block was randomized. Additionally, two central cases were added in each block to enable direct estimation of the experimental variance of the response, required for the statistical significance test of the estimated effects. Central cases were executed at the average level of factors, in fixed order within each block (cases 5 and 14). For all cases in the design only one observation was performed for each response at each of the testing dates (7, 28 and 90 days). Nevertheless, due to the large number of cases in the design, the influence of potential outliers is reduced in the estimation of factor and factor interaction effects.

The main interest responses were the compressive strength of RCM-based pastes, at 7, 28 and 90 days of hydration (responses Y1, Y2 and Y3 respectively). Compressive strength was assessed on cubic specimens 20mm in size. Additionally, the average Saturated Surface Dry (SSD) density of the specimens was measured to determine potential correlation between strength and density results.

### 3.2.2 Materials and methods

Source pastes to supply HCP for the reactivation process were prepared using ordinary Portland cement conforming to ASTM C150-09 type I. The SCM used was a commercially available condensed Silica fume, composed of over 99% SiO<sub>2</sub> according to XRF analysis. Pastes were mixed using distilled water, and cast into shallow plastic molds of 2.0 L capacity (~250x200x40mm). As shown in **Table 3.2**, five pastes were prepared to account for the four combinations and average values of factors X2 and X7. Pastes were kept in the molds for 24 hours in a fog room at 23°C, and then unmolded and cured under water at 23°C until 28 days of hydration. The resulting paste slabs were crushed in chunks of 40mm maximum size which were then dried at 105°C until constant weight to stop hydration, and stored when still hot in sealed plastic containers to prevent hydration to proceed.

**Table 3.2** Composition of source pastes to supply HCP wastes (~2 L).

Mix	Composition				Curing	Weight loss % (105 °C)
	OPC	SCM	Water	W/CM		
W1	2700 g	300 g	1050 g	0.35	28 d	17.7 %
W2	3000 g	0	1050 g	0.35	28 d	16.9 %
W3	2520 g	280 g	1400 g	0.50	28 d	25.2 %
W4	2800 g	0	1400 g	0.50	28 d	21.8 %
W5	2850 g	150 g	1275 g	0.425	28 d	21.3 %

For the inert siliceous fines, Chilean standard sand (comparable to ASTM C778-06) was used. The inert clay brick fines were derived from fragments of calcined clay bricks from a local factory. These materials were proportioned according to the indicated levels of the factors for each experimental case and grinded together in batches with the corresponding amount of source HCP. Each batch totaled 150g of material including the HCP and the indicated amount of sand (0g or 15g) and brick fragments (0g or 15g) according to the levels of factors X8 and X9 respectively. For

the central cases 7.5g of sand and 7.5g of brick fragments were added to 135g of HCP.

Grinding was performed in dry state, in a 600-watt vibratory mill comprised of a stainless steel container where samples are placed together with a steel cylinder and a steel ring that move freely hitting the sample. All batches, including those for central cases, were grinded for an initial period of 10 minutes using the central cylinder only. Batches requiring higher fineness according to factor X1 were grinded for 20 additional minutes adding the ring. For the central cases the additional grinding time was 10 minutes. Grinded materials were stored in sealed plastic containers. Between grinding of each batch the mill was cleaned by grinding coarse sand until metal surfaces were free of residues.

Dehydration was performed in an electric muffle oven, in batches of 85g each. The maximum dehydration temperature, indicated by factor X5, was reached at a temperature increase rate of 10°/min starting from room temperature. Samples were kept at the maximum temperature for 1.5 hours, and then left to cool down at free rate inside the oven. When the temperature inside the oven reached below 300°C the samples were removed, weighed, and stored in sealed glass flasks while still hot.

The RCM-based pastes were mixed at 0.70 W/CM due to the high water demand of the RCM (Shui et al., 2009). For each case a total of 35g of cementitious material was mixed including the RCM and the indicated amount of OPC (0g or 1.75g) and silica fume (0g or 3.5g) according to the levels of factors X4 and X6 respectively. For the central cases the substituted amounts of RCM were 0.88g by OPC and 1.75g by silica fume. Distilled water was added at the fixed W/CM, incorporating either 0g or 2.10g of NaOH 8M solution as substitution by volume of water, as indicated by the level of factor X3. For the central cases 1.05g of NaOH 8M solution was used. For each case a total of 59.5g of mix was prepared, producing ~35mL of paste. Each resulting paste was cast in three 20mm-side cubic molds. Pastes were kept in the

molds for 24h at 23°C in a fog room at 100% R.H. After unmolding, the cubes were cured underwater at 23°C until the date of testing (7, 28 or 90 days).

Each cubic specimen was weighed in SSD condition to 0.01g precision before testing. At 7 days of hydration, the cube weighing the median value of the three cubes available was selected for compressive strength testing. At 28 days the cube with the highest weight was selected, leaving the cube with the lowest weight to be tested at 90 days. Compressive strength testing was performed at a loading rate of 0.100 kN/s, equivalent to 0.25 MPa/s. Fracture was automatically detected by the testing machine and maximum load reported with 0.01 kN precision.

### **3.3 Results and discussion**

Observations have no significant sign of autocorrelation which is consistent with the randomization of case execution within each block. The time order scatter plot for strength observations (**Figure 3.2**) shows no correlation of response with execution order, and no significant location or scale shift over time despite the execution in four separated blocks. The histogram of the observations shows a bi-modal distribution spreading over a wider range of values with increasing hydration time, attributed to a factorial design in two levels in which a reduced number of factors has a strong effect on the response.

Both compressive strength and SSD density increased with hydration time in all the cases observed. The relative strength of individual cases within each block varied significantly from 7 to 28 days of hydration. As seen in **Figure 3.3**, a wide range of 28-day strength results was observed for cases having similar 7-day strength, making early strength a bad predictor of long term strength ( $R^2=0.42$ ). Conversely, good agreement was found between 28-day and 90-day strength results ( $R^2=0.90$ ), and between 7, 28 and 90-day SSD density results.

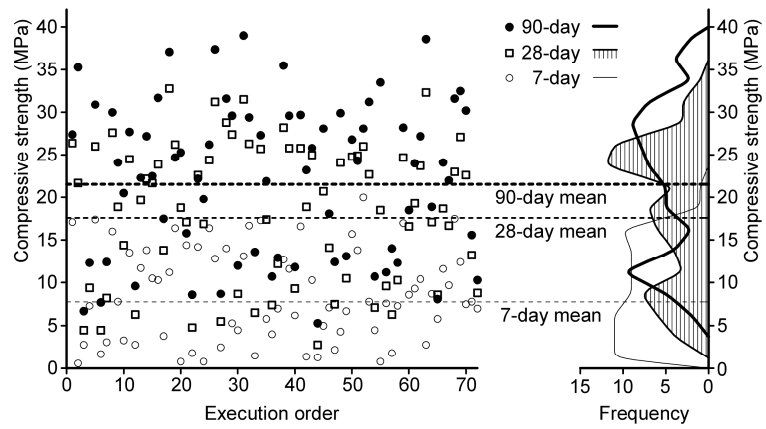


**Figure 3.2** Time order scatter plot of observed strength for all cases. Frequency shows bi-modal distribution of response spreading over hydration time.

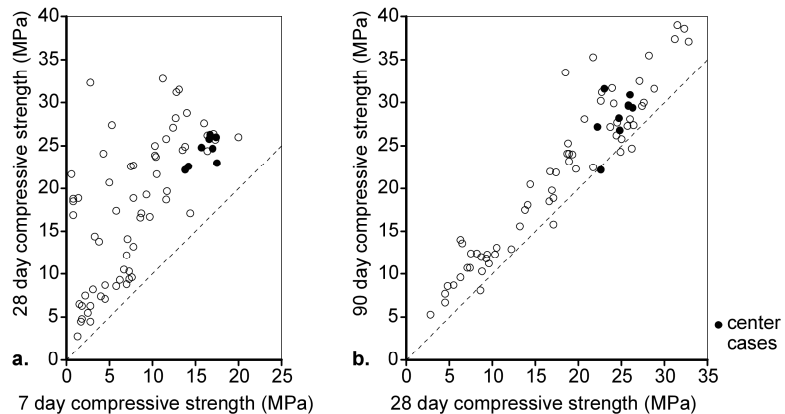


**Figure 3.3** Scatter plots of compressive strength observations. a) 28-day strength versus 7-day strength, b) 90-day strength versus 28-day strength.

No correlation was found between SSD density and compressive strength observations at 28 days of hydration (**Figure 3.4**). The observed variation of the compressive strength response is therefore attributed to the variation of the cementitious characteristics of the RCM produced.

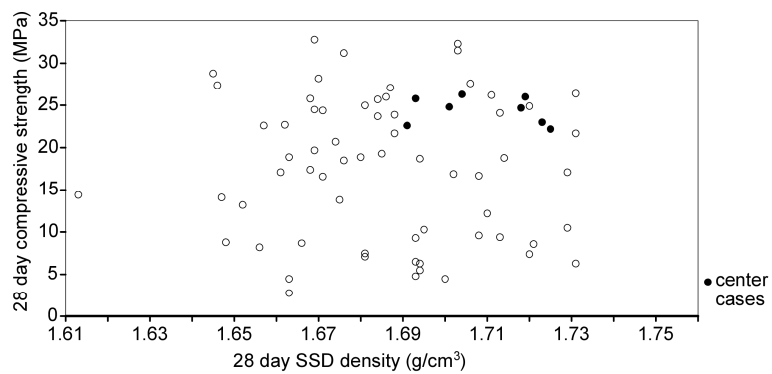


**Figure 3.4** Scatter plot of compressive strength observations versus SSD density observations for recycled paste specimens tested at 28 days.

Despite being produced at the average level of all experimental factors, central case specimens within each block displayed compressive strength and SSD density results significantly higher than block averages, indicating strong non-linearity of the responses in the experimental region explored. At 7 days of hydration, compressive strengths of central cases are consistently located in the upper quartile of results for each block. Although the difference is seen to decrease over time, the non-linearity is still significant at 90 days of hydration (**Figure 3.5**).

A temperature increase was observed on the fresh paste at the moment of mixing, which is indicative of a variable amount of free lime present in the RCM. Consistency of fresh pastes also varied considerably between different cases at the fixed W/CM used. Only a

subjective assessment of paste consistency was recorded during mixing, relative to which no evident correlation was found with results for compressive strength of RCM pastes.

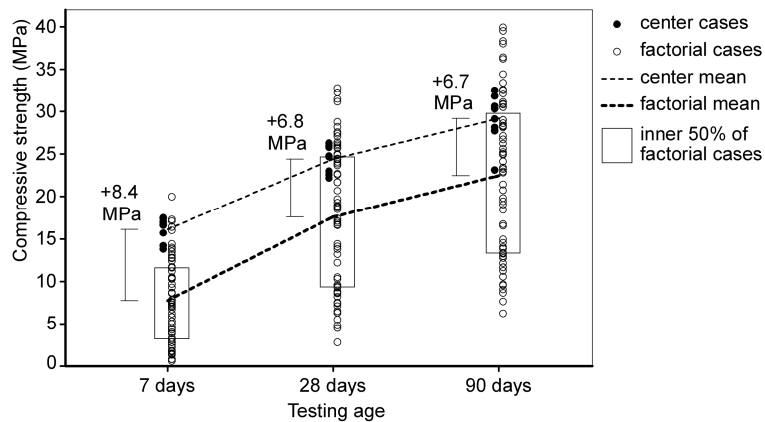


**Figure 3.5** Compressive strength observations at different testing ages. Average results of central cases deviate from average results of factorial cases.

### 3.3.1 Estimated effects of factors and factor interactions

Significance of factor and interaction effects was assessed using a statistical method complemented with a graphical method based on the normal probability plot of effects' estimates. For the statistical method, experimental variance of each response was determined from the median of the variance of the central cases within each block (4 degrees of freedom). The variance of the effects' estimates was calculated from the variance of the response considering the number of cases averaged to estimate the effects (i.e. variance of effects = 2/32 times the variance of the response). A 95% confidence interval was determined from the standard deviation of the effects' estimates and the corresponding points of the *t* distribution for a 5% probability with 4 degrees of freedom (**Table 3.3**).

**Table 3.3** Variance ( $S^2_R$ ) and standard deviation ( $S_R$ ) of responses and effects ( $S_{Ef}$ )

	Compressive strength		
	Y1 (7 days)	Y2 (28 days)	Y3 (90 days)
$S^2_R$	1.83 (4 DoF)	4.12 (4 DoF)	6.31 (4 DoF)
$S_R$	1.35 MPa	2.03 MPa	2.51 MPa
$S_{Ef}$	0.34 MPa	0.51 MPa	0.63 MPa
95% C.I. Effects	$\pm 0.94$ MPa	$\pm 1.41$ MPa	$\pm 1.74$ MPa

The estimates for effects of factors and two-factor interactions on compressive strength of RCM-based pastes at 7, 28, and 90 days of hydration are shown in **Tables 3.4, 3.5, and 3.6**, respectively. Effects exceeding the 95% confidence interval criteria are marked in bold typeface. Estimates for aliased effects are marked in italic typeface. All reported values are in units of the response, *i.e.* MPa. A relevance index is proposed for each factor, calculated as the ratio of the sum of the magnitude of its significant effects only, over the average maximum range of the response. If the main and interaction effects of a single factor could explain all the observed range of the response its relevance index would be close to one.

**Table 3.4** Effect of factors and interactions on response Y1: 7-day compressive strength of RCM pastes (MPa). 95% confidence interval:  $\pm 0.94$  MPa

Factor	Main effects	Two-factor interaction effects									Relevance (*)
		X2	X3	X4	X5	X6	X7	X8	X9		
		<i>DoH-s</i>	<i>NaOH</i>	<i>OPC</i>	<i>T°DH</i>	<i>SCM</i>	<i>SCM-s</i>	<i>F.Si-s</i>	<i>F.Al-s</i>		
X1 <i>FGR</i>	-0.68	<b>-1.23</b>	<b>1.69</b>	-0.05	<b>-1.36</b>	<b>-1.23</b>	<b>3.36</b>	0.05	0.55	<b>0.53</b>	
X2 <i>DoH-s</i>	<b>2.46</b>		0.13	0.20	0.01	0.36	<b>1.12</b>	0.55	0.05	<b>0.29</b>	
X3 <i>NaOH</i>	<b>1.86</b>			-0.91	<b>2.15</b>	<b>2.01</b>	<b>1.24</b>	-0.36	0.18	<b>0.53</b>	
X4 <i>OPC</i>	0.05				0.40	-0.41	-0.44	-0.37	0.15	0.00	
X5 <i>T°DH</i>	<b>-1.55</b>					<b>-1.04</b>	<b>-3.07</b>	0.31	-0.07	<b>0.55</b>	
X6 <i>SCM</i>	<b>4.76</b>						-0.05	0.86	-0.36	<b>0.54</b>	
X7 <i>SCM-s</i>	<b>1.77</b>							-0.05	<b>-1.30</b>	<b>0.71</b>	
X8 <i>F.Si-s</i>	<b>-1.70</b>								<b>-1.23</b>	0.18	
X9 <i>F.Al-s</i>	<b>-1.11</b>									0.14	

\* Sum of absolute values of significant effects of factor compared to maximum range of response.

**Table 3.5** Effect of factors and interactions on response Y2: 28-day compressive strength of RCM pastes (MPa). 95% confidence interval:  $\pm 1.41$  MPa

Factor	Main effects	Two-factor interaction effects									Relevance (*)
		X2	X3	X4	X5	X6	X7	X8	X9		
		<i>DoH-s</i>	<i>NaOH</i>	<i>OPC</i>	<i>T°DH</i>	<i>SCM</i>	<i>SCM-s</i>	<i>F.Si-s</i>	<i>F.Al-s</i>		
X1 <i>FGR</i>	0.35	-1.13	<b>1.51</b>	-0.45	-1.22	-0.13	<b>3.61</b>	1.12	1.37	<b>0.19</b>	
X2 <i>DoH-s</i>	<b>3.04</b>		-0.10	-0.56	0.68	0.61	<b>1.53</b>	1.37	1.12	<b>0.17</b>	
X3 <i>NaOH</i>	<b>-5.16</b>			<b>-1.45</b>	-0.10	<b>1.49</b>	-1.38	0.69	0.60	<b>0.36</b>	
X4 <i>OPC</i>	-0.14				-0.02	-1.08	-0.65	0.47	0.58	0.06	
X5 <i>T°DH</i>	<b>2.65</b>					-0.95	<b>-1.50</b>	0.29	-0.25	<b>0.16</b>	
X6 <i>SCM</i>	<b>12.37</b>						-1.10	1.25	-0.30	<b>0.52</b>	
X7 <i>SCM-s</i>	<b>3.85</b>							0.17	<b>-2.02</b>	<b>0.47</b>	
X8 <i>F.Si-s</i>	<b>-2.50</b>								-1.13	0.09	
X9 <i>F.Al-s</i>	-1.18									0.08	

\* Sum of absolute values of significant effects of factor compared to maximum range of response.

**Table 3.6** Effect of factors and interactions on response Y3: 90-day compressive strength of RCM pastes (MPa). 95% confidence interval:  $\pm 1.74$  MPa

Factor	Main effects	Two-factor interaction effects									Relevance (*)
		X2	X3	X4	X5	X6	X7	X8	X9		
		<i>DoH-s</i>	<i>NaOH</i>	<i>OPC</i>	<i>T°DH</i>	<i>SCM</i>	<i>SCM-s</i>	<i>F.Si-s</i>	<i>F.Al-s</i>		
X1 <i>FGR</i>	0.93	-0.89	1.58	0.63	-1.60	0.12	<b>2.87</b>	0.73	0.68	<b>0.09</b>	
X2 <i>DoH-s</i>	<b>2.17</b>		0.05	-1.07	-0.08	0.65	0.34	0.68	0.73	0.07	
X3 <i>NaOH</i>	<b>-8.50</b>			-1.23	-1.45	0.23	-1.56	0.57	0.20	<b>0.28</b>	
X4 <i>OPC</i>	-0.07				-0.52	-0.74	-0.55	0.17	1.01	0.00	
X5 <i>T°DH</i>	<b>2.83</b>					-0.62	-0.20	0.83	-0.02	<b>0.09</b>	
X6 <i>SCM</i>	<b>13.85</b>						-0.56	<b>2.04</b>	-0.14	<b>0.52</b>	
X7 <i>SCM-s</i>	<b>3.92</b>							0.30	-0.89	<b>0.22</b>	
X8 <i>F.Si-s</i>	<b>-2.16</b>								-0.89	<b>0.14</b>	
X9 <i>F.Al-s</i>	-0.27									0.00	

\* Sum of absolute values of significant effects of factor compared to maximum range of response.

### 3.3.2 Identification of significant factor and factor-interaction effects

Half-normal probability plots of the 63 effects of factors and factor interactions which can be estimated using the selected experimental design display good overall agreement between the selected 95% confidence interval and the graphical assessment of significance of effects. In these plots significant effects are expected to deviate from the line representing a normal distribution of effect estimates, meaning they cannot be explained by random errors. In the half normal plot of effects on 7-day compressive strength (**Figure 3.6**), several effects exceeding the selected confidence interval lay on the normal distribution line and thus they were screened out. Consequently, 6 factors and 5 two-factor interactions were identified as having a significant effect on 7-day strength of RCM-based pastes.

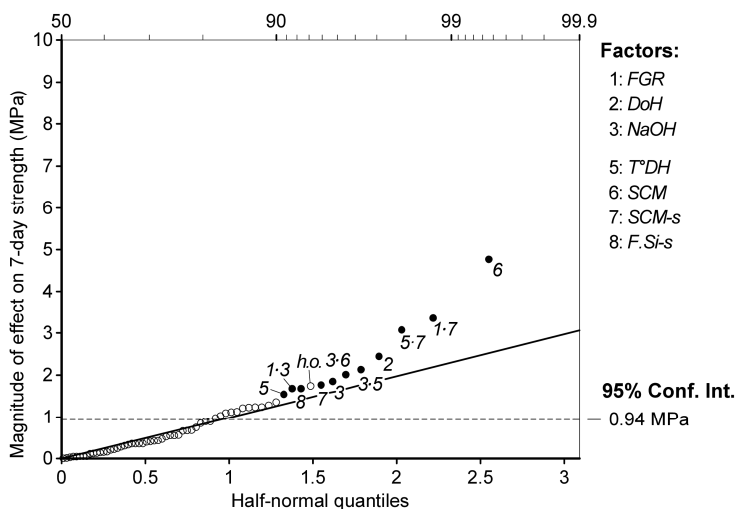


**Figure 3.6** Half-normal probability plot of estimated effects on 7-day compressive strength (h.o.: higher order effect, not considered).

In the half-normal probability plot of effects on 28-day compressive strength (**Figure 3.7**) it is evident that several effects just exceeding the selected confidence interval lay on the normal distribution line and thus they were screened out. Consequently, a total of 6 factors and 2 two-factor interactions were identified as having a significant

effect on 28-day strength of RCM-based pastes. Several of these factors and interactions also have a significant effect on 7-day strength; however, their relative importance differs substantially between the two testing ages.

Conversely, in the half normal plot of effects on 90-day compressive strength (**Figure 3.8**), several estimated effects not exceeding the selected confidence interval deviate from the normal distribution line and thus they were included in the analysis of effects. The set of factors and interactions considered is similar to the corresponding set of factors and interactions having a significant effect on 28-day compressive strength, with minor differences in the relative importance of their effects. Consequently, a total of 6 factors and 6 two-factor interactions were identified as having a significant effect on 90-day compressive strength of RCM-based pastes.

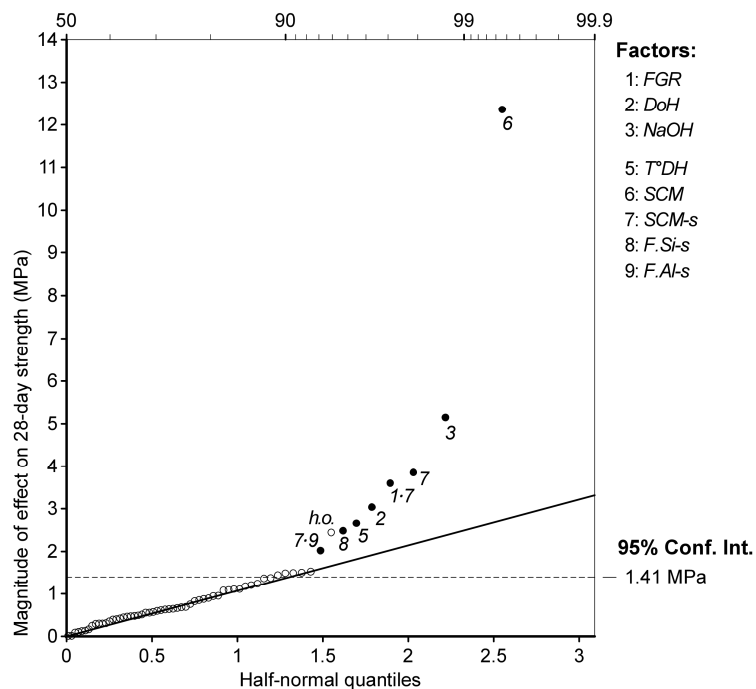


**Figure 3.7** Half-normal probability plot of estimated effects on 28-day compressive strength (h.o.: higher order effect, not considered).

Considering all hydration ages, a total of 6 factors and 9 two-factor interactions were identified as having a significant effect on compressive strength of the RCM-based pastes. Factors due to characteristics of HCP wastes displaying significant main effects were: the degree of hydration of the HCP wastes (X2), the use of silica fume in the composition of the HCP (X7) and the presence of inert siliceous fines intermixed in the HCP wastes (X8). Factor X7 was also involved in 4 significant two-factor interaction effects. Among reactivation process factors temperature of dehydration (X5) displayed a significant main effect, while the fineness of the wastes (X1) was involved only in significant two-factor interaction effects. Factors due to the proportioning of RCM-based pastes displaying significant main effects were: the addition of sodium hydroxide to the RCM-based pastes (X3) and the substitution of RCM by silica fume (X6), with both factors involved in several significant two-factor interaction effects.

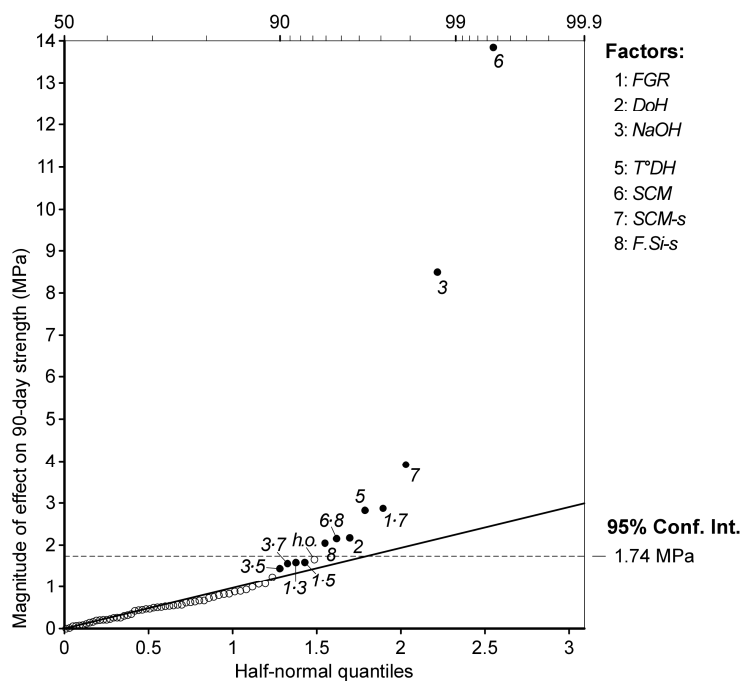


**Figure 3.8** Half-normal probability plot of estimated effects on 90-day compressive strength (h.o.: higher order effect, not considered).

### **3.3.3 Analysis of estimated effects on compressive strength of RCM-based pastes**

Compressive strength of RCM-based pastes was most affected by the level of substitution of RCM by silica fume (factor X6). In the experimental region explored, increasing the level of silica fume substitution in the RCM-based mixtures from 0% to 10% significantly increases average strength of the resulting pastes at all ages tested (**Figure 3.9**). This indicates RCM have a significant capacity for activating pozzolanic reactions. In addition, the estimated effect of silica fume substitution is higher when 5% NaOH solution is added to the RCM-based mixtures (interaction X6·X3). This interaction effect decreases gradually, being insignificant at 90 days. A possible explanation might be that the addition of NaOH solution potentiates the reactions involving silica fume in the RCM-based pastes at early ages, as OH<sup>-</sup> ions promote the dissolution of the amorphous silica. Similarly, the effect of silica fume substitution is higher when the HCP wastes contain 10% inert siliceous fines (interaction X6·X8). At 90 days of hydration this interaction effect is of similar magnitude than the negative effect of the inert siliceous fines on strength.

The effect of NaOH addition to the RCM-based mixtures (factor X3) was seen to evolve over hydration time. In the experimental region explored, increasing the addition of NaOH solution from 0% to 5% increases average strength of the resulting pastes at 7 days but decreases it at 28 and 90 days (**Figure 3.10**). Similar behavior has been observed in OPC-based and C<sub>3</sub>S-based pastes incorporating NaOH solutions. A reduced induction period and a general acceleration of initial hydration reactions are reported, however resulting in lower long term strength, probably due to replacement of Ca<sup>2+</sup> ions by Na<sup>+</sup> affecting the microstructure of the formed C-S-H (Juenger & Jennings, 2001). The effect of the NaOH addition is affected by the level of grinding of the HCP wastes (interaction X3·X1) and by the dehydration temperature used in the reactivation process (interaction X3·X5). When the HCP are grinded to higher fineness, the estimated effect of the NaOH addition is higher at 7 days, but lower at 28 and 90 days. This interaction increases the positive effect of

NaOH on 7-day strength and decreases its negative effect at later ages. When HCP wastes are dehydrated at 800°C, the estimated effect of the NaOH addition is higher at 7 and 90 days, increasing its positive effect on early strength, however, also increasing its negative effect on long term strength. It is suspected that both interactions are related to the availability of  $\text{Ca}^{2+}$  ions affecting the activity of  $\text{Na}^+$  ions in the RCM-based mixtures (Peterson, Neumann, & Livingston, 2006). Extended grinding process can result in extended carbonation of calcium bearing compounds, decreasing the availability of calcium ions in solution due to the low solubility of  $\text{CaCO}_3$ . Conversely, a higher dehydration temperature involves more decomposition of calcium bearing compounds into  $\text{CaO}$ , which readily combines with water to form soluble  $\text{Ca}(\text{OH})_2$ , increasing the availability of  $\text{Ca}^{2+}$  ions.

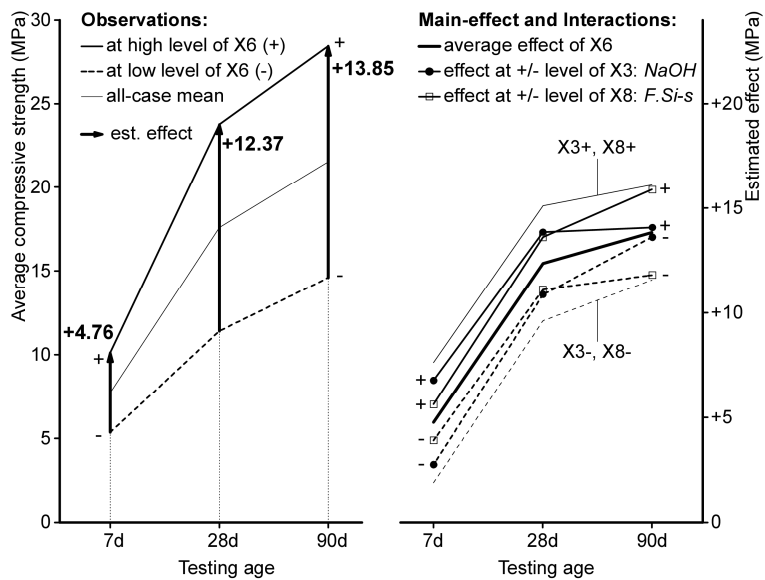


**Figure 3.9** Average compressive strength of RCM-based pastes at different levels of substitution of RCM by silica fume in the mixtures (factor X6), showing factor and interaction effects.

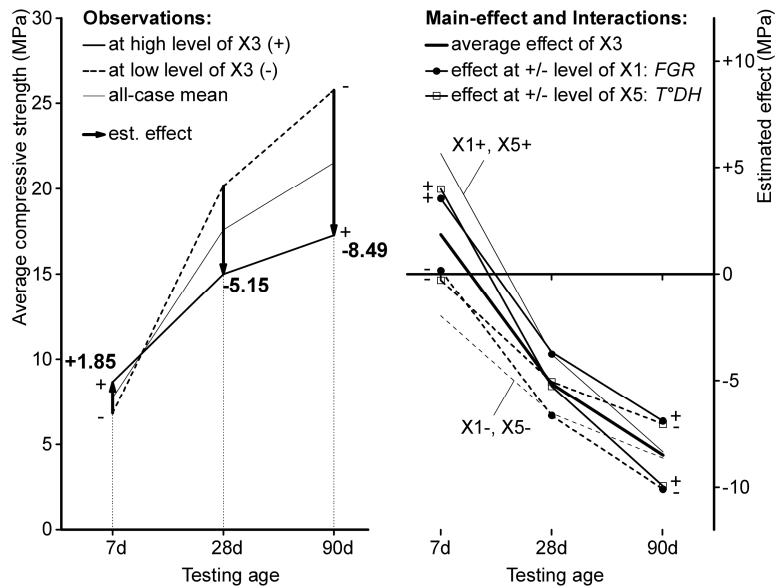


**Figure 3.10** Average compressive strength of RCM-based pastes at different levels of incorporation of NaOH solution to the mixtures (factor X3), showing factor and interaction effects.

Presence of silica fume substituting OPC in the original composition of the HCP wastes (factor X7) had a positive effect on compressive strength. In the experimental region explored, increasing the level of silica fume substitution in the source HCP from 0% to 10% increases average strength of RCM-based pastes (**Figure 3.11**). This is consistent with the product from C-S-H dehydration having a significant role in the strength gain of the RCM-based pastes, assuming more C-S-H should have formed as a product of pozzolanic reactions in the HCP incorporating silica fume. The estimated effect of silica fume substitution in the source HCP is higher when the HCP wastes are grinded to higher fineness (interaction X7·X1). It is believed that through extended grinding a significant amount of unreacted silica fume from the HCP wastes becomes available for pozzolanic reactions in the RCM-based pastes, increasing strength in agreement with the estimated effect of factor X6. Conversely, when the HCP are dehydrated at 800°C the estimated effect of the silica fume

substitution in the source HCP is lower at 7 and 28 days (interaction X7·X5). Likewise, the estimated effect of the silica fume substitution in the source HCP is lower at all ages tested when the HCP contain 10% inert fines from clay bricks (interaction X7·X9). It must be noted that the combined effect of the three interactions involving this factor can increase or decrease its effect by more than 7 MPa at 7 and 28 days, when the other factors involved are set at the appropriate levels.

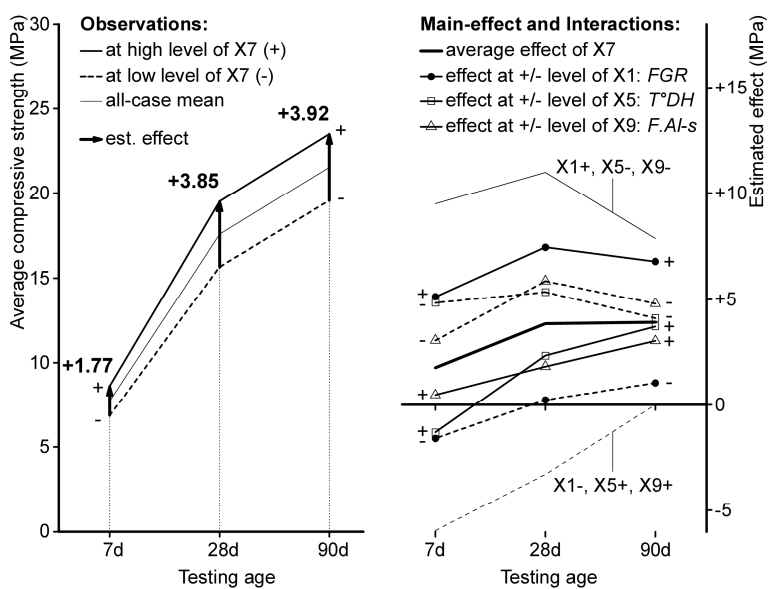


**Figure 3.11** Average compressive strength of RCM-based pastes at different levels of presence of silica fume in original composition of HCP wastes (factor X7), showing factor and interaction effects.

The effect of the dehydration temperature during the reactivation process (factor X5) was seen to evolve over time. In the experimental region explored, increasing the dehydration temperature from 700°C to 800°C decreases average strength of the RCM-based pastes at 7 days, but increases it at 28 and 90 days (**Figure 3.12**). A varying proportion of different dehydrated products in the RCM, resulting from the different dehydration temperatures used, could be the cause of the observed effect.

The estimated effect of the dehydration temperature depends on the extent of grinding of the HCP wastes (interaction X5·X1), being higher when the HCP wastes are grinded to higher fineness.

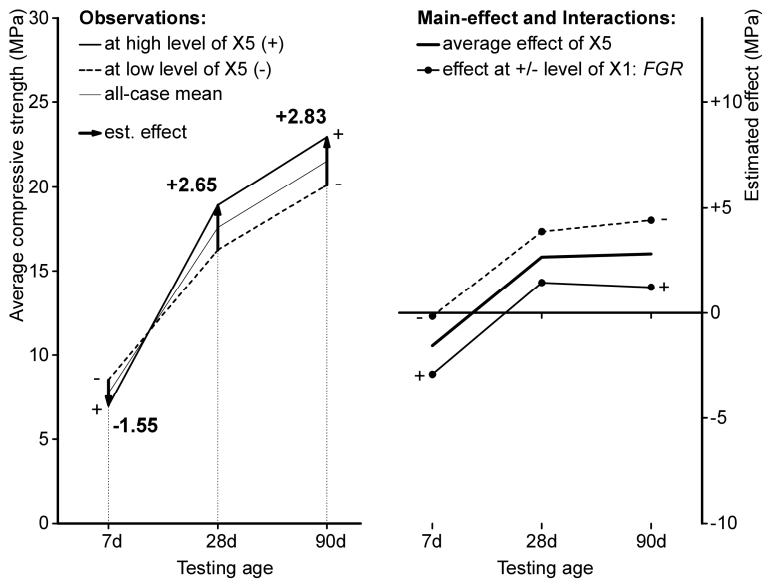


**Figure 3.12** Average compressive strength of RCM-based pastes at different levels of dehydration temperature (factor X5), showing factor and interaction effects.

Remaining significant main-factor effects are shown in **Figure 3.13**. In the experimental region explored, increasing the W/CM ratio of the source HCP from 0.35 to 0.50, i.e. increasing the degree of hydration of the HCP (factor X2), increases average strength of RCM-based pastes at all ages tested. A higher degree of hydration involves more C-S-H available for reactivation. However, the higher degree of hydration also means less unreacted cement remaining in the HCP wastes. Nevertheless, the calcium silicate produced from the dehydration of C-S-H probably has a high surface area, and could be more active during rehydration than the remaining unreacted cement grains which are usually concealed under a layer of

dense hydration products. Finally, in the experimental region explored, increasing the content of inert siliceous fines in the HCP (factor X8) from 0% to 10% decreases average strength of RCM-based pastes at all ages tested.

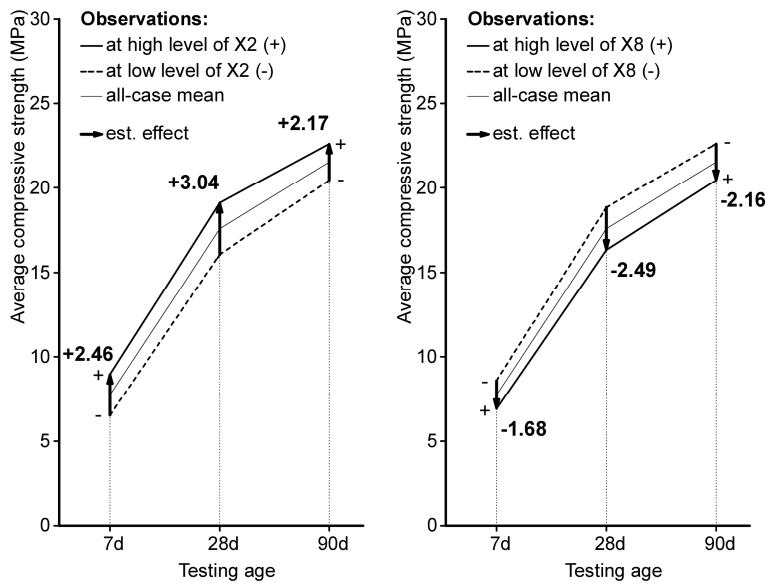


**Figure 3.13** Average compressive strength of RCM-based pastes at different levels of degree of hydration of HCP wastes (factor X2) and at different levels of presence of inert siliceous fines along the HCP wastes (factor X8).

### 3.3.4 Response models

The factorial experimental design performed allows for the fitting of a linear model of the response based on the estimated effects of factors and interactions. Although results from central cases indicate the response is strongly non-linear in the experimental region explored, the source of this non-linearity cannot be identified from the experiment as designed and performed. Consequently, the models reported were fitted to the factorial experimental cases only. These models are meant solely to confirm the selection of significant factors according to the screening and

identification purposes of the study, and, therefore, they include only the non-confounded main-factor and two-factor interaction effects identified as significant. Models for compressive strength of recycled pastes at 7, 28, and 90 days, are respectively:

$$Y_{i1} = 7.73 + 1.23 X_{i2} + 0.93 X_{i3} - 0.77 X_{i5} + 2.38 X_{i6} + 0.89 X_{i7} - 0.85 X_{i8} \\ + 0.85 X_{i1}X_{i3} - 0.68 X_{i1}X_{i5} + 1.68 X_{i1}X_{i7} + 1.07 X_{i3}X_{i5} + 1.01 X_{i3}X_{i6} \\ - 1.53 X_{i5}X_{i7} + \varepsilon_{i1} \quad (3.1)$$

$$Y_{i2} = 17.57 + 1.52 X_{i2} - 2.58 X_{i3} + 1.33 X_{i5} + 6.18 X_{i6} + 1.92 X_{i7} - 1.25 X_{i8} \\ + 1.81 X_{i1}X_{i7} - 1.01 X_{i7}X_{i9} + \varepsilon_{i2} \quad (3.2)$$

$$Y_{i3} = 21.51 + 1.08 X_{i2} - 4.25 X_{i3} + 1.41 X_{i5} + 6.92 X_{i6} + 1.96 X_{i7} - 1.08 X_{i8} \\ + 0.79 X_{i1}X_{i3} - 0.80 X_{i1}X_{i5} + 1.44 X_{i1}X_{i7} - 0.72 X_{i3}X_{i5} + 0.78 X_{i3}X_{i7} \\ + 1.02 X_{i6}X_{i8} + \varepsilon_{i3} \quad (3.3)$$

Where, for any particular observation  $i$ ,  $Y_{iz}$  is the predicted response,  $X_{ij}$  is the coded level of every  $X_j$  factor (-1, +1), and  $\varepsilon_{iz}$  is the random error of the respective response. In these equations the regression coefficients are in response units (MPa).

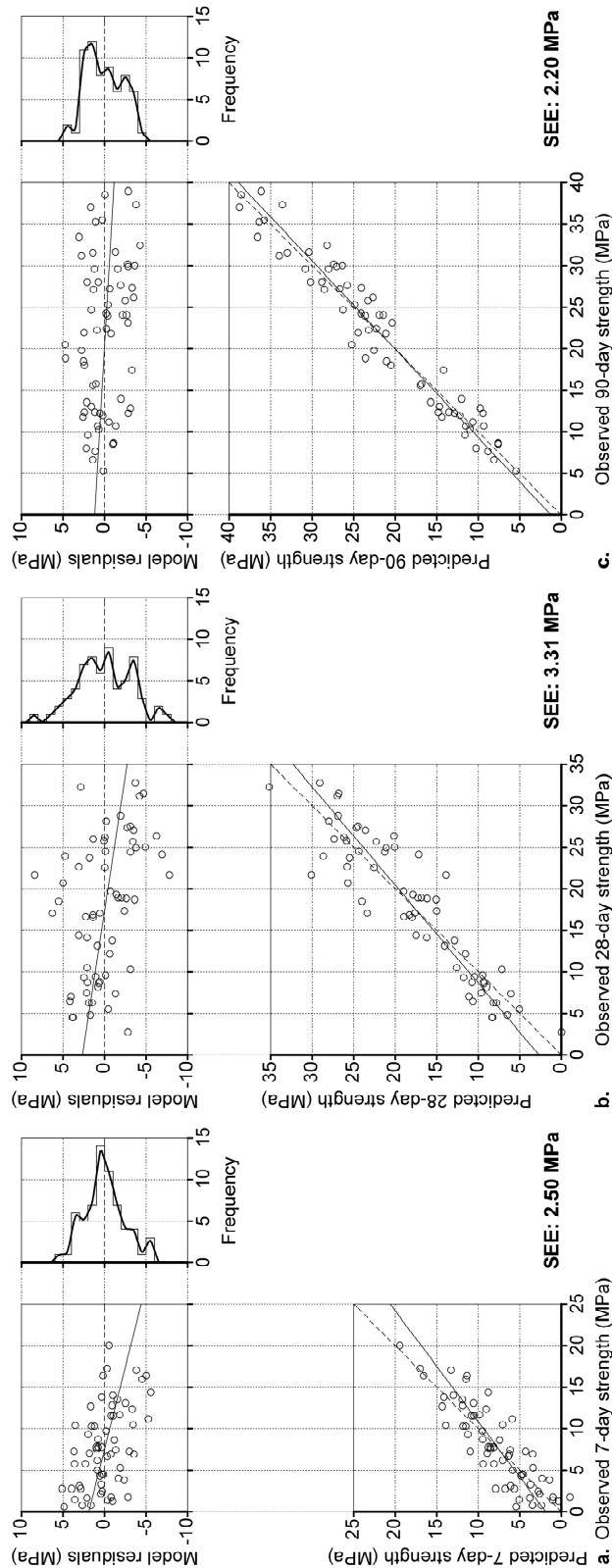


**Figure 3.14** Scatter plots of predicted (model) versus observed compressive strength at 7, 28, and 90 days, including residual values, and histogram of residuals.

As seen in **Figure 3.14**, the models fit the experimental data and display approximately normal distributions for the residuals. The model for the compressive strength at 90 days displays the least amount of deviation from the observed values, with the lowest standard error of the estimate (2.20 MPa). This error compares well with the standard deviation of the response calculated from the central case results at 90 days (2.51 MPa). The model for compressive strength at 28 days, which includes the least number of effects, displays the largest deviation from the observed values. The model for 7-day compressive strength displays normally distributed residuals, however with a marked drift towards under estimation of the response for higher strength observations. The general fit of the models indicates a substantial portion of the range of strength results is explained by the effect of the selected factors and interactions. Additionally, the selection of factors is confirmed to be particularly adequate to explain and predict long term strength response.

### **3.3.5      Optimum levels of factors**

Within the experimental region explored the models can be used to predict combinations of factor levels yielding highest strength. Since the effect of factors and interactions evolve over time, there is not a particular combination of factors that can maximize early and long term strength simultaneously. Considering 90-day strength of RCM-based pastes as the most relevant response, optimal levels of factors for four different initial conditions (a, b, c and d) are given in **Table 3.7**. In all cases higher strength of RCM-based paste would be obtained at a high level of substitution of RCM by silica fume. For HCP wastes including inert fines from either sand or brick residues (condition a), highest long term strength of RCM-based pastes would be obtained if wastes have a high degree of hydration, and reactivating them at the higher temperature of dehydration. However, for HCP wastes including silica fume (condition b), the highest strength would be obtained increasing the time of grinding of the wastes.

**Table 3.7** Combinations of factor levels for optimum long term strength

Conditions	Factors (coded levels)												Predicted responses			
	HCP waste composition				Reactivation		RCM-paste mixture			Strength		Density				
	X2	X7	X8	X9	X1	X5	X3	X4	X6	(MPa)	(g/cm <sup>3</sup> )					
	<i>DoH-s</i>	<i>SCM-s</i>	<i>F.Si-s</i>	<i>F.Al-s</i>	<i>FGR</i>	<i>T°DH</i>	<i>NaOH</i>	<i>OPC</i>	<i>SCM</i>	7-d	28-d	90-d	28-d			
a	+	-	+	+	-	+	-	-	+	10.6	28.8	36.1	1.686			
b	+	+	+	+	+	+	-	-	+	6.2	30.7	38.4	1.686			
c	+	+	+	+	-	-	-	-	+	11.3	24.4	32.9	1.643			
d	+	-	-	-	-	+	-	-	+	12.3	29.3	36.3	1.708			

If grinding time and temperature of dehydration are set at their low levels less energy would be required for the reactivation process (condition c). In this scenario, higher strengths would be obtained from HCP wastes including silica fume and having a high degree of hydration. An additional waste beneficiation process might be implemented, incorporating a silica-rich SCM and improving hydration of the wastes, for instance by wet grinding of the wastes. Finally, for HCP wastes from pure pastes (condition d) the highest strengths would be obtained for HCP having a high degree of hydration, reactivating them at the higher dehydration temperature.

### 3.4 Conclusions

In order to evaluate a process for the recycling of HCP wastes based reactivation of their cementitious characteristics by dehydration, it was first necessary to identify material and process parameters affecting the binding performance of the RCM obtained. This study has contributed to our knowledge of the reactivation process and its products, screening relevant factors to identify significant factor and factor interaction effects on compressive strength of RCM-based pastes.

RCM display significant cementitious behavior as indicated by the strength gain of pastes made with them at 0.7 W/CM ratio. Maximum individual case values were: 20.0 ( $\pm 1.4$ ), 32.8 ( $\pm 2.0$ ), and 39.0 ( $\pm 2.5$ ) MPa at 7, 28, and 90 days, respectively. However, these

maximum values were observed at different combinations of factor levels at the different testing ages. Therefore, the effects of factors on compressive strength evolve over time. This is particularly evident between 7 and 28 days of hydration. Since no correlation was found between strength and density results, differences in strength among individual cases are likely explained by the different cementitious characteristics of the RCM produced at the different levels of the factors.

Average strength of central cases, i.e. those performed at the medium level of the factors, was significantly higher than the average strength of the rest of the cases in the experiment. This indicates a large non-linearity of the response in the experimental region explored. However, identification of factors causing the reported non-linearity is beyond the possibilities of the selected factorial experimental design in two levels.

Effects of factors were estimated by linear regression of the results of the experimental design. Significance of estimated effects was determined by comparing their magnitude with the standard deviation of the effects, with a 95% confidence interval, and by a graphical method. Considering results from the 3 testing ages covered, 6 main-factor and 9 two-factor interactions, involving 7 of the factors under study, were identified as having a significant effect on strength of RCM-based pastes.

In the experimental region explored:

1. Increasing RCM substitution by silica fume as SCM in RCM-based pastes significantly increases their average strength, indicating RCM have substantial pozzolanic activation capacity. Additionally, this effect is higher for RCM produced from HCP wastes containing inert siliceous fines.
2. Increasing addition of NaOH alkaline activator in RCM-based pastes increases their early age strength, but decreases their long term strength. Although the activator is involved in several significant interactions, the combined effect of the factor and its interactions did not prove beneficial for the strength of RCM-based pastes.

3. Increasing the degree of hydration of the HCP wastes increases average strength of RCM-based pastes. At a high degree of hydration HCP is expected to contain a higher concentration of C-S-H. Therefore, the dehydrated product of C-S-H is regarded as a significant cementitious component of RCM.
4. Increasing substitution of OPC by silica fume in the source HCP increases average strength of RCM-based pastes. This effect increases significantly when the wastes are grinded to higher fineness. Conversely, it decreases when the wastes are dehydrated at the higher temperature or when the wastes contain fines from clay bricks.
5. Increasing the dehydration temperature used to reactivate the HCP wastes decreases average early strength of RCM-pastes, but significantly increases their long term strength. However, the effect of dehydration temperature is shifted up when the wastes are grinded to a lower fineness, rendering the negative effect on early strength insignificant.
6. Increasing the content of inert fines in the HCP wastes decreases the average strength of RCM-based pastes due to dilution of the cementitious material. However, this negative effect is significant only for the fines from siliceous sand. In the range of substitution levels studied, the effect of fines from clay bricks is hardly detectable at 90 days of hydration, suggesting these fines are better incorporated in the hydration products responsible for strength gain.

Based on the number of their significant factor and factor interaction effects the following factors have the highest potential for optimization of strength of RCM-based pastes:

Source material factors (group I):

Degree of hydration of the HCP wastes

Use of silica fume in the original composition of the HCP

Presence of inert siliceous fines along the HCP wastes

Reactivation process factors (group II):

Extent of grinding of the HCP wastes

Maximum dehydration temperature

Proportioning factors for RCM-based mixtures (group III):

Substitution of RCM by silica fume

Besides the exploration of the selected factors through a wider set of levels and on a wider set of interest responses, a better understanding of the physical and chemical processes explaining the estimated effects would be required to implement this recycling alternative for HCP wastes from concretes. Developing of alternative or additional process steps and optimization of the reactivation process to accommodate the relevant characteristics of real wastes will undoubtedly follow. However, the great potential of these materials has been established.

### **3.5 Acknowledgments**

The authors wish to thank the Laboratorio de Resistencia de Materiales, RESMAT (DICTUC) for its collaboration, and Mr. Mauricio Guerra of the Construction Materials Laboratory of the School of Engineering at Pontificia Universidad Católica de Chile for his work to support this study.

### **3.6 References**

Abbas, A., Fathifazl, G., Isgor, O. B., Razaqpur, a. G., Fournier, B., & Foo, S. (2009).

Durability of recycled aggregate concrete designed with equivalent mortar volume method. *Cement and Concrete Composites*, 31(8), 555–563.  
doi:10.1016/j.cemconcomp.2009.02.012

Achtemichuk, S., Hubbard, J., Sluce, R., & Shehata, M. H. (2009). The utilization of recycled concrete aggregate to produce controlled low-strength materials without

- using Portland cement. *Cement and Concrete Composites*, 31(8), 564–569. doi:10.1016/j.cemconcomp.2008.12.011
- Ai, H. M., Wei, J., Bai, J. Y., & Lu, P. G. (2011). Properties of Recycled-Cement Produced from Waste Concrete. *Advanced Materials Research*, 194-196, 1170–1175. doi:10.4028/www.scientific.net/AMR.194-196.1170
- Alonso, C., & Fernandez, L. (2004). Dehydration and rehydration processes of cement paste exposed to high temperature environments. *Journal of Materials Science*, 39, 3015–3024.
- Arioz, O. (2007). Effects of elevated temperatures on properties of concrete. *Fire Safety Journal*, 42(8), 516–522. doi:10.1016/j.firesaf.2007.01.003
- Box, G. E. P., & Hunter, J. S. (2005). *Statistics for Experimenters* (2nd Ed., p. 212). Hoboken, New Jersey: John Wiley & Sons, Inc.
- Castellote, M., Alonso, C., Andrade, C., Turrillas, X., & Campo, J. (2004). Composition and microstructural changes of cement pastes upon heating, as studied by neutron diffraction. *Cement and Concrete Research*, 34(9), 1633–1644. doi:10.1016/S0008-8846(03)00229-1
- DeJong, M. J., & Ulm, F.-J. (2007). The nanogranular behavior of C-S-H at elevated temperatures (up to 700 °C). *Cement and Concrete Research*, 37(1), 1–12. doi:10.1016/j.cemconres.2006.09.006
- Dombrowski, K., Buchwald, A., & Weil, M. (2006). The influence of calcium content on the structure and thermal performance of fly ash based geopolymers. *Journal of Materials Science*, 42(9), 3033–3043. doi:10.1007/s10853-006-0532-7

- Farage, M. C. R., Sercombe, J., & Gallé, C. (2003). Rehydration and microstructure of cement paste after heating at temperatures up to 300 °C. *Cement and Concrete Research*, 33(7), 1047–1056. doi:10.1016/S0008-8846(03)00005-X
- Fridrichová, M. (2007). Hydration of belite cements prepared from recycled concrete residues. *Ceramics-Silikaty*, 51(1), 45–51. Retrieved from [http://www.ceramics-silikaty.cz/2007/2007\\_01\\_045.htm](http://www.ceramics-silikaty.cz/2007/2007_01_045.htm)
- Gartner, E. (2004). Industrially interesting approaches to “low-CO<sub>2</sub>” cements. *Cement and Concrete Research*, 34(9), 1489–1498. doi:10.1016/j.cemconres.2004.01.021
- Handoo, S. K., Agarwal, S., & Agarwal, S. K. (2002). Physicochemical, mineralogical, and morphological characteristics of concrete exposed to elevated temperatures. *Cement and Concrete Research*, 32(7), 1009–1018. doi:10.1016/S0008-8846(01)00736-0
- Huntzinger, D. N., & Eatmon, T. D. (2009). A life-cycle assessment of Portland cement manufacturing: comparing the traditional process with alternative technologies. *Journal of Cleaner Production*, 17(7), 668–675. doi:10.1016/j.jclepro.2008.04.007
- Janotka, I., & Mojumdar, S. C. (2005). Thermal analysis at the evaluation of concrete damage by high temperatures. *Journal of Thermal Analysis and Calorimetry*, 81(1), 197–203. doi:10.1007/s10973-005-0767-6
- Juenger, M. C. G., & Jennings, H. M. (2001). Effects of High Alkalinity on Cement Pastes. *ACI Materials Journal*, 98, 251–255.
- Juenger, M. C. G., Winnefeld, F., Provis, J. L., & Ideker, J. H. (2011). Advances in alternative cementitious binders. *Cement and Concrete Research*, 41(12), 1232–1243. doi:10.1016/j.cemconres.2010.11.012
- Kasai, Y. (2004). Recent Trends in Recycling of Concrete Waste and Use of Recycled Aggregate Concrete in Japan. In T. C. Liu & C. Meyer (Eds.), *SP-219-Recycling*

- concrete and other materials for sustainable development* (pp. 11–34). Farmington Hills: American Concrete Institute International.
- Lauritzen, E. K. (2004). Recycling concrete-An Overview of Challenges and Opportunities. In T. C. Liu & C. Meyer (Eds.), *SP-219-Recycling concrete and other materials for sustainable development* (pp. 1–10). Farmington Hills: American Concrete Institute International.
- Lin, Y.-H., Tyan, Y.-Y., Chang, T.-P., & Chang, C.-Y. (2004). An assessment of optimal mixture for concrete made with recycled concrete aggregates. *Cement and Concrete Research*, 34(8), 1373–1380. doi:10.1016/j.cemconres.2003.12.032
- Mendes, A., Sanjayan, J., & Collins, F. (2007). Phase transformations and mechanical strength of OPC/Slag pastes submitted to high temperatures. *Materials and Structures*, 41(2), 345–350. doi:10.1617/s11527-007-9247-8
- Meyer, C. (2009). The greening of the concrete industry. *Cement and Concrete Composites*, 31(8), 601–605. doi:10.1016/j.cemconcomp.2008.12.010
- NIST/SEMATECH. (2003). e-Handbook of Statistical Methods. Retrieved from <http://www.itl.nist.gov/div898/handbook/>
- Okada, Y., Sasaki, K., Zhong, B., Ishida, H., & Mitsuda, T. (1994). Formation Processes of  $\beta$ -C<sub>2</sub>S by the Decomposition of Hydrothermally Prepared C-S-H with Ca(OH)2. *Journal of the American Ceramic Society*, 77, 1319–1323. doi:DOI: 10.1111/j.1151-2916.1994.tb05409.x
- Peterson, V. K., Neumann, D. a., & Livingston, R. a. (2006). Effect of NaOH on the kinetics of tricalcium silicate hydration: A quasielastic neutron scattering study. *Chemical Physics Letters*, 419(1-3), 16–20. doi:10.1016/j.cplett.2005.11.032

- Phan, L. T., Lawson, J. R., & Davis, F. L. (2001). Effects of elevated temperature exposure on heating characteristics, spalling, and residual properties of high performance concrete. *Materials and Structures*, 34(March), 83–91.
- Poon, C. S., Azhar, S., Anson, M., & Wong, Y. L. (2001). Strength and durability recovery of fire-damaged concrete after post-fire-curing. *Cement and Concrete Research*, 31(9), 1307–1318. doi:10.1016/S0008-8846(01)00582-8
- Poon, C. S., Qiao, X. C., & Chan, D. (2006). The cause and influence of self-cementing properties of fine recycled concrete aggregates on the properties of unbound sub-base. *Waste management (New York, N.Y.)*, 26(10), 1166–72. doi:10.1016/j.wasman.2005.12.013
- Poon, C. S., Shui, Z. H., & Lam, L. (2004). Effect of microstructure of ITZ on compressive strength of concrete prepared with recycled aggregates. *Construction and Building Materials*, 18(6), 461–468. doi:10.1016/j.conbuildmat.2004.03.005
- Shui, Z., Xuan, D., Chen, W., Yu, R., & Zhang, R. (2009). Cementitious characteristics of hydrated cement paste subjected to various dehydration temperatures. *Construction and Building Materials*, 23(1), 531–537. doi:10.1016/j.conbuildmat.2007.10.016
- Shui, Z., Xuan, D., Wan, H., & Cao, B. (2008). Rehydration reactivity of recycled mortar from concrete waste experienced to thermal treatment. *Construction and Building Materials*, 22(8), 1723–1729. doi:10.1016/j.conbuildmat.2007.05.012
- Shui, Z., Yu, R., & Dong, J. (2012). Activation of Fly Ash with Dehydrated Cement Paste, *ACI Materials Journal*, 108 (2), 204-208.
- U.S. Geological Survey. (2009). *Mineral Commodity Summaries* (pp. 40–41). Reston.

#### **4. USE OF REACTIVATED CEMENTITIOUS MATERIALS FOR THE PRODUCTION OF MORTARS**

Ricardo Serpell, Mauricio López

Submitted, August 2013: *Cement and Concrete composites.*

##### **Abstract**

The production of reactivated cementitious materials is an alternative for the recycling of hydrated-cement-rich fines left from the crushing of concrete wastes to produce recycled aggregates. Reactivation is a thermal process where calcium silicate hydrates present in the fines dehydrate and form compounds which can develop cementitious behavior upon rehydration. In this study, a central composite experimental design was used to assess and model the effects of the reactivation temperature and of the substitution level of reactivated material by supplementary cementitious material on the flowability, compressive strength, and expansion of reactivated cementitious material mortars. Effects of reactivation temperature correlated with the content of reactive phases identified in the materials, particularly a stabilized form of alpha'-C<sub>2</sub>S. Effects of substitution depended on the supplementary material used, but were generally similar to the effects equivalent substitutions have on the properties of Portland cement mortars.

**Keywords:** Cement recycling, concrete recycling, silica fume, fly ash, dehydrated cement paste.

#### **4.1        Introduction**

Concrete contributes a large fraction of the solid wastes generated in developed countries, constituting the largest single component of the construction and demolition wastes (Meyer, 2009; Tam & Tam, 2006). In order to reduce the environmental impact of the construction industry, increasing amounts of concrete wastes are crushed to produce recycled aggregates for future construction work, particularly in countries with limited access to appropriate landfill areas and reduced availability of natural aggregate sources (Lopes de Brito, Gonçalves, & dos Santos, 2006). Reclamation process is based on the mechanical separation of the original aggregates from the mortar (cement paste and sand) adhered to them, which would otherwise adversely affect the fresh and hardened properties of concretes made with the recycled aggregates (Sanchez de Juan & Alaejos Gutiérrez, 2009; Shayan & Xu, 2003). In order to obtain higher quality aggregates successive crushing stages and additional thermal or chemical processes can be combined to enhance the separation of the adhered mortar. However, as separation improves, the weight percent of crushed concrete reclaimed as aggregates decreases. In addition, since attached mortar content increases as the size fraction of the aggregate decreases (Sanchez de Juan & Alaejos Gutiérrez, 2009), production is usually limited to coarse recycled aggregates. As a consequence, the largest part of the concrete wastes is transformed into fines and powder, which find little use in construction except as a backfilling material.

Due to their high concentration of residual hydrated cement paste, fines left from the production of recycled aggregates are avoided in conventional concrete mixtures (Kenai et al., 2002; Khatib, 2005). However, their chemical composition, also a result of their high content of hydrated cement, makes them an interesting raw material for the production of recycled cementitious materials. Through a thermal reactivation process the binding capacity of the cementitious material can be partially recovered. Dehydration of calcium silicate hydrates over 600 °C leads to the formation of unhydrated compounds which have been described as similar in composition and structure to the dicalcium silicate present in Portland cement (Alonso & Fernandez, 2004). The rehydration of these compounds displays cementitious behavior, developing strength and thus potentially enabling the

recycling of the hydrated cement wastes as a valuable construction material (Shui et al., 2008). Using laboratory sourced pastes as raw material, Shui, Xuan, Chen, Yu, & Zhang (2009), found that the temperature used in the dehydration process significantly affect the water requirement for standard consistency, the degree of hydration and the compressive strength of pastes based on the reactivated material. Compressive strength was found to increase with increasing dehydration temperature between 300 and 800 °C. The 28-day compressive strength of pastes based on material dehydrated at 800 °C was reported to be 60% of the strength achieved by the original Portland cement paste. However, compressive strength decreased when dehydration temperature was further increased to 900 °C.

In a previous study, we investigated the main and interaction effects of nine material and process factors on the 7, 28 and 90-day compressive strength of pastes based on reactivated cementitious material (RCM) using a factorial experimental design in two-levels (Serpell & Lopez, 2013). Higher compressive strengths observed were 20.0, 32.4 and 39.0 MPa at 7, 28 and 90 days, respectively. According to the estimated effects, increasing the temperature used in the reactivation process from 700 to 800 °C decreases 7-day strength but increases 28 and 90-day strength of RCM pastes. It was found that RCM have a substantial capacity to promote pozzolanic reactions, as indicated by the significant increase in strength observed when the reactivated material is partially substituted by silica fume in the new mixtures. In addition, results from experiments performed at the average level of the factors evidenced significant non-linearity of the response. The source of the non-linearity could not be identified from the results of the experimental design used, as it was limited to first order effects and interactions.

The second phase of the study, reported in this paper, investigated the process factor and mixture proportioning factor previously identified as having the largest effect on strength of RCM pastes: the maximum temperature used in the reactivation process and, the level of substitution of RCM by a supplementary cementitious material (SCM) in the new mixtures. Since these factors have the largest potential for optimization, the purpose of the study was to determine if an optimal value exists for either of them, where specific responses are maximized, and to evaluate if the optimal value of either factor depends on

the level of the other due to factor interaction. A central composite experimental design for two factors was selected in order to explore the factor-response relationship over a wider range of factor levels.

As opposed to previous studies based exclusively on pastes, this study evaluated the performance of the RCM as a binder for the production of mortars. Consequently, selected responses were: the flow behavior, expansion and 28-day compressive strength of RCM mortars. In order to compare results with our previous study, silica fume was used as the main SCM. However, fly ash was also used to contrast the effect of silica fume on flow and strength of RCM mortars. In addition to studying the binder performance of the RCM, complementary tests were carried out in order to explain the observed behavior, including: density measurements and sieving of raw and reactivated materials, XRD analysis of RCM and measurements of evaporated water during mixing of RCM pastes.

## **4.2        Experimental Design**

Considering results from previous studies, an experimental region of interest was defined, limiting the range of reactivation temperatures and RCM substitution levels to be explored. The base range of reactivation temperatures was centered on  $800\text{ }^{\circ}\text{C} \pm 100\text{ }^{\circ}\text{C}$ . Pastes of RCM produced over this range of temperatures are known to develop significantly different strengths (Shui et al., 2009). The base range of RCM substitution levels was centered on  $20\% \pm 10\%$ . According to previous results using silica fume was as the substituting material (Serpell & Lopez, 2013), the range selected extends the experimental region in the direction of increasing strength. The factor-response relationship in the selected experimental region was explored using a rotatable central composite experimental design for two factors (**Figure 4.1**). Central composite designs enable efficient second order regression of the factor-response relationship and thus provide a quadratic model to fit the response surface in the experimental region (Box & Wilson, 1951). The core of the design is a full factorial design in two levels that allows estimation of the linear effects of factors and factor interactions. This core is augmented with axial

and central points, which allow estimation of the second order effects of the factors and the experimental variance of the responses, respectively. Whereas factorial points are located at  $\pm 1$  coded units from the center of the experimental region, axial points are located at  $\pm \alpha$  coded units from the center of the experimental region, with  $\alpha$  being greater than 1. In order to obtain a rotatable design, i.e. one in which the variance of the response depends only on the distance from the center of the experimental region, the value of  $\alpha$  was chosen to be  $(n_f)^{1/4}$ , where  $n_f$  is the number of factorial cases, thus for the selected design  $\alpha$  equals  $4^{1/4} = 1.414$ . The resulting experimental and coded levels for the reactivation temperature (factor X1: R-Temp) and for the RCM substitution level (factor X2: SCM) are shown in **Table 4.1**. For execution purposes the experiment was divided in two blocks: one comprising the four axial cases and two of the central cases, and one comprising the four factorial cases and the remaining two central cases. Execution of individual cases within each block was randomized.

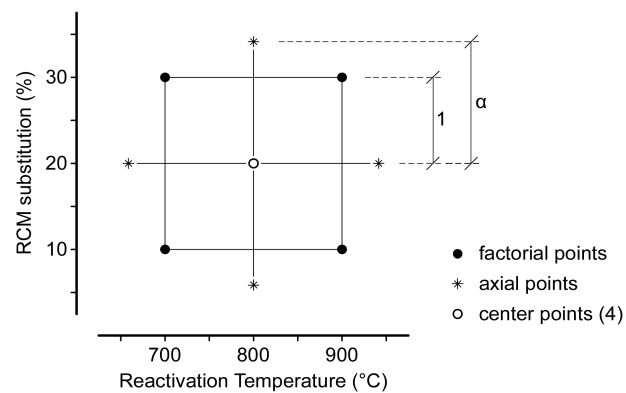


**Figure 4.1** Experimental region covered by the central composite experimental design

**Table 4.1** Design factor levels

Coded levels	Experimental levels	
	X1: R-Temp °C	X2: SCM %
-1.414	659	6
-1	700	10
0	800	20
1	900	30
1.414	941	34

After the main experiment was performed, three sets of additional experiments followed. One set of experiments was intended to extend the range of substitution levels explored beyond the range covered by the central composite experiment. The other two sets were meant to compare the results obtained using silica fume as the substituting material with results obtained using fly ash at different water to cementitious material ratios. The additional cases were limited to RCM produced at 800 °C.

#### **4.2.1 Mixture Design**

As prescribed by the experimental program, individual mixtures incorporated RCM produced at a specific temperature and at a specific level of substitution by either silica fume or fly ash. The substitution was performed in a volumetric basis replacing a given percent of RCM by the specific amount of silica fume or fly ash having the same volume. The water content was held constant in order to fix the water to cementitious material (W/CM) volumetric ratio. Consequently, a constant volume of paste is obtained, thus fixing the paste to fine aggregate ratio and the volume of mortar produced. However, as the total weight of the cementitious material changes at the different levels of substitution the above method results in a small variation of the water to cementitious material mass ratio across the mixtures. Mixture recipes for the individual cases in the central composite experiment and in the additional experiments are shown in **Tables 4.2** and **4.3**, respectively. Effective water

to cementitious material mass and volume ratios shown consider water absorption by the aggregate (0.6% by weight).

**Table 4.2** Mixture recipes: cases from the central composite experiment

Case	Block	Factor Levels				Mixture recipe (kg/m <sup>3</sup> )				Effective	
		Coded		Experimental		RCM	Si fume	Sand	Water	W/CM ratios	mass
X1	X2	R-Temp	SCM								volume
C1	1	-1.414	0	659	20%	346.2	63.5	1190	409.6	0.98	2.8
C2	1	1.414	0	941	20%	346.2	63.5	1190	409.6	0.98	2.8
C3	1	0	-1.414	800	6%	406.7	19.0	1190	409.6	0.95	2.8
C4	1	0	1.414	800	34%	285.6	107.9	1190	409.6	1.02	2.8
C5	1	0	0	800	20%	346.2	63.5	1190	409.6	0.98	2.8
C6	1	0	0	800	20%	346.2	63.5	1190	409.6	0.98	2.8
C7	2	-1	-1	700	10%	389.4	31.7	1190	409.6	0.96	2.8
C8	2	-1	1	700	30%	302.9	95.2	1190	409.6	1.01	2.8
C9	2	1	-1	900	10%	389.4	31.7	1190	409.6	0.96	2.8
C10	2	1	1	900	30%	302.9	95.2	1190	409.6	1.01	2.8
C11	2	0	0	800	20%	346.2	63.5	1190	409.6	0.98	2.8
C12	2	0	0	800	20%	346.2	63.5	1190	409.6	0.98	2.8

**Table 4.3** Mixture recipes: additional cases

Case	Factor Levels		Mixture recipe (kg/m <sup>3</sup> )					Effective W/CM	
	R-Temp	SCM	RCM	Si fume	Fly Ash	Sand	Water	mass	volume
C0	800	0%	432.7	0.0		1190	409.6	0.93	2.8
C13	800	40%	259.6	133.1		1190	409.6	1.02	2.8
C14	800	50%	216.4	166.4		1190	409.6	1.05	2.8
A0	800	0%	432.7		0.0	1190	409.6	0.93	2.8
A1	800	10%	389.4		34.5	1190	409.6	0.95	2.8
A2	800	20%	346.2		69.0	1190	409.6	0.97	2.8
A3	800	30%	302.9		103.5	1190	409.6	0.99	2.8
A4	800	40%	259.6		138.0	1190	409.6	1.01	2.8
A5	800	50%	216.4		172.5	1190	409.6	1.00*	2.7*
A6	800	60%	173.1		207.0	1190	409.6	0.98*	2.6*
A7	800	70%	129.8		241.5	1190	409.6	0.98*	2.5*
B0	800	0%	470.9		0.0	1295	362.6	0.75	2.3
B1	800	10%	423.8		36.3	1295	362.6	0.77	2.3
B2	800	20%	376.7		72.5	1295	362.5	0.79	2.3
B3	800	30%	329.6		108.8	1295	362.5	0.81	2.3
B4	800	40%	282.5		145.0	1295	362.5	0.83	2.3
B5	800	50%	235.4		181.3	1295	362.5	0.84	2.3
B6	800	60%	188.4		217.5	1295	362.5	0.84*	2.2*
B7	800	70%	141.3		253.8	1295	362.5	0.85*	2.2*

\* Values account for significant bleeding observed

### 4.3 Materials and methods

The wastes that serve as the raw material for the production of RCM were obtained from cement pastes made specifically for this purpose under laboratory conditions. These pastes were produced using ordinary Portland cement conforming to ASTM C150 type I, having a density of 3.140 g/cm<sup>3</sup>. In the production of the RCM mortars either silica fume or fly ash were used as SCM. Silica fume was a commercially available condensed type, composed of over 99% SiO<sub>2</sub> according to XRF analysis, and having a density of 2.307 g/cm<sup>3</sup>. Fly ash was obtained from a local power plant. According to the oxide analysis shown in **Table 4.4**, its chemical composition conforms to the ASTM C618 class F

specification. This fly ash has a density of 2.392 g/cm<sup>3</sup>. Mortars were produced using natural siliceous sand, graded as specified in Chilean standard NCh-158 (**Table 4.5**).

**Table 4.4** XRF analysis of fly ash

		ASTM C 618 % Class F specification
Al <sub>2</sub> O <sub>3</sub>	21.0	
Fe <sub>2</sub> O <sub>3</sub>	8.31	
SiO <sub>2</sub>	55.8	
SiO <sub>2</sub> +Al <sub>2</sub> O <sub>3</sub> + Fe <sub>2</sub> O <sub>3</sub>	85.1	70.0 min.
CaO	5.87	
MgO	2.70	
Na <sub>2</sub> O	1.54	
K <sub>2</sub> O	1.07	
TiO <sub>2</sub>	0.95	
P <sub>2</sub> O <sub>5</sub>	0.63	
SO <sub>3</sub>	0.44	5.0 max.
BaO	0.27	
SrO	0.24	
Loss On Ignition	1.01	6.0 max.

**Table 4.5** NCh-158 normalized sand gradation

Mesh opening (mm)	Sieve No	Cumulative % retained
2.00	10	0
1.68	12	5 ± 5
1.00	18	33 ± 5
0.50	35	67 ± 5
0.150	100	88 ± 5
0.075	200	98 ± 2

Source pastes were produced mixing Portland cement at 0.50 water to cement mass ratio, and cast in roughly square molds, 500 mm a side and 40 mm deep. The resulting slabs were unmolded at 24 hours and placed under water for curing. At 28 days they were hammered into chunks of 40mm maximum size, which were then placed in a drying oven at 105°C until constant weight was achieved. A jaw crusher and a ball mill were used to reduce the material to a fine powder. To control the milling process, materials were sieved using a #200 mesh (75 $\mu$ m opening size). Milling continued until only 20% of the material was retained (average of 2 sieving tests).

Dehydration of the powdered material was performed in batches of 400g using a programmable electric muffle oven. Heating cycle started at room temperature and proceeded at 10 °C per minute to the maximum temperature indicated by the experimental program for each batch. The material remained at the maximum temperature for 150 minutes, and then the oven was left to cool down to room temperature at free rate. The resulting RCMs were stored in sealed plastic containers until the date of mixture. Samples of RCM produced at each of the five prescribed temperatures were sieved with a #200 mesh to measure changes in the fineness of the powdered material due to the reactivation process. Density of RCMs was measured using a Nitrogen gas pycnometer (Ultrapyc 1200e). RCM samples were also analyzed by powder X-ray diffraction (XRD), using a Bruker D2 Phaser diffractometer, scanning between 5 and 70 degrees.

For the production of the RCM mortars, the prescribed amount of RCM was first manually mixed with 80% of the prescribed water. The steel bowl containing the resulting paste was weighed and then placed in a water bath at room temperature. This procedure was meant to control the temperature raise of the RCM paste, which can evolve a significant amount of heat of hydration in the first minutes depending on the amount of free lime present in the RCM. The paste was remixed constantly during the 5 minute long water bath period. After the water bath the bowl was dried and weighed to determine the amount of water lost to evaporation. Additional water was incorporated to the mixture to compensate for the evaporated water. The sand, the silica fume or fly ash, the additional water and the rest of

the prescribed water were added to the RCM paste in the bowl and mixed in a laboratory mixer until a uniform mixture was obtained ( $3 \pm 1$  minutes).

Five mixtures were produced for each case in the central composite experiment: Two mixtures for 7-day strength testing and two mixtures for 28-day strength testing –using one of them also to measure flowability–, and one mixture for mortar expansion testing. Only one mixture was produced for each case in the additional experimental program for flowability and 28-day compressive strength testing. Flowability was measured according to procedures specified in ASTM C1437, within 1 minute of the end of mixing. For strength testing purposes, the remainder of the mixture was casted in 50mm cubic molds, and stored in a moist room at  $23^{\circ}\text{C}$  and 100% R.H for 48 hrs. Specimens were then unmolded, weighed and left to cure in lime water at  $23^{\circ}\text{C}$  until the prescribed date of testing. Strength testing was performed on the saturated surface dry specimens at a load rate of 1350 N/s (equivalent to 0.52 MPa/s). Mortar expansion was tested according to ASTM C1038. Mixtures were casted in 25 by 25 by 285 mm prism molds and stored in a moist room at  $23^{\circ}\text{C}$  and 100% R.H. Specimens were unmolded at 48 hrs. to avoid damage due to the low initial strength. Initial length was measured after placing them in saturated lime water at  $23^{\circ}\text{C}$  for 30 minutes. Final length was measured at the age of 14 days.

#### **4.4 Results and discussion**

According to results from sieving, fineness of the RCM is higher than that of the original powdered raw material they were produced from. In addition, the fraction of material retained in the #200 mesh decreased for materials reactivated at higher temperatures (**Figure 4.2**), indicating that the fineness of RCMs increases with increasing reactivation temperature. Density of RCMs also varied, linearly increasing with reactivation temperature, from  $2.81 \text{ g/cm}^3$  for RCM produced at  $660^{\circ}\text{C}$  to  $3.12 \text{ g/cm}^3$  for RCM produced at  $940^{\circ}\text{C}$ . Both phenomena can be related to the decrease in specific volume associated with the dehydration of hydrated phases in the cement paste and the

decomposition of carbonated compounds. The increase in fineness can also be related to the fractioning of bigger particles during the heat cycle.

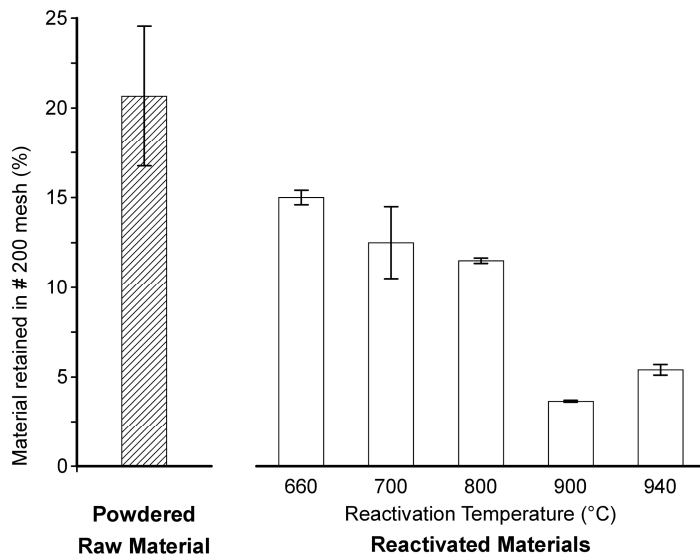


**Figure 4.2** Percent of raw and reactivated material retained in #200 mesh (75 µm)

Results for all cases in the central composite experiment are shown in **Table 4.6**. As expected, the amount of water lost by evaporation during RCM paste mixing varied according to the level of substitution used. Increased substitution means less RCM is incorporated in a fixed volume of mixture therefore less heat is evolved. However, for mixtures incorporating the same amount of RCM the amount of evaporated water increased with increasing reactivation temperature, particularly in the range from 660 to 800 °C (**Figure 4.3**). During the initial mixing of the RCM pastes false set was also observed. Both, the heat evolved and false set, are related to the formation of calcium hydroxide from free lime present in the RCM. During the reactivation process, free lime is first formed from the dehydration of calcium hydroxide between 400 and 550 °C. Then, when the materials reach the maximum temperature used in the process, i.e. above 550 °C, free lime is also formed from the decomposition of calcium carbonate. Since the rate of

decomposition increases with increasing temperature, the amount of free lime present in the resulting RCM depends on the maximum temperature reached during the fixed length reactivation process. Whereas at 660°C only a fraction of the calcium carbonate can decompose in the process, above 900 °C all of it is expected to be decomposed. Consequently, the initial heat evolved by the pastes increased with increasing reactivation temperature due to increasing free lime content in the RCM. Pastes based on RCMs produced above 800 °C evolved more heat and displayed stronger false set behavior.

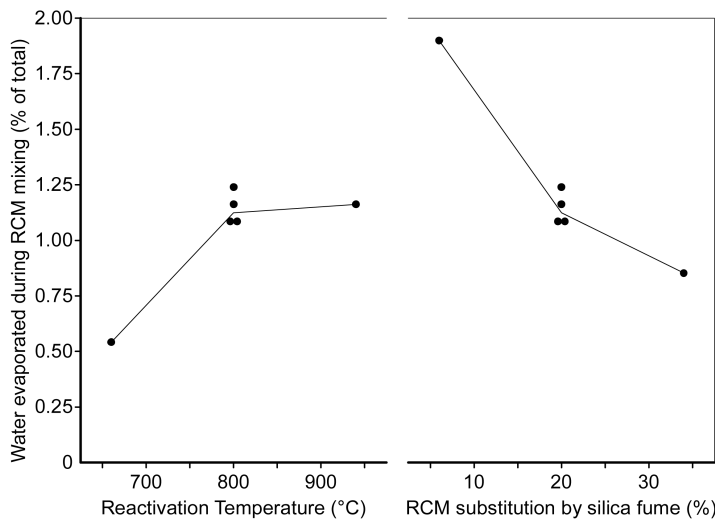


**Figure 4.3** Evaporated water during initial mixing versus RCM reactivation temperature and RCM substitution level

**Table 4.6** Results: cases from the central composite experiment

Case	Factor levels		Evaporated	Flow	Weight	Expansion	Compressive strength*	
	R-Temp °C	Si-fume %	water %	C1437 %	gain %	C1038 %	7-day MPa	28-day MPa
C1	659	20	0.54%	69.5	0.88	0.014	8.55	18.18
C2	941	20	1.16%	67.5	0.25	0.073	7.13	19.60
C3	800	6	1.90%	76.0	0.42	0.017	8.29	14.92
C4	800	34	0.85%	48.0	0.34	0.045	11.58	23.94
C5	800	20	1.08%	57.5	0.32	0.020	9.62	20.67
C6	800	20	1.24%	51.0	0.37	0.017	9.70	21.10
C7	700	10	0.74%	84.5	0.65	0.015	7.52	16.18
C8	700	30	0.58%	55.7	0.63	0.018	10.36	21.83
C9	900	10	1.70%	72.2	0.24	0.026	7.32	18.72
C10	900	30	1.01%	53.9	0.31	0.059	9.68	22.22
C11	800	20	1.08%	55.8	0.42	0.020	9.53	22.49
C12	800	20	1.16%	57.5	0.42	0.017	10.21	22.18

\* 7 and 28-day strength results shown are the average of two replicates

Effects of reactivation temperature and substitution level on flow, compressive strength and expansion of RCM mortars were estimated by second order regression of the experimental results shown in **Table 4.6**. Significant effects were identified using analysis of variance (ANOVA) at a 5% significance level (95% confidence interval). Effects exceeding the selected confidence interval are marked in bold in the ANOVA tables accompanying the discussion of effects (**Tables 4.8, 4.9, 4.10 and 4.11**). In the response models discussed and plotted, only these effects are included. In addition, estimated effects on flow and on compressive strength are compared to results obtained from RCM mortars where fly ash was used as the substituting material (**Table 4.7**).

**Table 4.7** Results: cases from additional experiments

Case	Factor levels		Flow C1437 %	Strength 28-day MPa
	R-Temp °C	Fly Ash %		
C0	800	0	80.0	11.70
C13	800	40	*	25.80
C14	800	50	*	25.24
A0	800	0	76.3	11.50
A1	800	10	103.3	6.98
A2	800	20	108.0	7.01
A3	800	30	129.0	5.15
A4	800	40	**	3.69
A5	800	50	**	2.45
A6	800	60	**	1.40
A7	800	70	**	0.88
B0	800	0	***	***
B1	800	10	20.5	17.52
B2	800	20	47.5	13.56
B3	800	30	76.5	10.22
B4	800	40	106.5	7.89
B5	800	50	121.0	5.08
B6	800	60	146.0	3.64
B7	800	70	**	1.76

\* no flow, \*\* exceeded flow table diameter, \*\*\* unable to compact

#### 4.4.1 Flow of RCM mortars

Regression of the flow test results indicates both the RCM substitution level and the temperature used to produce the RCM significantly affect the flow of RCM mortars.

**Table 4.8** shows the analysis of variance of the response model fitted, including the estimated effect of factors and their significance level (p-values). As indicated by the estimated effect of the factor (X2), in the experimental region explored, increasing the RCM substitution by silica fume decreases flow of RCM mortars. The factor also appears to have a significant second order effect (X2·X2). According to its estimated second order effect, the net effect of the substitution decreases as the substitution

level increases. In the range of substitution levels covered by the response model the second order component is unable to overcome the main negative effect of the substitution, and therefore flow continues to drop as more RCM is substituted by silica fume.

**Table 4.8** ANOVA: flow test results

Source	Estimate (% flow)	Sum of Squares	DoF	Mean of Squares	F-Ratio	P-Value
<b>Average</b>	<b>55.45</b>					
X1: R-Temp	-2.12	35.82	1	35.82	3.87	0.1062
<b>X2: Si-fume</b>	<b>-10.84</b>	939.57	1	939.57	101.56	<b>0.0002</b>
X1·X2	+2.63	27.56	1	27.56	2.98	0.1449
<b>X1·X1</b>	<b>+6.86</b>	300.85	1	300.85	32.52	<b>0.0023</b>
<b>X2·X2</b>	<b>+3.61</b>	83.23	1	83.23	9.00	<b>0.0301</b>
Blocks	+0.84	8.50	1	8.50	0.92	0.3818
Total error		46.26	5	9.25		
Total		1391.86	11			

According to the model, the reactivation temperature effect on flow is characterized by its second order component ( $X_1 \cdot X_1$ ). At any substitution level, minimum flow is predicted for mortars based on RCM produced at 800 °C. From this point, either increasing or decreasing the reactivation temperature increases flow of RCM mortars (**Figure 4.4**). Although not statistically significant, the estimated first order effect of the reactivation temperature ( $X_1$ ) suggests the increase in flow is higher in the direction of lower reactivation temperatures. Absence of significant interaction between the reactivation temperature and the substitution level indicates factor effects on flow are independent. According to this lack of interaction, in the experimental region explored, substitution effect on flow is largely unaffected by the varying characteristics of the RCM produced at different temperatures, and reactivation temperature effect on flow is unaffected by the level of substitution.

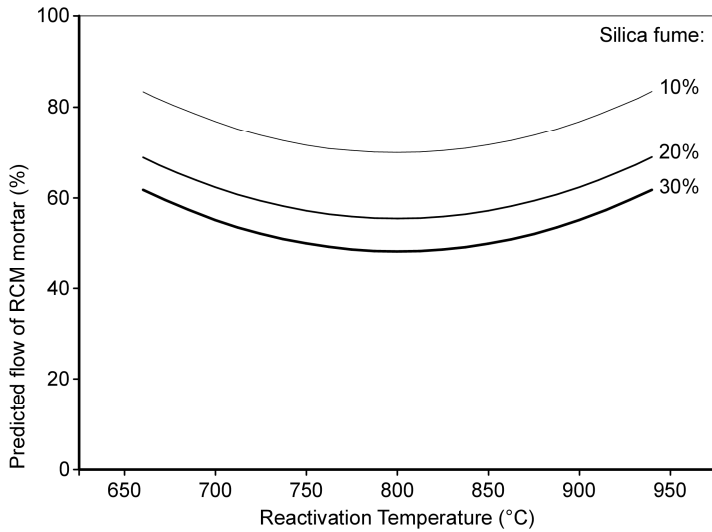


**Figure 4.4** Predicted response for flow of RCM mortars at different RCM substitution levels

The effect of substitution level was observed to depend on the characteristics of the SCM used. In the additional experiments performed using fly ash as the substituting material, substitution level had the opposite effect of that previously estimated using silica fume. In fly ash incorporated RCM mortars mixed at 0.8 and 1.0 W/CM ratios flow increased as the substitution level increased (**Figure 4.5**). These observations suggest that the effect of substitution by SCM in RCM mortars can be compared to the effect of a similar substitution in Portland cement mortars, where the impact of a given SCM on flowability depends largely on its mean particle size, density, shape, and specific surface. Whereas fly ash is usually reported to improve the rheological properties of cement pastes, mortars and concretes, the opposite has been reported for silica fume (Ferraris, Obla, & Hill, 2001; Rao, 2003). As in cement based mortars, differences observed in RCM mortars can be explained by the larger specific surface and smaller mean particle size of silica fume increasing water demand and cohesiveness of the mixture, respectively.

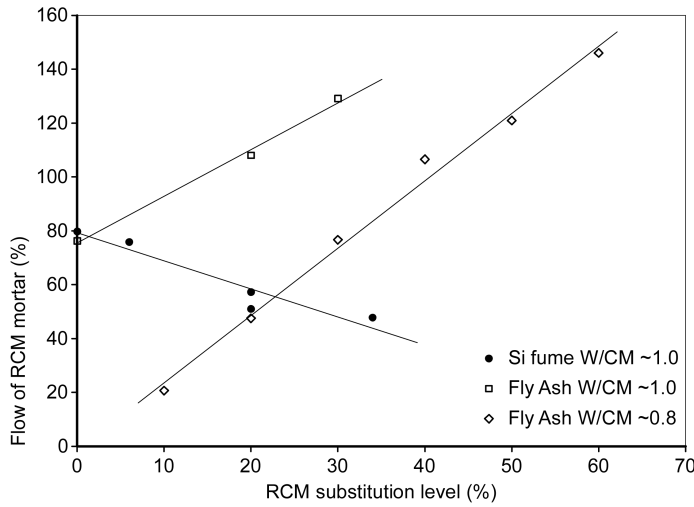


**Figure 4.5** Flow of RCM mortars versus RCM substitution level

#### 4.4.2 Strength of RCM mortars

Regression of 7 and 28-day results shows both RCM substitution level and reactivation temperature significantly affect compressive strength of RCM mortars (**Table 4.9** and **Table 4.10**). According to the response model fitted, at either of the tested ages, compressive strength of RCM mortars increases as substitution by silica fume is increased ( $X_2$ ). However, for 28-day strength the estimated effect decreases with increasing substitution level, as indicated by the significant second order effect of the factor ( $X_2 \cdot X_2$ ). Considering both the first and second order effects estimated, the model predicts maximum strength at 28 days would be achieved at approximately 35% substitution. In additional experiments maximum 28-day strength was found at 40% substitution confirming the existence of an optimum substitution level when using silica fume as predicted by the model (**Figure 4.6**). Additional experiments also showed that the model predictions are valid only for RCM mortars where silica fume is used as the substituting material. In RCM mortars using fly ash as the substituting material 28-day compressive strength decreased as substitution level increased. This behavior was observed across the range of substitution levels

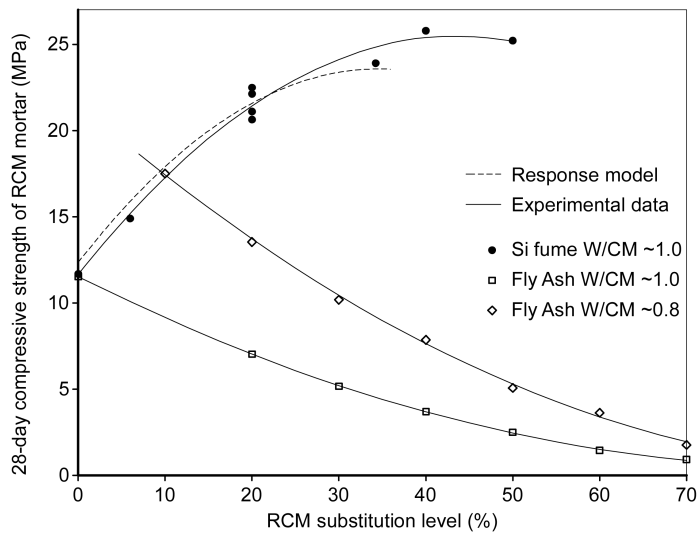
explored, for mortars mixed at either 1.0 or 0.8 W/CM ratio. In the range explored these SCMs had opposite impact on strength. Although their chemical composition differs, both SCMs are high in amorphous silica. Therefore, at higher substitution levels the fly-ash can provide as much soluble silica as silica fume can at lower levels. Consequently, differences in chemical composition alone cannot explain the observed behavior. As in Portland cement based mortars, physical properties of the SCM such as its particle size significantly affect 28-day compressive strength of RCM mortars. In Portland cement based mortars where 25% of the cement is substituted by either inert or pozzolanic mineral admixtures, Lawrence, Cyr, & Ringot (2005), found the effect of fineness to be significant for pozzolanic materials. Compressive strength was found to increase with increasing fineness at all ages tested. In the same study, when class F fly ash with a particle size similar to that of cement was used, compressive strength was found to decrease linearly with substitution level for hydration times up to 28 days. However, at 180 days of hydration mixtures incorporating up to 35% fly ash had developed compressive strengths exceeding the control mixture (0% replacement). Therefore, it remains to be observed how strength of RCM mortars incorporating fly ash evolves over longer hydration periods as fly ash has a lower rate of reaction and much smaller specific surface compared to silica fume.

**Table 4.9** ANOVA: 7-day strength results

Source	Estimate (MPa)	Sum of Squares	DoF	Mean of Squares	F-Ratio	P-Value
Average	<b>9.77</b>					
X1: R-Temp	<b>-0.36</b>	2.103	1	2.103	5.91	<b>0.0264</b>
<b>X2: Si-fume</b>	<b>+1.23</b>	24.279	1	24.279	68.24	<b>0.0000</b>
X1·X2	-0.12	0.118	1	0.118	0.33	0.5729
<b>X1·X1</b>	<b>-1.00</b>	12.872	1	12.872	36.18	<b>0.0000</b>
<b>X2·X2</b>	+0.04	0.023	1	0.023	0.06	0.8033
Blocks	-0.02	0.010	1	0.010	0.03	0.8715
Total error		6.048	17	0.356		
Total		46.216	23			

**Table 4.10** ANOVA: 28-day strength results

Source	Estimate (MPa)	Sum of Squares	DoF	Mean of Squares	F-Ratio	P-Value
<b>Average</b>	<b>21.61</b>					
X1: R-Temp	+0.62	6.096	1	6.096	5.82	<b>0.0275</b>
<b>X2: Si-fume</b>	<b>+2.74</b>	119.970	1	119.970	114.43	<b>0.0000</b>
X1·X2	-0.54	2.311	1	2.311	2.20	0.1559
<b>X1·X1</b>	<b>-1.22</b>	18.915	1	18.915	18.04	<b>0.0005</b>
<b>X2·X2</b>	<b>-0.95</b>	11.446	1	11.446	10.92	<b>0.0042</b>
Blocks	+0.43	4.524	1	4.524	4.32	0.0532
Total error		17.823	17	1.048		
Total		176.220	23			


**Figure 4.6** 28-day compressive strength of RCM mortars at different RCM substitution levels

Regression of 7 and 28-day results also shows reactivation temperature significantly affects compressive strength, with a markedly second order effect estimated at both testing ages ( $X_1 \cdot X_1$ ). According to the estimated effect, increasing reactivation temperature in the range from 660 to 800 °C increases compressive strength of RCM

mortars whereas increasing reactivation temperature in the range from 800 to 940 °C decreases compressive strength (**Figure 4.7**). Lack of significant interaction effects indicate that the effect of reactivation temperature is independent of the RCM substitution level when using silica fume. Consequently, at any given substitution level, highest compressive strength is achieved using RCM produced at 800 °C.

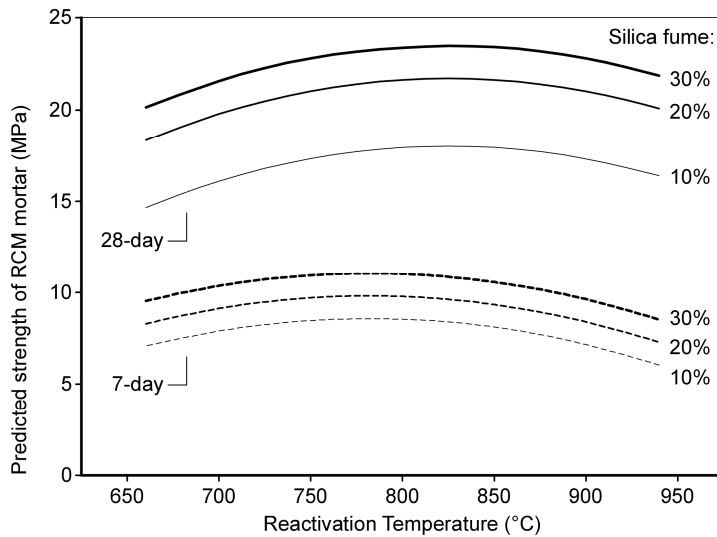


**Figure 4.7** Predicted response for 7 and 28-day compressive strength of RCM mortars at different RCM substitution levels

Results from XRD analysis of the reactivated materials provide clues to the cause of the observed behavior. As seen in **Figure 4.8**, two broad peaks present in the XRD scan of the RCM heated to 660 °C, roughly centered at 32.5 and 33.1 degrees, appear with progressively higher intensity in the scans of the RCMs heated to 700 and 800 °C. These peaks match the pattern of a stabilized form of alpha'-C<sub>2</sub>S. Although best matching pattern corresponds to alpha'-Ca<sub>2</sub>SiO<sub>4</sub> 0.05-Ca<sub>3</sub>(PO<sub>4</sub>)<sub>2</sub> (PDF2 database reference code: 00-049-1674), it is not possible to determine if the stabilizing agent is phosphate or other species with the information gathered in this study alone.

Nevertheless, the almost perfect match supports the identification of alpha'-C<sub>2</sub>S, which is also compatible with the raw materials and temperatures involved in the reactivation process. In the scan of the RCM produced at 900 °C the referred peaks appear in a shifted position and with decreased intensity. Consequently, the alpha'-C<sub>2</sub>S pattern no longer matches the profile. Peak position and intensity continues to change with increasing temperature. For RCM produced at 940 °C the beta-C<sub>2</sub>S (Larnite) pattern best matches the profile in the same region.

According to Taylor (1997), when the hydration products of Portland cement are decomposed at temperatures between 800 and 1000 °C, beta-C<sub>2</sub>S is the normal product. However, since alpha'-C<sub>2</sub>S forms at temperatures around 630-680 °C, it must be present in all the materials during the high temperature phase of the reactivation process. The fact that it remains stable at ambient temperature only in the materials that were heated up to 800 °C or less means the stabilizing agent is removed from the structure at higher temperatures. It remains to be explained if this happens because the stabilizing agent is a volatile compound, or because it is taken up by other phase formed at the higher temperature, or because it is exsolved on cooling when the structure was formed at a higher temperature.

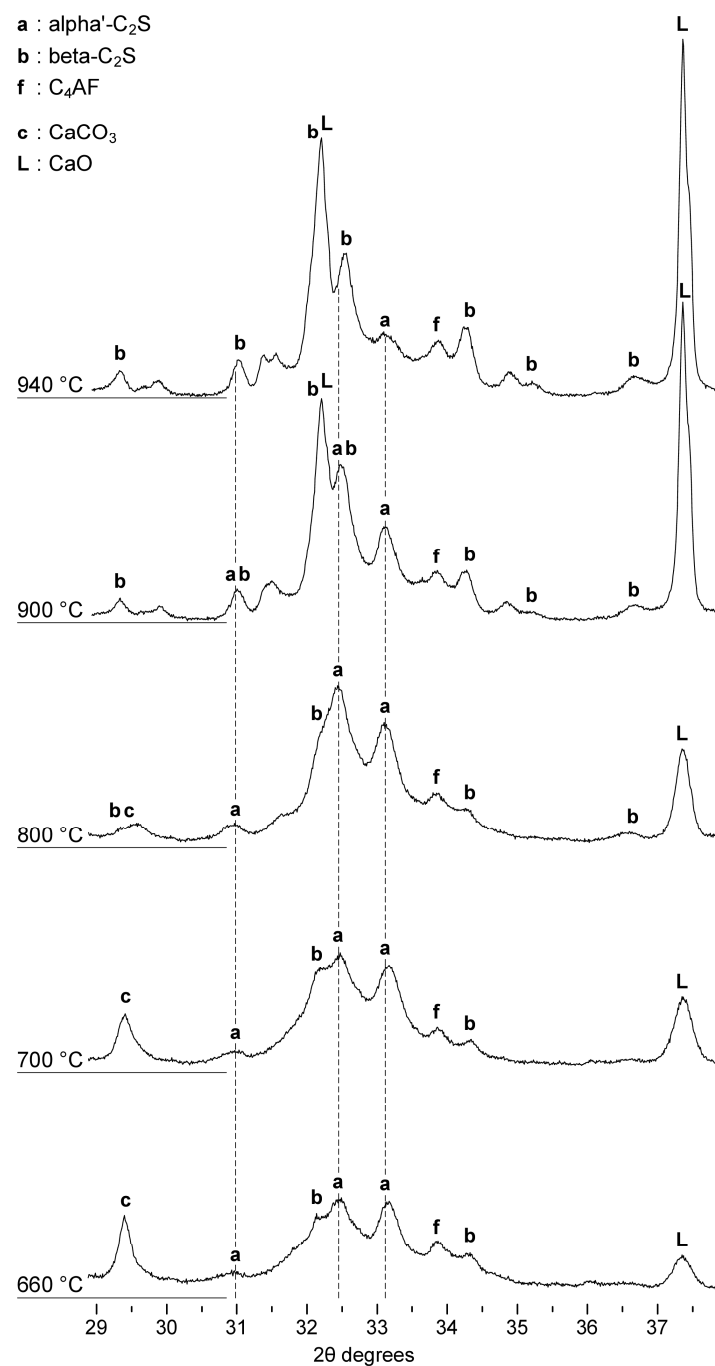


**Figure 4.8** XRD scans of RCM produced at different reactivation temperatures

The relative XRD intensities of several interest phases as observed in RCMs produced at different temperatures are shown in **Figure 4.9**. Intensities were normalized relative to the highest intensity observed for each particular phase. Therefore, the graph represents the evolution of each phase as reactivation temperature is changed, but not the relative abundance of phases at any given temperature. Intensity of free lime was determined from the height of the peak at an angle of 37.36 degrees. Intensity of alpha'-C<sub>2</sub>S was determined from the height of the peaks at 32.45 and 33.11 degrees. Intensity of beta-C<sub>2</sub>S was determined from the height of the peaks at 32.09, 32.59 and 34.32 degrees. Intensity of the amorphous phases was determined from the average height of the profile between 30.4 and 30.7 degrees.

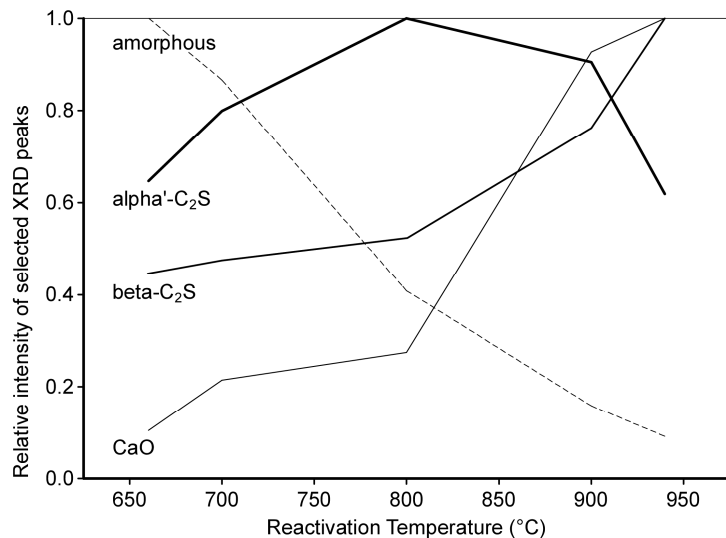


**Figure 4.9** Relative intensity of interest phases identified in the XRD scans of the RCM produced at different reactivation temperatures

As expected, free lime is seen to increase intensity at a higher rate in the range from 800 to 900 °C where the Calcium carbonate decomposes at a higher rate. Amorphous phases are seen to decrease in intensity with increasing temperature. The decrease can be related to the dehydration of C-S-H and the formation of more crystalline phases due to slow cooling from higher temperatures. Beta-C<sub>2</sub>S is seen to increase with increasing temperature in the range from 800 to 940 °C. In the range from 660 to 800 °C, as the amorphous phases decrease, alpha'-C<sub>2</sub>S increases with increasing temperature. Conversely, in the range from 800 to 940 °C, as beta-C<sub>2</sub>S increases, alpha'-C<sub>2</sub>S decreases with increasing temperature. Consequently, alpha'-C<sub>2</sub>S produced from the dehydration of C-S-H at up to 800 °C appears to remains stable on cooling, whereas when the same phase is heated to higher temperatures progressively more of it reverts to beta-C<sub>2</sub>S on cooling.

Identification of a stabilized form of alpha'-C<sub>2</sub>S is compatible with the strength observations, as it is known to react much faster than beta-C<sub>2</sub>S, gaining strength at a higher rate over a period of several months (Benarchid, Diouri, Boukhari, Aride, & Elkhadiri, 2005; Cuberos et al., 2009). Therefore, 28-day compressive strength increases as the reactivation temperature of the RCM is increased from 660 to 800°C, due to increasing content of alpha'-C<sub>2</sub>S in the reactivated materials. Conversely, 28-day compressive strength decreases as the reactivation temperature of the RCM is increased from 800 to 940 °C, due to increasing amount of alpha'-C<sub>2</sub>S reverted to beta-C<sub>2</sub>S in the materials.

#### **4.4.3 Expansion of RCM mortars**

The regression model of expansion test results indicates expansion of RCM mortars is affected by both the reactivation temperature and the substitution level used (**Table 4.11**). In the experimental region explored, increasing the reactivation temperature (X1) increases expansion of RCM mortars. In addition, the effect of the factor increases with increasing reactivation temperature as indicated by the significant second order effect estimated (X1·X1). As predicted by the model,

expansion increases at a significantly higher rate as reactivation temperature is increased above 800 °C (**Figure 4.10**). Increasingly higher amounts of free lime are expected to be found in the RCM produced between 800 and 940°C due to decomposition of Calcium carbonate during the reactivation process. Although the reaction of free lime with water forms larger volume  $\text{Ca}(\text{OH})_2$ , in order to produce expansion it must occur after the mortar has set. Most free lime reacts with water during mixing of RCMs. However, reaction rate is slowed down as mix water is rapidly saturated with  $\text{Ca}^{2+}$  and  $\text{OH}^-$  ions and  $\text{Ca}(\text{OH})_2$  layers grow on the surface of the free lime grains. Consequently, depending on the initial concentration, a fraction of the free lime can remain unreacted after setting. In the set mortar, saturation of the pore solution with  $\text{OH}^-$  ions means  $\text{Ca}(\text{OH})_2$  from the hydration of remaining free lime must be formed in situ producing expansion (Deng, Hong, Lam, & Tang, 1995).

**Table 4.11** ANOVA: Expansion results

Source	Estimate (%)	Sum of Squares	DoF	Mean of Squares	F-Ratio	P-Value
<b>Average</b>	<b>0.017</b>					
X1: R-Temp	<b>+0.015</b>	1.9E-03	1	1.9E-03	63.77	<b>0.0005</b>
<b>X2: Si-fume</b>	<b>+0.009</b>	5.8E-04	1	5.8E-04	19.58	<b>0.0069</b>
X1·X2	+0.007	1.8E-04	1	1.8E-04	6.11	0.0564
<b>X1·X1</b>	<b>+0.010</b>	6.2E-04	1	6.2E-04	20.92	<b>0.0060</b>
<b>X2·X2</b>	+0.004	1.1E-04	1	1.1E-04	3.65	0.1143
Blocks	-0.002	7.0E-05	1	7.0E-05	2.35	0.1859
Total error		1.5E-04	5	3.0E-05		
Total		3.5E-03	11			

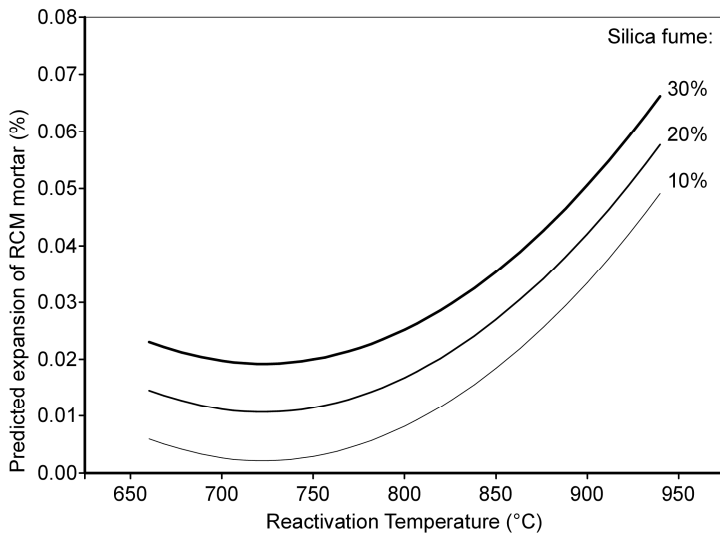


**Figure 4.10** Predicted response for expansion of RCM mortars at different RCM substitution levels.

The estimated effect of substitution level indicates expansion of RCM mortars increases when the level of substitution by silica fume increases (X2). Generally, lower expansion is reported for silica fume incorporated pastes and concretes compared to control mixtures using pure Portland cement (Mazloom, Ramezanianpour, & Brooks, 2004). Nevertheless, the opposite effect has also been observed. According to Rao (1998), although cement pastes without silica fume exhibited higher expansion than silica fume incorporated pastes, in the later expansion gradually increased as the content of silica fume increased from 5% to 30%. Likewise, Igarashi, Kubo, & Kawamura (2000) observed high initial expansion followed by shrinkage for silica fume incorporated mortars at low water to binder ratios (<0.30), but found that at high water to binder ratio (0.55) the expansion of silica fume incorporated mortars was almost the same as that of corresponding mortars without silica fume. Consequently, to explain the effect of silica fume substitution level on expansion of RCM mortars, an interaction between the silica fume and the RCM, different than that expected between silica fume and Portland

cement, is not required. As in cement mortars, the increase in expansion observed as silica fume content is increased is believed to be caused by the reduction of the average pore size of the paste obtained as substitution levels are increased. The delayed hydration of unreacted phases, such as remaining free lime in this case, within the limited pore space available, results in internal pressure causing expansion of the mortar.

## **4.5        Conclusions**

Fresh and hardened properties of mortars based on reactivated cementitious materials (RCM) are significantly affected by the reactivation temperature used to produce the RCM and by the level to which it is substituted by a supplementary cementitious material (SCM) in the mortar mixture. Response models developed in this study indicate these factors do not have interaction effects on flow, compressive strength and expansion of RCM mortars and, accordingly, their main effects can be analyzed independently.

### **4.5.1      Substitution level:**

Substitution of RCM by a suitable SCM can decrease the concentration of free lime in the mixture, thus decreasing the initial heat and the false set behavior as the substitution level increases. The general effect of the substitution by SCM in RCM mortars was found to be comparable to the effect of similar substitutions in Portland cement based mortars. As in cement based mortars, flow of RCM mortars can be adjusted by varying the substitution level of the SCM. When substituting RCM by silica fume, flow decreases with increasing substitution level. Conversely, when substituting RCM by class F fly ash, flow increases with increasing substitution level. Likewise, strength of RCM mortars is affected by the substitution level depending on the type of SCM used. When substituting RCM by fly ash 28-day compressive strength decreases with increasing substitution. Conversely, when substituting RCM by silica fume strength increases with increasing substitution until reaching an optimum level. In this study, maximum strength was achieved at 40%

substitution by silica fume. Finally, expansion of RCM mortars was studied using silica fume as the substituting material. In the range of substitution levels explored, expansion increases as the substitution by silica fume increases.

#### **4.5.2 Reactivation temperature:**

Performance of the RCM as a binder for mortars is affected by the relative abundance and chemical composition of its phases, which are, in turn, a result of the temperature history of the reactivation process. Among the phases identified in the XRD of the RCMs produced in this study, the contents of free lime and of two polymorphs of calcium disilicate, beta-C<sub>2</sub>S and a stabilized form of alpha'-C<sub>2</sub>S, are seen to evolve with reactivation temperature.

Free lime content in the RCM increases with increasing reactivation temperature. The rate of increase is higher above 800°C due to faster decomposition of calcium carbonate. Hydration of free lime evolves a significant amount of heat and can produce false set behavior. Consequently, the heat evolved and the false set behavior of RCM increase with increasing reactivation temperature. Likewise, delayed hydration of free lime remaining in the set mortar is a source of expansion, and thus, expansion of RCM mortars increases with increasing reactivation temperature, particularly for materials produced above 800°C.

Depending on the reactivation temperature used, alpha'-C<sub>2</sub>S produced from the decomposition of calcium silicate hydrates above 600 °C can remain stable at ambient temperature in the RCM. Between 660 and 800 °C, alpha-C<sub>2</sub>S content in the RCM increases with increasing reactivation temperature. Conversely, above 800 °C alpha'-C<sub>2</sub>S content decreases with increasing reactivation temperature, partially reverting to beta-C<sub>2</sub>S on cooling. Strength developed by RCM mortars at 7 and 28 days is significantly affected by alpha'-C<sub>2</sub>S content. Consequently, in order to maximize 28-day strength, a RCM having the largest content of alpha'-C<sub>2</sub>S must be obtained by careful selection of the reactivation temperature. The effect of

reactivation temperature on flow of RCM mortars is the opposite as that on strength. Minimum flow is obtained using RCM produced at 800 °C which has the highest alpha'-C<sub>2</sub>S content. Therefore, in order to obtain a workable mortar and at the same time maximize strength, plasticizing admixtures would be required.

#### **4.6 Acknowledgments**

We acknowledge support from project CONICYT/ FONDAP 15110020. We express our gratitude to Professor Pablo Pasten of the Department of Hydraulic and Environmental Engineering, Mr. Iván Navarrete from the Department of Construction Engineering and Management, Mr. Patricio Pérez from the Metallurgy Laboratory of the Department of Mechanical and Metallurgical Engineering, and the staff at the Materials Strength Laboratory, RESMAT, all of them from the School of Engineering of Pontificia Universidad Católica de Chile.

#### **4.7 References**

- Alonso, C., & Fernandez, L. (2004). Dehydration and rehydration processes of cement paste exposed to high temperature environments. *Journal of Materials Science*, 39, 3015–3024.
- Benachrid, M. Y., Diouri, A., Boukhari, A., Aride, J., & Elkhadiri, I. (2005). Hydration of iron–phosphorus doped dicalcium silicate phase. *Materials Chemistry and Physics*, 94(2-3), 190–194. doi:10.1016/j.matchemphys.2005.04.047
- Box, G. E. P., & Wilson, K. B. (1951). On the experimental attainment of optimum conditions. *Journal of the Royal Statistical Society Series B (Statistica Methodology)*, 13(1), 1–45.

- Cuberos, A. J. M., De la Torre, Á. G., Martín-Sedeño, M. C., Moreno-Real, L., Merlini, M., Ordóñez, L. M., & Aranda, M. a. G. (2009). Phase development in conventional and active belite cement pastes by Rietveld analysis and chemical constraints. *Cement and Concrete Research*, 39(10), 833–842. doi:10.1016/j.cemconres.2009.06.017
- Deng, M., Hong, D., Lam, X., & Tang, M. (1995). Mechanism of expansion in hardened cement pastes with hard-burnt free lime. *Cement and Concrete Research*, 25, 440–448.
- Ferraris, C. F., Obla, K. H., & Hill, R. (2001). The influence of mineral admixtures on the rheology of cement paste and concrete. *Cement and Concrete Research*, 31(2), 245–255. doi:10.1016/S0008-8846(00)00454-3
- Igarashi, S., Kubo, H. R., & Kawamura, M. (2000). Long-term volume changes and microcracks formation in high strength mortars. *Cement and Concrete Research*, 30(6), 943–951. doi:10.1016/S0008-8846(00)00251-9
- Kenai, S., Debieb, F., & Azzouz, L. (2002). Mechanical Properties and Durability of Concrete made with Coarse and Fine Recycled Aggregates. In R. K. Dhir, T. D. Dyer, & J. E. Halliday (Eds.), Sustainable Concrete Construction: *Proceedings of the International Conference Held at the University of Dundee, Scotland, UK on 9-11 September, 2002* (pp. 383–392). London: Thomas Telford.
- Khatib, J. M. (2005). Properties of concrete incorporating fine recycled aggregate. *Cement and Concrete Research*, 35(4), 763–769. doi:10.1016/j.cemconres.2004.06.017
- Lawrence, P., Cyr, M., & Ringot, E. (2005). Mineral admixtures in mortars effect of type, amount and fineness of fine constituents on compressive strength. *Cement and Concrete Research*, 35(6), 1092–1105. doi:10.1016/j.cemconres.2004.07.004

- Lopes de Brito, J. M. C., Gonçalves, A. P., & dos Santos, J. R. (2006). Recycled concrete production: Multiple recycling of concrete coarse aggregates. *Revista Ingeniería de Construcción*, 21, 33–40.
- Mazloom, M., Ramezanianpour, a. a., & Brooks, J. J. (2004). Effect of silica fume on mechanical properties of high-strength concrete. *Cement and Concrete Composites*, 26(4), 347–357. doi:10.1016/S0958-9465(03)00017-9
- Meyer, C. (2009). The greening of the concrete industry. *Cement and Concrete Composites*, 31(8), 601–605. doi:10.1016/j.cemconcomp.2008.12.010
- Rao, G. A. (1998). Influence of Silica fume replacement of cement on expansion and drying shrinkage. *Cement and Concrete Research*, 28(10), 1505–1509.
- Rao, G. A. (2003). Investigations on the performance of silica fume-incorporated cement pastes and mortars. *Cement and Concrete Research*, 33(11), 1765–1770. doi:10.1016/S0008-8846(03)00171-6
- Sanchez de Juan, M., & Alaejos Gutiérrez, P. (2009). Study on the influence of attached mortar content on the properties of recycled concrete aggregate. *Construction and Building Materials*, 23(2), 872–877. doi:10.1016/j.conbuildmat.2008.04.012
- Serpell, R., & Lopez, M. (2013). Reactivated cementitious materials from hydrated cement paste wastes. *Cement and Concrete Composites*, 39, 104–114. doi:10.1016/j.cemconcomp.2013.03.020
- Shayan, A., & Xu, A. (2003). Performance and Properties of Structural Concrete Made with Recycled Concrete Aggregate. *ACI Materials Journal*, 100(5), 371–380.
- Shui, Z., Xuan, D., Chen, W., Yu, R., & Zhang, R. (2009). Cementitious characteristics of hydrated cement paste subjected to various dehydration temperatures. *Construction and Building Materials*, 23(1), 531–537. doi:10.1016/j.conbuildmat.2007.10.016

- Shui, Z., Xuan, D., Wan, H., & Cao, B. (2008). Rehydration reactivity of recycled mortar from concrete waste experienced to thermal treatment. *Construction and Building Materials*, 22(8), 1723–1729. doi:10.1016/j.conbuildmat.2007.05.012
- Tam, V. W. Y., & Tam, C. M. (2006). A review on the viable technology for construction waste recycling. *Resources, Conservation and Recycling*, 47(3), 209–221. doi:10.1016/j.resconrec.2005.12.002
- Taylor, H. F. W. (1997). *Cement Chemistry* (2nd ed.). London: Thomas Telford.

## GENERAL REFERENCES

- Abbas, A., Fathifazl, G., Isgor, O. B., Razaqpur, a. G., Fournier, B., & Foo, S. (2009). Durability of recycled aggregate concrete designed with equivalent mortar volume method. *Cement and Concrete Composites*, 31(8), 555–563.  
doi:10.1016/j.cemconcomp.2009.02.012
- Achtemichuk, S., Hubbard, J., Sluce, R., & Shehata, M. H. (2009). The utilization of recycled concrete aggregate to produce controlled low-strength materials without using Portland cement. *Cement and Concrete Composites*, 31(8), 564–569.  
doi:10.1016/j.cemconcomp.2008.12.011
- ACI. (2008). Sustainability takes the spotlight at the American Concrete Institute. *Press release, American Concrete Institute*. Retrieved August 23, 2013, from <http://www.concrete.org/GENERAL/PressReleases/Dec162008Release.htm>
- ACI Committee 229. (2013). *ACI 229R-99 Controlled Low-Strength Materials* (pp. 1–13). Farmington Hills.
- Ai, H. M., Wei, J., Bai, J. Y., & Lu, P. G. (2011). Properties of Recycled-Cement Produced from Waste Concrete. *Advanced Materials Research*, 194-196, 1170–1175.  
doi:10.4028/www.scientific.net/AMR.194-196.1170
- Alizadeh, V., Helwany, S., Ghorbanpoor, A., & Sobolev, K. (2014). Design and application of controlled low strength materials as a structural fill. *Construction and Building Materials*, 53, 425–431. doi:10.1016/j.conbuildmat.2013.12.006
- Alonso, C., & Fernandez, L. (2004). Dehydration and rehydration processes of cement paste exposed to high temperature environments. *Journal of Materials Science*, 39, 3015–3024.

- Annerel, E., & Taerwe, L. (2009). Revealing the temperature history in concrete after fire exposure by microscopic analysis. *Cement and Concrete Research*, 39(12), 1239–1249. doi:10.1016/j.cemconres.2009.08.017
- Arioz, O. (2007). Effects of elevated temperatures on properties of concrete. *Fire Safety Journal*, 42(8), 516–522. doi:10.1016/j.firesaf.2007.01.003
- Aspdin, J. (1824). An improvement in the modes of producing an artificial stone. U.K.: British Patent Office.
- Benarchid, M. Y., Diouri, A., Boukhari, A., Aride, J., & Elkhadiri, I. (2005). Hydration of iron–phosphorus doped dicalcium silicate phase. *Materials Chemistry and Physics*, 94(2-3), 190–194. doi:10.1016/j.matchemphys.2005.04.047
- Bhat, S. T., & Lovell, C. W. (1997). Flowable Fill Using Waste Foundry Sand: A Substitute for Compacted or Stabilized Soil. In M. A. Wasemiller & K. B. Hoddinott (Eds.), *Testing Soil Mixed With Waste or Recycled Materials, ASTM STP 1275*. American Society for Testing and Materials.
- Box, G. E. P., & Hunter, J. S. (1957). Multifactor experimental designs for exploring response surfaces. *Annals of Mathematical Statistics*, 28(1), 195–241.
- Box, G. E. P., & Hunter, J. S. (2005). *Statistics for Experimenters* (2nd Ed., p. 212). Hoboken, New Jersey: John Wiley & Sons, Inc.
- Box, G. E. P., & Wilson, K. B. (1951). On the experimental attainment of optimum conditions. *Journal of the Royal Statistical Society Series B (Statistica Methodology)*, 13(1), 1–45.
- Brown, M. T., & Buranakarn, V. (2003). Emergy indices and ratios for sustainable material cycles and recycle options. *Resources, Conservation and Recycling*, 38(1), 1–22. doi:10.1016/S0921-3449(02)00093-9

- Castellote, M., Alonso, C., Andrade, C., Turrillas, X., & Campo, J. (2004). Composition and microstructural changes of cement pastes upon heating, as studied by neutron diffraction. *Cement and Concrete Research*, 34(9), 1633–1644. doi:10.1016/S0008-8846(03)00229-1
- Cody, A. M., Lee, H., Cody, R. D., & Spry, P. G. (2004). The effects of chemical environment on the nucleation, growth, and stability of ettringite  $[Ca_3Al(OH)_6]_2(SO_4)_3 \cdot 26H_2O$ . *Cement and Concrete Research*, 34(5), 869–881.
- Cuberos, A. J. M., De la Torre, Á. G., Martín-Sedeño, M. C., Moreno-Real, L., Merlini, M., Ordóñez, L. M., & Aranda, M. a. G. (2009). Phase development in conventional and active belite cement pastes by Rietveld analysis and chemical constraints. *Cement and Concrete Research*, 39(10), 833–842. doi:10.1016/j.cemconres.2009.06.017
- DeJong, M. J., & Ulm, F.-J. (2007). The nanogranular behavior of C-S-H at elevated temperatures (up to 700 °C). *Cement and Concrete Research*, 37(1), 1–12. doi:10.1016/j.cemconres.2006.09.006
- Deng, M., Hong, D., Lam, X., & Tang, M. (1995). Mechanism of expansion in hardened cement pastes with hard-burnt free lime. *Cement and Concrete Research*, 25, 440–448.
- Dombrowski, K., Buchwald, A., & Weil, M. (2006). The influence of calcium content on the structure and thermal performance of fly ash based geopolymers. *Journal of Materials Science*, 42(9), 3033–3043. doi:10.1007/s10853-006-0532-7
- Du, L., & Folliard, K. (2002). Effects of constituent materials and quantities on water demand and compressive strength of controlled low-strength material. *Journal of materials in civil engineering*, 14(6), 485–495. doi:10.1061/(ASCE)0899-1561(2002)14:6(485)

- Du, L., Folliard, K., & Trejo, D. (2004). A New Unbonded Capping Practice for Evaluating the Compressive Strength of Controlled Low-Strength Material Cylinders. *Cement, Concrete, and Aggregates*, 26(1), 1–8. doi:10.1520/CCA11895
- Etxeberria, M., Ainchil, J., Pérez, M. E., & González, A. (2013). Use of recycled fine aggregates for Control Low Strength Materials (CLSMs) production. *Construction and Building Materials*, 44, 142–148. doi:10.1016/j.conbuildmat.2013.02.059
- Etxeberria, M., Vázquez, E., Marí, A., & Barra, M. (2007). Influence of amount of recycled coarse aggregates and production process on properties of recycled aggregate concrete. *Cement and Concrete Research*, 37(5), 735–742. doi:10.1016/j.cemconres.2007.02.002
- Evangelista, L., & de Brito, J. (2007). Mechanical behaviour of concrete made with fine recycled concrete aggregates. *Cement and Concrete Composites*, 29(5), 397–401. doi:10.1016/j.cemconcomp.2006.12.004
- Farage, M. C. R., Sercombe, J., & Gallé, C. (2003). Rehydration and microstructure of cement paste after heating at temperatures up to 300 °C. *Cement and Concrete Research*, 33(7), 1047–1056. doi:10.1016/S0008-8846(03)00005-X
- Ferraris, C. F., Obla, K. H., & Hill, R. (2001). The influence of mineral admixtures on the rheology of cement paste and concrete. *Cement and Concrete Research*, 31(2), 245–255. doi:10.1016/S0008-8846(00)00454-3
- Fridrichová, M. (2007). Hydration of belite cements prepared from recycled concrete residues. *Ceramics-Silikaty*, 51(1), 45–51. Retrieved from [http://www.ceramics-silikaty.cz/2007/2007\\_01\\_045.htm](http://www.ceramics-silikaty.cz/2007/2007_01_045.htm)
- Gartner, E. (2004). Industrially interesting approaches to “low-CO<sub>2</sub>” cements. *Cement and Concrete Research*, 34(9), 1489–1498. doi:10.1016/j.cemconres.2004.01.021

- Handoo, S. K., Agarwal, S., & Agarwal, S. K. (2002). Physicochemical, mineralogical, and morphological characteristics of concrete exposed to elevated temperatures. *Cement and Concrete Research*, 32(7), 1009–1018. doi:10.1016/S0008-8846(01)00736-0
- Hansen, T. C., & Boegh, E. (1985). Elasticity and Drying Shrinkage of Recycled Aggregate Concrete. *ACI Journal*, 82(5), 648–652.
- Hanson, J. L., Stone, G. M., & Yesiller, N. (2012). Use of Post-Consumer Corrugated Fiberboard as Fine Aggregate Replacement in Controlled Low-Strength Materials. *Journal of ASTM International*, 9(2), 562–579. doi:10.1520/JAI103843
- Hendricks, C. A., Jager, D. De, Blok, K., & Riemer, P. (1998). Emission Reduction of Greenhouse Gases from the Cement Industry. In *Proceedings of the Fourth International Conference on Greenhouse Gas Control Technologies, Interlaken, Austria*. Retrieved from <http://citeseerx.ist.psu.edu/viewdoc/summary?doi=10.1.1.133.9042>
- Huntzinger, D. N., & Eatmon, T. D. (2009). A life-cycle assessment of Portland cement manufacturing: comparing the traditional process with alternative technologies. *Journal of Cleaner Production*, 17(7), 668–675. doi:10.1016/j.jclepro.2008.04.007
- Igarashi, S., Kubo, H. R., & Kawamura, M. (2000). Long-term volume changes and microcracks formation in high strength mortars. *Cement and Concrete Research*, 30(6), 943–951. doi:10.1016/S0008-8846(00)00251-9
- Janotka, I., & Mojumdar, S. C. (2005). Thermal analysis at the evaluation of concrete damage by high temperatures. *Journal of Thermal Analysis and Calorimetry*, 81(1), 197–203. doi:10.1007/s10973-005-0767-6
- Juenger, M. C. G., & Jennings, H. M. (2001). Effects of High Alkalinity on Cement Pastes. *ACI Materials Journal*, 98, 251–255.

- Juenger, M. C. G., Winnefeld, F., Provis, J. L., & Ideker, J. H. (2011). Advances in alternative cementitious binders. *Cement and Concrete Research*, 41(12), 1232–1243. doi:10.1016/j.cemconres.2010.11.012
- Kasai, Y. (2004). Recent Trends in Recycling of Concrete Waste and Use of Recycled Aggregate Concrete in Japan. In T. C. Liu & C. Meyer (Eds.), *SP-219-Recycling concrete and other materials for sustainable development* (pp. 11–34). Farmington Hills: American Concrete Institute International.
- Katz, A., & Kovler, K. (2004). Utilization of industrial by-products for the production of controlled low strength materials (CLSM). *Waste management (New York, N.Y.)*, 24(5), 501–12. doi:10.1016/S0956-053X(03)00134-X
- Kenai, S., Debieb, F., & Azzouz, L. (2002). Mechanical Properties and Durability of Concrete made with Coarse and Fine Recycled Aggregates. In R. K. Dhir, T. D. Dyer, & J. E. Halliday (Eds.), *Sustainable Concrete Construction: Proceedings of the International Conference Held at the University of Dundee, Scotland, UK on 9-11 September, 2002* (pp. 383–392). London: Thomas Telford.
- Khatib, J. M. (2005). Properties of concrete incorporating fine recycled aggregate. *Cement and Concrete Research*, 35(4), 763–769. doi:10.1016/j.cemconres.2004.06.017
- Kou, S. C., & Poon, C. S. (2009). Properties of self-compacting concrete prepared with coarse and fine recycled concrete aggregates. *Cement and Concrete Composites*, 31(9), 622–627. doi:10.1016/j.cemconcomp.2009.06.005
- Lachemi, M., Şahmaran, M., Hossain, K. M. a., Lotfy, a., & Shehata, M. (2010). Properties of controlled low-strength materials incorporating cement kiln dust and slag. *Cement and Concrete Composites*, 32(8), 623–629. doi:10.1016/j.cemconcomp.2010.07.011
- Lauritzen, E. K. (2004). Recycling concrete-An Overview of Challenges and Opportunities. In T. C. Liu & C. Meyer (Eds.), *SP-219-Recycling concrete and other*

- materials for sustainable development* (pp. 1–10). Farmington Hills: American Concrete Institute International.
- Lawrence, P., Cyr, M., & Ringot, E. (2005). Mineral admixtures in mortars effect of type, amount and fineness of fine constituents on compressive strength. *Cement and Concrete Research*, 35(6), 1092–1105. doi:10.1016/j.cemconres.2004.07.004
- Lin, Y.-H., Tyan, Y.-Y., Chang, T.-P., & Chang, C.-Y. (2004). An assessment of optimal mixture for concrete made with recycled concrete aggregates. *Cement and Concrete Research*, 34(8), 1373–1380. doi:10.1016/j.cemconres.2003.12.032
- Lo Presti, A., Artioli, G., Bravo, A., Cella, F., Cerulli, T., & Magistri, M. (2007). Study of the Influence of Soluble Ions on Morphological and Microstructural Properties of Synthetic Ettringite. In *Proceedings of the 12th International Congress on the Chemistry of Cement*. Montreal, Canada.
- Lopes de Brito, J. M. C., Gonçalves, A. P., & dos Santos, J. R. (2006). Recycled concrete production: Multiple recycling of concrete coarse aggregates. *Revista Ingeniería de Construcción*, 21, 33–40.
- Madlool, N. a., Saidur, R., Hossain, M. S., & Rahim, N. a. (2011). A critical review on energy use and savings in the cement industries. *Renewable and Sustainable Energy Reviews*, 15(4), 2042–2060. doi:10.1016/j.rser.2011.01.005
- Mazloom, M., Ramezanianpour, a. a., & Brooks, J. J. (2004). Effect of silica fume on mechanical properties of high-strength concrete. *Cement and Concrete Composites*, 26(4), 347–357. doi:10.1016/S0958-9465(03)00017-9
- Mehta, P. K., & Monteiro, P. J. M. (2006). *Concrete: microstructure, properties and materials* (Third Ed.). New York: McGraw-Hill Companies, Inc.

- Mendes, A., Sanjayan, J., & Collins, F. (2007). Phase transformations and mechanical strength of OPC/Slag pastes submitted to high temperatures. *Materials and Structures*, 41(2), 345–350. doi:10.1617/s11527-007-9247-8
- Meyer, C. (2009). The greening of the concrete industry. *Cement and Concrete Composites*, 31(8), 601–605. doi:10.1016/j.cemconcomp.2008.12.010
- Naganathan, S., Razak, H. A., & Hamid, S. N. A. (2012). Properties of controlled low-strength material made using industrial waste incineration bottom ash and quarry dust. *Materials & Design*, 33, 56–63. doi:10.1016/j.matdes.2011.07.014
- Nagataki, S., Gokce, a, Saeki, T., & Hisada, M. (2004). Assessment of recycling process induced damage sensitivity of recycled concrete aggregates. *Cement and Concrete Research*, 34(6), 965–971. doi:10.1016/j.cemconres.2003.11.008
- Naik, Tarum R, & Singh, S. S. (1997). Influence of Fly Ash on Setting and Hardening Characteristics of Concrete Systems. *ACI Materials Journal*, 94(5), 355–360.
- Naik, Tarun R, Asce, F., Kraus, R. N., Ramme, B. W., Chun, Y., & Kumar, R. (2006). High-Carbon Fly Ash in Manufacturing Conductive CLSM and Concrete. *Journal of materials in civil engineering*, 18(6), 743–746. doi:10.1061/(ASCE)0899-1561(2006)18:6(743)
- Nataraja, M. C., & Nalanda, Y. (2008). Performance of industrial by-products in controlled low-strength materials (CLSM). *Waste Management*, 28(7), 1168–1181. Retrieved from <http://www.sciencedirect.com/science/article/pii/S0956053X07001456>
- NIST/SEMATECH. (2003). e-Handbook of Statistical Methods. Retrieved from <http://www.itl.nist.gov/div898/handbook/>
- Odum, H. T. (1996). *Environmental Accounting: Energy and Environmental Decision Making* (1st ed.). New York: John Wiley & Sons, Inc.

- Okada, Y., Sasaki, K., Zhong, B., Ishida, H., & Mitsuda, T. (1994). Formation Processes of  $\beta$ -C<sub>2</sub>S by the Decomposition of Hydrothermally Prepared C-S-H with Ca(OH)2. *Journal of the American Ceramic Society*, 77, 1319–1323. doi:DOI: 10.1111/j.1151-2916.1994.tb05409.x
- Padmini, A. K., Ramamurthy, K., & Mathews, M. S. (2009). Influence of parent concrete on the properties of recycled aggregate concrete. *Construction and Building Materials*, 23(2), 829–836. doi:10.1016/j.conbuildmat.2008.03.006
- PCA. (2008). Top ten reasons to use concrete for sustainable design. *Portland Cement Association*. Retrieved August 22, 2013, from [http://www.cement.org/newsroom/AIA08/Top\\_Ten.htm](http://www.cement.org/newsroom/AIA08/Top_Ten.htm)
- Peterson, V. K., Neumann, D. a., & Livingston, R. a. (2006). Effect of NaOH on the kinetics of tricalcium silicate hydration: A quasielastic neutron scattering study. *Chemical Physics Letters*, 419(1-3), 16–20. doi:10.1016/j.cplett.2005.11.032
- Phan, L. T., Lawson, J. R., & Davis, F. L. (2001). Effects of elevated temperature exposure on heating characteristics, spalling, and residual properties of high performance concrete. *Materials and Structures*, 34(March), 83–91.
- Pierce, C. E., Tripathi, H., & Brown, T. W. (2003). Cement Kiln Dust in Controlled Low-Strength Materials. *ACI Materials Journal*, 100(6), 455–462. doi:10.14359/12951
- Poon, C. S., Azhar, S., Anson, M., & Wong, Y. L. (2001). Strength and durability recovery of fire-damaged concrete after post-fire-curing. *Cement and Concrete Research*, 31(9), 1307–1318. doi:10.1016/S0008-8846(01)00582-8
- Poon, C. S., Qiao, X. C., & Chan, D. (2006). The cause and influence of self-cementing properties of fine recycled concrete aggregates on the properties of unbound sub-base. *Waste management (New York, N.Y.)*, 26(10), 1166–72. doi:10.1016/j.wasman.2005.12.013

- Poon, C. S., Shui, Z. H., & Lam, L. (2004). Effect of microstructure of ITZ on compressive strength of concrete prepared with recycled aggregates. *Construction and Building Materials*, 18(6), 461–468. doi:10.1016/j.conbuildmat.2004.03.005
- Powers, T. C. (1968). *The properties of fresh concrete*. New York: John Wiley & Sons, Inc.
- Powers, T. C., & Brownyard, T. L. (1947). Studies of the Physical Properties of Hardened Portland Cement Paste. *Journal American Concrete Institute*, 18(7), 933–992.
- Rao, G. A. (1998). Influence of Silica fume replacement of cement on expansion and drying shrinkage. *Cement and Concrete Research*, 28(10), 1505–1509.
- Rao, G. A. (2003). Investigations on the performance of silica fume-incorporated cement pastes and mortars. *Cement and Concrete Research*, 33(11), 1765–1770. doi:10.1016/S0008-8846(03)00171-6
- Richardson, M. G. (2002). *Fundamentals of durable reinforced concrete*. London & New York: Spon Press.
- RILEM. (2009). 1st announcement & call for papers, 2nd international RILEM conference: progress of recycling in the built environment. *RILEM*. Retrieved November 30, 2009, from <http://www.rilem.net/manifs/2009-020412.doc>
- Roesler, J., Lange, D., Salas, A., Brand, A., & Arboleda, C. (2013). *COE Report No. 34: Properties of recycled concrete aggregates for airfield rigid pavements* (pp. 1–98). Urbana, IL.
- Sanchez de Juan, M., & Alaejos Gutiérrez, P. (2009). Study on the influence of attached mortar content on the properties of recycled concrete aggregate. *Construction and Building Materials*, 23(2), 872–877. doi:10.1016/j.conbuildmat.2008.04.012

- Serpell, R., & Lopez, M. (2013). Reactivated cementitious materials from hydrated cement paste wastes. *Cement and Concrete Composites*, 39, 104–114. doi:10.1016/j.cemconcomp.2013.03.020
- Shayan, A., & Xu, A. (2003). Performance and Properties of Structural Concrete Made with Recycled Concrete Aggregate. *ACI Materials Journal*, 100(5), 371–380.
- Shui, Z., Xuan, D., Chen, W., Yu, R., & Zhang, R. (2009). Cementitious characteristics of hydrated cement paste subjected to various dehydration temperatures. *Construction and Building Materials*, 23(1), 531–537. doi:10.1016/j.conbuildmat.2007.10.016
- Shui, Z., Xuan, D., Wan, H., & Cao, B. (2008). Rehydration reactivity of recycled mortar from concrete waste experienced to thermal treatment. *Construction and Building Materials*, 22(8), 1723–1729. doi:10.1016/j.conbuildmat.2007.05.012
- Shui, Z., Yu, R., & Dong, J. (2011). Activation of Fly Ash with Dehydrated Cement Paste. *ACI Materials Journal*, 108(2), 204–208.
- Stark, J., & Bollmann, K. (2000). Delayed Ettringite Formation in Concrete. *Nordic Concrete Research Publications*, 23, 4–28.
- Taha, R. A., Alnuaimi, A. S., Al-Jabri, K. S., & Al-Harthy, A. S. (2007). Evaluation of controlled low strength materials containing industrial by-products. *Building and Environment*, 42(9), 3366–3372.
- Tam, V. W. Y., & Tam, C. M. (2006). A review on the viable technology for construction waste recycling. *Resources, Conservation and Recycling*, 47(3), 209–221. doi:10.1016/j.resconrec.2005.12.002
- Tanikella, P., & Olek, J. (2009). Incorporating physical and chemical characteristics of fly ash in statistical modeling of binder properties. *Masters Abstracts International*, 48(2).
- Taylor, H. F. W. (1997). *Cement Chemistry* (2nd ed.). London: Thomas Telford.

- Tikalsky, P., Gaffney, M., & Regan, R. (2000). Properties of Controlled Low-Strength Material Containing Foundry Sand. *ACI Materials Journal*, 97(6), 698–702.  
doi:10.14359/9984
- U.S. Geological Survey. (2009). *Mineral Commodity Summaries 2009* (pp. 40–41). Reston, Virginia.
- U.S. Geological Survey. (2013). *Mineral Commodity Summaries 2013* (pp. 38–39). Reston, Virginia.
- Yuan, F., Shen, L., & Li, Q. (2011). Energy analysis of the recycling options for construction and demolition waste. *Waste management (New York, N.Y.)*, 31(12), 2503–11. doi:10.1016/j.wasman.2011.07.001

## **APPENDICES**

## Appendix A: Supplementary data from the FRCA-based CLSM study

Data and figures provided in this section supplement information reported in the manuscript “Relative proportioning of Controlled Low-Strength Materials” submitted to *ACI Materials Journal*.

**Table A.1** Mixture compositions for the three replications of the CLSM central composite experiment

Case	Coded levels			Mixture constituents (kg/m <sup>3</sup> )												
				FVA + FA1				FRCA + FA1				FRCA + FA2				
	1:	2:	3:	Agg.	OPC	SCM	Water	Agg.	OPC	SCM	Water	Agg.	OPC	SCM	Water	W/OPC
R1	-1	-1	-1	1644	37	332	240	1507	37	332	240	1507	37	331	239	6.50
R2	1	-1	-1	1644	26	238	278	1507	26	238	278	1507	26	238	277	10.50
R3	-1	1	-1	1381	47	421	304	1266	47	421	304	1266	47	419	302	6.50
R4	1	1	-1	1381	34	302	352	1266	34	302	352	1266	33	301	351	10.50
R5	-1	-1	1	1644	74	297	241	1507	74	297	241	1507	74	296	240	3.25
R6	1	-1	1	1644	53	213	279	1507	53	213	279	1507	53	212	278	5.25
R7	-1	1	1	1381	94	376	306	1266	94	376	306	1266	94	375	304	3.25
R8	1	1	1	1381	67	270	354	1266	67	270	354	1266	67	269	353	5.25
R9	0	0	0	1513	53	298	298	1386	53	298	298	1386	52	297	297	5.67
R10	-1.682	0	0	1513	73	412	249	1386	73	412	249	1386	72	410	248	3.42
R11	1.682	0	0	1513	41	233	326	1386	41	233	326	1386	41	232	324	7.91
R12	0	-1.682	0	1735	42	239	239	1589	42	239	239	1589	42	238	238	5.67
R13	0	1.682	0	1291	63	357	357	1183	63	357	357	1183	63	355	355	5.67
R14	0	0	-1.682	1513	23	326	297	1386	23	326	297	1386	23	325	295	12.90
R15	0	0	1.682	1513	82	270	299	1386	82	270	299	1386	82	269	298	3.63
R16	0	0	0	1513	53	298	298	1386	53	298	298	1386	52	297	297	5.67
R17	0	0	0	1513	53	298	298	1386	53	298	298	1386	52	297	297	5.67

Notes: 1 Kg/m<sup>3</sup> = 1.685 lb/yd<sup>3</sup>; Aggregate weight is in SSD condition; FA1: Class C fly ash; FA2.: highly reactive class C fly ash

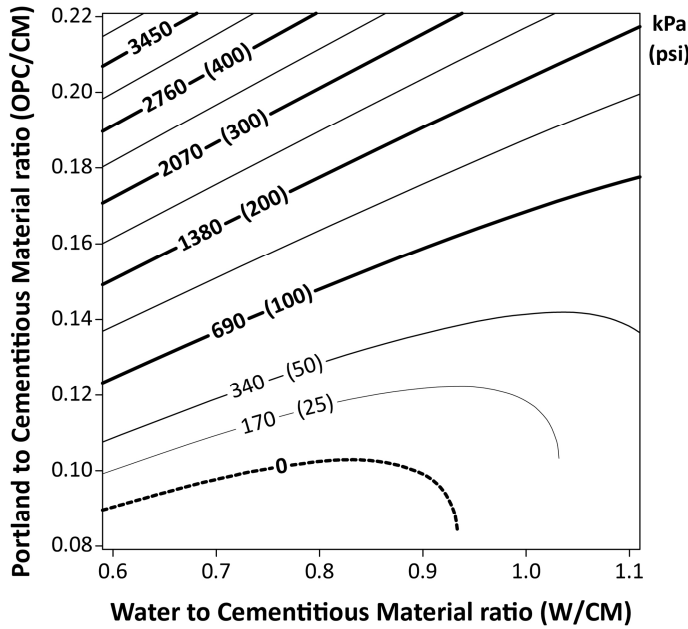


**Figure A.1** Predicted response surface for 28-day compressive strength as a function of the W/CM and OPC/CM ratios for FVA-based CLSM incorporating class C fly ash.

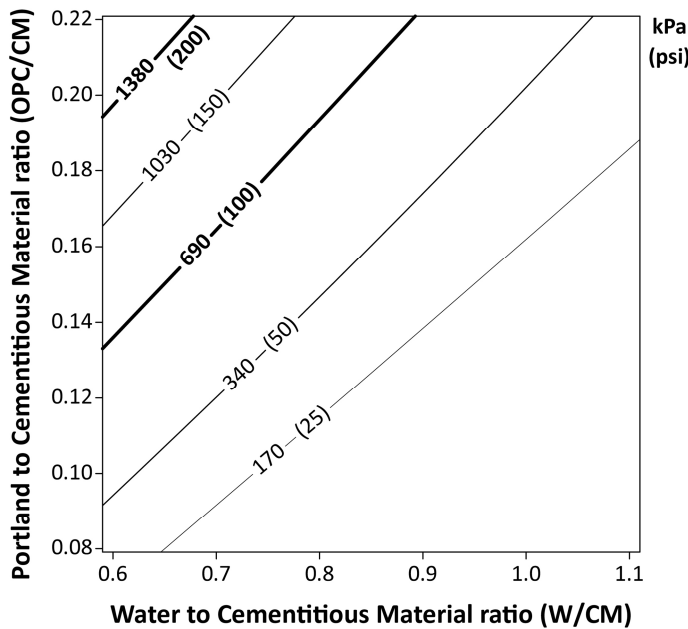


**Figure A.2** Predicted response surface for 28-day compressive strength as a function of the W/CM and OPC/CM ratios for FRCA-based CLSM incorporating class C fly ash.

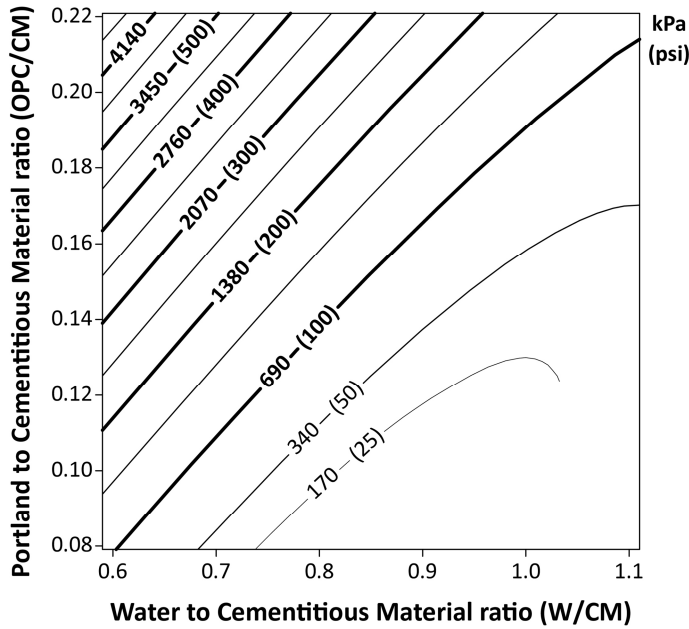


**Figure A.3** Predicted response surface for 28-day compressive strength as a function of the W/CM and OPC/CM ratios for FRCA-based CLSM incorporating a highly reactive class C fly ash.



**Figure A.4** Comparison of slump-flow results for FRCA-based CLSM at high (left) and low (right) volumetric paste percent.

## Appendix B: Supplementary data from the multifactorial study of RCM

Data and figures provided in this section supplement information reported in the paper “Reactivated cementitious materials from hydrated cement paste wastes” published in *Cement and Concrete Composites*.

**Table B.1** Weight loss on dehydration of source materials

D. Temp.	w/c Si fume	0.35		0.425	0.50		row averages
		10 %	0 %	5 %	10 %	0 %	
800 °C		11.8 %	12.3 %		13.0 %	13.1 %	12.5%
750 °C				12.5%			12.5%
700 °C		10.8 %	11.8 %		12.1 %	12.3 %	11.8%
column		11.3 %	12.0 %		12.5 %	12.7 %	12.1%
averages		11.7 %			12.6 %		



**Figure B.1** 3-gang 20mm side mold for RCM-based pastes

**Table B.2** RCM pastes: Individual case results for block 1, in execution order.

Case	Experimental factors (coded)									Responses					
	X1	X2	X3	X4	X5	X6	X7	X8	X9	7 days		28 days		90 days	
	FGR	DoH-s	NaOH	OPC	T°DH	SCM	SCM-s	F.Si-s	F.Al-s	SSD Den. (g/cm <sup>3</sup> )	Y1 Strength (MPa)	Y4 SSD Den. (g/cm <sup>3</sup> )	Y2 Strength (MPa)	SSD Den. (g/cm <sup>3</sup> )	Y3 Strength (MPa)
4	1	1	-1	-1	-1	-1	1	-1	-1	1.726	17.1	1.731	26.4	1.731	27.4
58	1	-1	-1	1	1	1	1	-1	1	1.642	0.6	1.688	21.7	1.690	35.3
21	-1	-1	1	-1	1	-1	-1	1	1	1.701	2.8	1.700	4.5	1.688	6.7
16	1	1	1	1	-1	-1	1	1	1	1.709	7.3	1.713	9.4	1.709	12.3
65 c	0	0	0	0	0	0	0	0	0	1.710	17.4	1.719	26.0	1.705	30.9
13	-1	-1	1	1	-1	-1	1	-1	-1	1.630	1.7	1.663	4.5	1.650	7.7
1	-1	-1	-1	-1	-1	-1	1	1	1	1.625	3.1	1.656	8.2	1.643	12.4
54	1	-1	1	-1	1	1	1	1	-1	1.700	16.0	1.706	27.6	1.703	30.0
46	1	-1	1	1	-1	1	-1	-1	1	1.645	7.8	1.663	18.9	1.655	24.1
34	1	-1	-1	-1	-1	1	-1	1	-1	1.611	3.3	1.613	14.4	1.606	20.5
55	-1	1	1	-1	1	1	1	-1	1	1.646	13.5	1.669	24.5	1.660	27.7
24	1	1	1	-1	1	-1	-1	-1	-1	1.716	2.8	1.731	6.3	1.735	9.6
47	-1	1	1	1	-1	1	-1	1	-1	1.663	11.7	1.669	19.7	1.654	22.3
66 c	0	0	0	0	0	0	0	0	0	1.709	13.8	1.725	22.2	1.733	27.2
25	-1	-1	-1	1	1	-1	-1	-1	-1	1.721	10.5	1.731	21.7	1.716	22.5
35	-1	1	-1	-1	-1	1	-1	-1	1	1.675	10.3	1.688	23.9	1.685	31.7
28	1	1	-1	1	1	-1	-1	1	1	1.664	3.8	1.675	13.8	1.676	17.5
59	-1	1	-1	1	1	1	1	1	-1	1.646	11.2	1.669	32.8	1.663	37.1
Block means (including central cases)										1.674	8.6	1.689	18.1	1.683	22.4

**Table B.3** RCM pastes: Individual case results for block 2, in execution order.

Case	Experimental factors (coded)									Responses					
	X1	X2	X3	X4	X5	X6	X7	X8	X9	7 days		28 days		90 days	
	FGR	DoH-s	NaOH	OPC	T°DH	SCM	SCM-s	F.Si-s	F.Al-s	SSD Den. (g/cm <sup>3</sup> )	Y1 Strength (MPa)	Y4 SSD Den. (g/cm <sup>3</sup> )	Y2 Strength (MPa)	SSD Den. (g/cm <sup>3</sup> )	Y3 Strength (MPa)
63	-1	1	1	1	1	1	-1	-1	1	1.707	16.4	1.711	26.2	1.710	24.7
17	-1	-1	-1	-1	1	-1	1	-1	-1	1.689	0.8	1.714	18.8	1.706	25.3
32	1	1	1	1	1	-1	1	-1	-1	1.721	14.4	1.729	17.1	1.730	15.8
29	-1	-1	1	1	1	-1	1	1	1	1.678	1.8	1.693	4.8	1.695	8.6
67 c	0	0	0	0	0	0	0	0	0	1.688	14.2	1.691	22.6	1.681	22.2
20	1	1	-1	-1	1	-1	1	1	1	1.671	0.8	1.702	16.9	1.688	19.8
39	-1	1	1	-1	-1	1	1	1	-1	1.657	16.4	1.671	24.4	1.670	26.2
42	1	-1	-1	1	-1	1	1	1	-1	1.665	12.8	1.676	31.2	1.658	37.4
8	1	1	1	-1	-1	-1	-1	1	1	1.688	2.5	1.694	5.5	1.691	8.7
43	-1	1	-1	1	-1	1	1	-1	1	1.631	14.0	1.645	28.8	1.643	31.6
50	1	-1	-1	-1	1	1	-1	-1	1	1.628	5.3	1.646	27.4	1.636	29.6
9	-1	-1	-1	1	-1	-1	-1	1	1	1.665	4.5	1.666	8.7	1.656	12.0
51	-1	1	-1	-1	1	1	-1	1	-1	1.698	13.1	1.703	31.5	1.693	39.0
68 c	0	0	0	0	0	0	0	0	0	1.696	16.7	1.704	26.3	1.700	29.4
12	1	1	-1	1	-1	-1	-1	-1	-1	1.684	1.5	1.693	6.5	1.694	13.6
38	1	-1	1	-1	-1	1	1	-1	1	1.674	17.3	1.684	25.7	1.684	27.3
62	1	-1	1	1	1	1	-1	1	-1	1.663	5.8	1.668	17.4	1.658	21.9
5	-1	-1	1	-1	-1	-1	-1	-1	-1	1.715	4.0	1.720	7.4	1.709	10.7
Block means (including central cases)										1.679	9.0	1.689	19.3	1.683	22.4

**Table B.4** RCM pastes: Individual case results for block 3, in execution order.

Case	Experimental factors (coded)									Responses					
	X1	X2	X3	X4	X5	X6	X7	X8	X9	7 days		28 days		90 days	
	<i>FGR</i>	<i>DoH-s</i>	<i>NaOH</i>	<i>OPC</i>	<i>T°DH</i>	<i>SCM</i>	<i>SCM-s</i>	<i>F.Si-s</i>	<i>F.Al-s</i>	SSD Den. (g/cm <sup>3</sup> )	Y1 Strength (MPa)	Y4 SSD Den. (g/cm <sup>3</sup> )	Y2 Strength (MPa)	SSD Den. (g/cm <sup>3</sup> )	Y3 Strength (MPa)
23	-1	1	1	-1	1	-1	1	1	-1	1.700	7.0	1.710	12.2	1.693	12.9
36	1	1	-1	-1	-1	1	1	1	1	1.655	12.7	1.670	28.2	1.663	35.5
33	-1	-1	-1	-1	-1	1	1	-1	-1	1.648	11.6	1.668	25.8	1.664	29.6
3	-1	1	-1	-1	-1	-1	-1	1	-1	1.692	6.2	1.693	9.3	1.675	11.8
69 c	0	0	0	0	0	0	0	0	0	1.683	16.6	1.693	25.8	1.695	29.7
26	1	-1	-1	1	1	-1	1	1	-1	1.657	1.4	1.680	18.9	1.669	23.2
56	1	1	1	-1	1	1	-1	1	1	1.669	10.3	1.681	25.0	1.679	25.8
14	1	-1	1	1	-1	-1	-1	1	-1	1.656	1.3	1.663	2.8	1.660	5.3
60	1	1	-1	1	1	1	-1	-1	-1	1.661	5.0	1.674	20.7	1.660	28.1
45	-1	-1	1	1	-1	1	1	1	1	1.634	7.1	1.647	14.1	1.644	18.1
2	1	-1	-1	-1	-1	-1	-1	-1	1	1.670	2.2	1.681	7.5	1.681	12.4
27	-1	1	-1	1	1	-1	1	-1	1	1.687	4.3	1.713	24.1	1.716	29.9
22	1	-1	1	-1	1	-1	1	-1	1	1.714	6.7	1.729	10.5	1.729	13.1
70 c	0	0	0	0	0	0	0	0	0	1.690	15.7	1.701	24.8	1.703	26.8
53	-1	-1	1	-1	1	1	-1	-1	-1	1.712	13.8	1.720	24.9	1.711	24.3
48	1	1	1	1	-1	1	1	-1	-1	1.678	20.0	1.686	26.0	1.678	28.1
57	-1	-1	-1	1	1	1	-1	1	1	1.649	7.8	1.662	22.7	1.658	31.2
15	-1	1	1	1	-1	-1	-1	-1	1	1.673	4.5	1.681	7.1	1.678	10.7
Block means (including central cases)										1.674	8.6	1.686	18.3	1.681	22.0

**Table B.5** RCM pastes: Individual case results for block 4, in execution order.

Case	Experimental factors (coded)									Responses					
	X1	X2	X3	X4	X5	X6	X7	X8	X9	7 days		28 days		90 days	
	FGR	DoH-s	NaOH	OPC	T°DH	SCM	SCM-s	F.Si-s	F.Al-s	SSD Den. (g/cm <sup>3</sup> )	Y1 Strength (MPa)	Y4 SSD Den. (g/cm <sup>3</sup> )	Y2 Strength (MPa)	SSD Den. (g/cm <sup>3</sup> )	Y3 Strength (MPa)
49	-1	-1	-1	-1	1	1	1	1	1	1.649	0.8	1.676	18.5	1.678	33.5
6	1	-1	1	-1	-1	-1	1	1	-1	1.700	7.6	1.708	9.6	1.700	11.2
18	1	-1	-1	-1	1	-1	-1	1	-1	1.690	1.8	1.694	6.3	1.678	14.0
30	1	-1	1	1	1	-1	-1	-1	1	1.691	7.3	1.695	10.3	1.690	12.3
71 c	0	0	0	0	0	0	0	0	0	1.711	17.0	1.718	24.7	1.706	28.2
37	-1	-1	1	-1	-1	1	-1	1	1	1.657	8.6	1.671	16.6	1.660	18.5
40	1	1	1	-1	-1	1	-1	-1	-1	1.674	9.3	1.685	19.3	1.685	24.0
64	1	1	1	1	1	1	1	1	1	1.673	10.4	1.684	23.7	1.683	27.2
52	1	1	-1	-1	1	1	1	-1	-1	1.671	2.8	1.703	32.3	1.701	38.6
61	-1	-1	1	1	1	1	1	-1	-1	1.649	8.7	1.661	17.1	1.660	18.9
31	-1	1	1	1	1	-1	-1	1	-1	1.722	5.8	1.721	8.6	1.733	8.1
10	1	-1	-1	1	-1	-1	1	-1	1	1.682	11.6	1.694	18.7	1.695	24.1
19	-1	1	-1	-1	1	-1	-1	-1	1	1.698	9.7	1.708	16.7	1.704	22.0
72 c	0	0	0	0	0	0	0	0	0	1.706	17.5	1.723	23.0	1.718	31.6
41	-1	-1	-1	1	-1	1	-1	-1	-1	1.677	12.4	1.687	27.1	1.680	32.5
44	1	1	-1	1	-1	1	-1	1	1	1.644	7.5	1.657	22.6	1.656	30.2
11	-1	1	-1	1	-1	-1	-1	1	-1	1.635	7.8	1.652	13.2	1.645	15.6
7	-1	1	1	-1	-1	-1	1	-1	1	1.622	7.0	1.648	8.8	1.636	10.3
Block means (including central cases)										1.675	8.5	1.688	17.6	1.684	22.3

### Appendix C: Supplementary data from the study of RCM-based mortars

Data and figures provided in this section supplement information reported in the paper “Use of reactivated cementitious materials for the production of mortars” submitted to *Cement and Concrete Composites*.

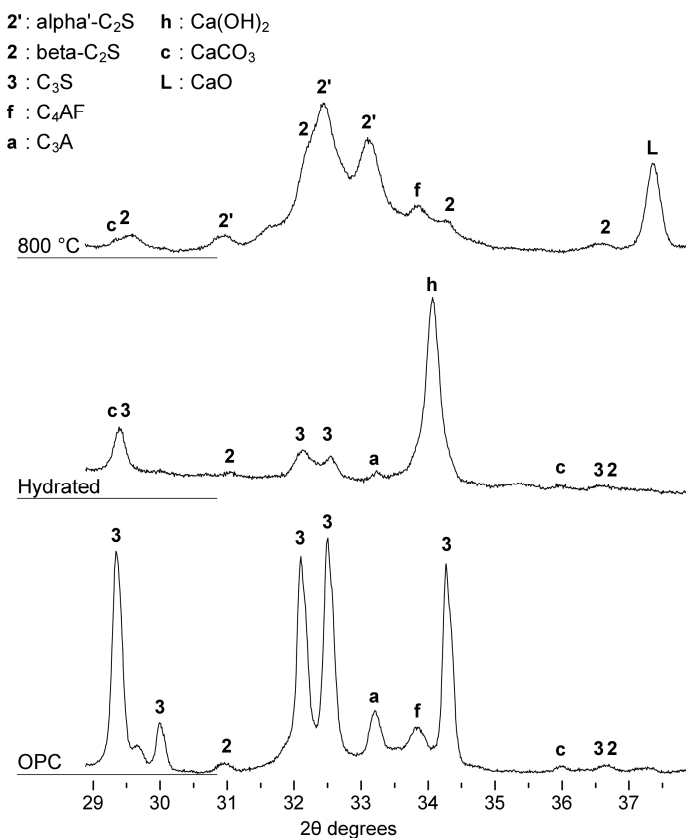


**Figure C.1** Comparison of XRD patterns of OPC, hydrated paste and RCM produced at 800 °C, between 29 and 38  $2\theta$  degrees.

Document revision: 2014/05/19